

**EURAD**  
**State of the Knowledge (SoK) Report**

**Spent Nuclear Fuel**  
**Domain 3.1.1**

**Kastriot Spahiu**  
**SKB, Stockholm and Chalmers University of Technology,**  
**Gothenburg, Sweden**

**Version : 1.0 ; 09 November 2021**

Please note: The statements made within this document are not necessarily the views of EURAD or any of its members. They represent the author(s) view on the most relevant knowledge about the topic at hand. The author(s) or EURAD assume no responsibility or liability for any errors or omissions in the content of this document. The information contained in this document is provided on an "as is" basis with no guarantees of completeness, accuracy, usefulness or timeliness.



*This project has received funding from the European Union's Horizon 2020 research and innovation programme under Grant Agreement n° 847593.*

## TABLE OF CONTENTS

Table of contents.....	I
Table of figures.....	II
List of Abbreviations.....	III
1. Introduction.....	1
2. General description of nuclear fuel types and reactors.....	1
3. The generation of fission products and higher actinides in a nuclear reactor-how does spent fuel get its actual composition. ....	2
4. The chemical state of the fission products and actinides in SNF. ....	4
5. Interim storage of spent nuclear fuel, wet and dry. ....	7
6. Damaged fuel rods .....	8
6.1 Oxidation of damaged fuel in reactor and during wet interim storage. ....	8
7. Fuel inventory and repository important parameters related to it. ....	9
8. Inventory of metallic parts of fuel assemblies, corrosion release fraction.....	10
9. Post-closure criticality. ....	11
10. Instant release fraction. ....	12
11. Radiolytically promoted fuel dissolution in presence of air.....	14
12. Spent fuel dissolution in deep repository: canister effects.....	16
12.1. Redox conditions in a failed canister.....	16
12.2. Spent fuel dissolution under reducing conditions. ....	17
13. Alpha doped UO <sub>2</sub> leaching under anoxic and reducing conditions. ....	19
13.1. Anoxic conditions and old fuel -Threshold of specific $\alpha$ -activity.....	20
13.2. Alpha doped UO <sub>2</sub> leaching under reducing conditions. ....	20
14. Fuel dissolution rates under reducing conditions. ....	21
15. Potential catalyst ( $\epsilon$ -particle) poisoning.....	22
16. Fuel dissolution modelling.....	22
17. Long-time structural stability of the fuel matrix. ....	25
References.....	26

## TABLE OF FIGURES

Figure 1: Fuel rod (left, from Olander 2009) and fuel assembly (right, <a href="http://www.world-nuclear.org">www.world-nuclear.org</a> ).....	2
Figure 2: Fission yields (in % per fission) of various fission products as function of the mass number for the thermal fission of $^{235}\text{U}$ , $^{239}\text{Pu}$ and $^{233}\text{U}$ .....	5
Figure 3: Relative partial molar Gibbs free energies of oxygen of the fission product oxides and of $\text{UO}_{2+x}$ and $\text{U}_{0.8}\text{Pu}_{0.2}\text{O}_{2\pm x}$ .....	6
Figure 4: Radioactivity, divided in total number of $\alpha$ - and $\beta$ -emissions, in $\text{UO}_2$ fuel with a burn-up of 40 GWd/tHM as a function of cooling time. ....	10
Figure 5: Redox conditions in a glovebox with 1 ppm (upper line) or 0.01 ppm $\text{O}_2$ (lower line), as compared to repository conditions, shown in a Eh-pH diagram for Pu (Eh (mV) = 59.16 pe). ....	17
Figure 6: Evolution of concentrations of actinides, lanthanides and $\text{Tc}$ (left) and fractional release rates (right) during fuel powder (0.25-0.5 mm) leaching under 1 bar $\text{H}_2$ , 25 °C. ....	18
Figure 7: Elementary processes for fuel dissolution by radiolytic oxidants in presence of $\text{H}_2$ . ....	24

## LIST OF ABBREVIATIONS

AGR	Advanced Gas-cooled Reactors
ASIED	Alpha Self-Irradiation Enhanced Diffusion
ASTAR	Alpha particle stopping power database, NIST
BET	Brunauer–Emmett–Teller theory
BU	BurnUp
BWR	Boiling Water Reactors
CAST	CARbon-14 Source Term (EC Project)
CIEMAT	Centro de Investigaciones Energéticas, Medioambientales y Tecnológicas (english: The Center for Energy, Environmental and Technological Research), Spanish public research institution in energy and the environment
CRUD	Chalk River Unidentified Deposits
DGR	Deep Geological Repository
DHC	Delayed Hydride Cracking
DISCO	Modern spent fuel dissolution and chemistry in failed container conditions (EC Project)
dpa	Displacement per atom
EC	European Commission
ENRESA	Empresa Nacional de Residuos Radiactivos (english: National Radioactive Waste Company), Spanish Radioactive Waste Management Organization
et al.	et alii, et aliae
FGR	Fission Gas Release
FIAP	Fraction of the Inventory in the Aqueous Phase
FIMA	Fissions per Initial Metal Atom
FIRST-Nuclides	Fast / Instant Release of Safety Relevant Radionuclides from Spent Nuclear Fuel (EC project)
FMDM	Fuel Matrix Dissolution Model
FP	Fission Product
GWd	Gigawatt days
HBS	High Burnup Structure
HDO	Deuterium Hydrogen monOxide; Semiheavy water
HM	Heavy Metal
IAEA	International Atomic Energy Agency
ICP-MS	Inductively coupled plasma mass spectrometry
INCAN	Rates and mechanisms of radioactive release and retention inside a waste disposal canister (EC project)
IRF	Instant Release Fraction
KIT-INE	Karlsruher Institut für Technologie - Institut für Nukleare Entsorgung (english: Karlsruhe Institute of Technology - Institute for Nuclear Waste Disposal)
KTH	Kungliga Tekniska Högskolan (english: KTH, Royal Institute of Technology)
LET	Linear Energy Transfer
LPR	Linear Power Rating
LWR	Light Water Reactors
MAM	Matrix-Alteration Model
MICADO	Model uncertainty for the mechanism of dissolution of spent fuel in a nuclear waste repository (EC-Project)
MIMAS-MOX	Micronized - MASTer blend mixed oxide

### 3.1.1 Spent Nuclear Fuel; State-of-Knowledge

MOX	Mixed Oxide Fuel
MWd, GWd	Megawatt days, Gigawatt days
NEA-TDB	Nuclear Energy Agency - Thermochemical DataBases
NF-PRO	Near Field Processes (EC-Project)
NPP	Nuclear Power Plant
ORIGEN	Oak Ridge Isotope GENERation
PA	Performance assessment
PCI	Pellet-Cladding Interaction
ppb	Parts per billion
ppm	Parts per million
PWR	Pressurized Water Reactors
QSS	Quasi Steady State
REE-oxides	Rare-Earth Element oxides
RWM	Radioactive Waste Management
SCALE	Standardized Computer Analyses for Licensing Evaluation
SCC	Stress Corrosion Cracking
SFS	Spent fuel stability under repository conditions (EC-Project)
SIMFUEL	Simulated nuclear fuel consisting of UO <sub>2</sub> doped with inactive lanthanides and other fission products, including metallic particles, in proportions corresponding to the simulated burnup.
SKB	Svensk Kärnbränslehantering Aktieföretag (english: Swedish Nuclear Fuel and Waste Management Company), Swedish Radioactive Waste Management Organization
SNF	Spent Nuclear Fuel
SPA	Spent fuel Performance Assessment (EC project)
SRIM	Stopping and Range of Ions in Matter; a group of computer programs which calculate interaction of ions with matter
SUBATECH	Laboratory of Subatomic Physics and related Technologies
T <sub>c</sub>	Temperature in the centre of the pellets
UO <sub>2</sub>	Uranium dioxide
UOX	Uranium oxide fuel
USSR	Union of Soviet Socialist Republics
UWO	The University of Western Ontario (Canada)
VVER	Water-Water Energetic Reactor (from Russian: vodo-vodyanoi energetichesky reactor) water-water power reactor
WMO	Waste Management Organisation
XPS	X-ray Photoelectron Spectroscopy
XRD	X-Ray Diffraction
ZVI	Zero Valent Iron

## 1. INTRODUCTION

The moment a nuclear fuel assembly is discharged from the reactor it becomes spent nuclear fuel (SNF). This term is much more used than e.g., “used” or “irradiated” nuclear fuel. The direct disposal of spent nuclear fuel first received consideration in the late 1970s (Johnson and Shoemith 1988) and is actually the main option for several European countries, such as Sweden, Finland, Spain, Germany, Switzerland.

This report will focus on SNF properties as waste material and has the double aim to be a short introduction to the field for non-specialists, generalists, young researchers, etc., as well as to be valuable for organizations involved in SNF management programs (e.g. Waste Management Organizations (WMO)), and their spent fuel specialists. This was attempted by discussing the most important issues for the performance assessment of a spent fuel repository, providing many references, and aiming to explain the concepts and the methods as simply as possible. The author is conscient that this is a very difficult task, much more so because no previous State of the Art reports exist, except one on instant release fraction (Kinzler and Gonzales-Robles 2013). On the other hand, reports on the same subject have been published more than two decades ago (Johnson and Shoemith 1988) and quite recently (Shoemith 2013, Carbol et al. 2020, Grambow 2021).

Many types of SNF exist, however as the vast majority of the SNF kept in storage in EC countries today is UO<sub>2</sub> and MOX (Mixed OXide of U and Pu) fuels, these fuel-types will be given most focus. Additionally, the accent in the chapter, when it comes to examples for a type of repository, is laid on a deep granitic repository since this one is closest to a step-wise implementation and also the author is most familiar with. EC-projects related to spent fuel: [Chemistry of the Reaction of Fabricated and High Burnup Spent UO<sub>2</sub> Fuel with Saline Brines](#) (Grambow et al. 1996), [Source term for performance of assessment of spent fuel as a waste form](#) (Grambow et al. 2000), [SFS](#) (Poinssot et al. 2005), [INCAN](#) (Oversby 2005), [NF-PRO](#) (Grambow et al. 2008), [MICADO](#) (Grambow et al. 2010), [FIRST-NUCLIDES](#) (Kienzler et al. 2014), [DISCO](#) (Evins et al. 2020) have contributed much to an increased knowledge in the field of spent fuel as a waste form-the author has had the privilege to participate in most of them.

The report starts with a discussion of how the spent fuel gets its actual composition during reactor operation, with emphasis on fuel properties important for its behavior in the repository, such as instant release fraction or fuel matrix dissolution behavior. A short description of interim fuel storage (wet or dry) follows, discussing also some specific issues such as fuel drying and damaged fuel rods. The inventory of spent fuel as a waste form, including radionuclides in the metallic parts of fuel assemblies is discussed next, as well as other repository relevant properties related to it, such as the radiation field, its evolution with time and the residual heat. A very short discussion of post-closure criticality follows, treating only its long-term repository aspects. The major emphasis is laid on spent fuel oxidative dissolution, first in presence of air, then under conditions relevant for European repository concepts. The progress in the recent years in spent fuel modelling by a more appropriate treatment of interfacial reactions is discussed next and the report finalizes with a treatment of long-term changes occurring in spent fuel in a sealed canister, such as radiation damage or helium buildup.

## 2. GENERAL DESCRIPTION OF NUCLEAR FUEL TYPES AND REACTORS.

There are several types on nuclear reactors including experimental, isotope production, ship propulsion and nuclear power reactors (that produce electricity). Nuclear power reactors are based on the use of thermal neutrons (slowed down from ~1 MeV to ~0.03 eV in an appropriate moderator, e.g. water, heavy water (D<sub>2</sub>O) or graphite), or fast neutrons (Olander 2009, Bailly 1999). The main types of nuclear power reactors developed that use thermal neutrons are LWR reactors, which include Boiling Water Reactors (BWR) and Pressurized Water Reactors (PWR). PWR reactors build in the former USSR, called VVER reactors, are present in some Eastern European countries and Finland. Pressurized Heavy Water Reactors that use heavy water as moderator, were developed mainly in Canada (CANDU reactors) and are also present in some Eastern European countries. Graphite moderated and gas cooled reactors were developed in UK and include Advanced Gas-cooled Reactors (AGR), which use UO<sub>2</sub> fuel and CO<sub>2</sub> gas as coolant.

### 3.1.1 Spent Nuclear Fuel; State-of-Knowledge

The light water reactor (LWR) fuel rod typically consists of a stack of  $\text{UO}_2$  pellets inside a Zircaloy cladding (Figure 1, left). The rods are assembled into arrays containing 50 to 300 rods which are called *fuel assemblies* (Figure 1, right). Several fuel assemblies constitute the *reactor core* in an arrangement that: (i) provides a rigid structure for holding fuel elements; (ii) delivers the desired thermal power to the coolant; (iii) provides a critical assembly with a minimum of neutron leakage (iv) provides adequate coolant flow to remove fission heat and sufficient coolant volume for thermalization of fission neutrons (v) accommodates control rods that maintain criticality as the fuel is consumed (Olander 2009). The predominant fuel for the present generation of nuclear power reactors is uranium dioxide in the form of ceramic pellets

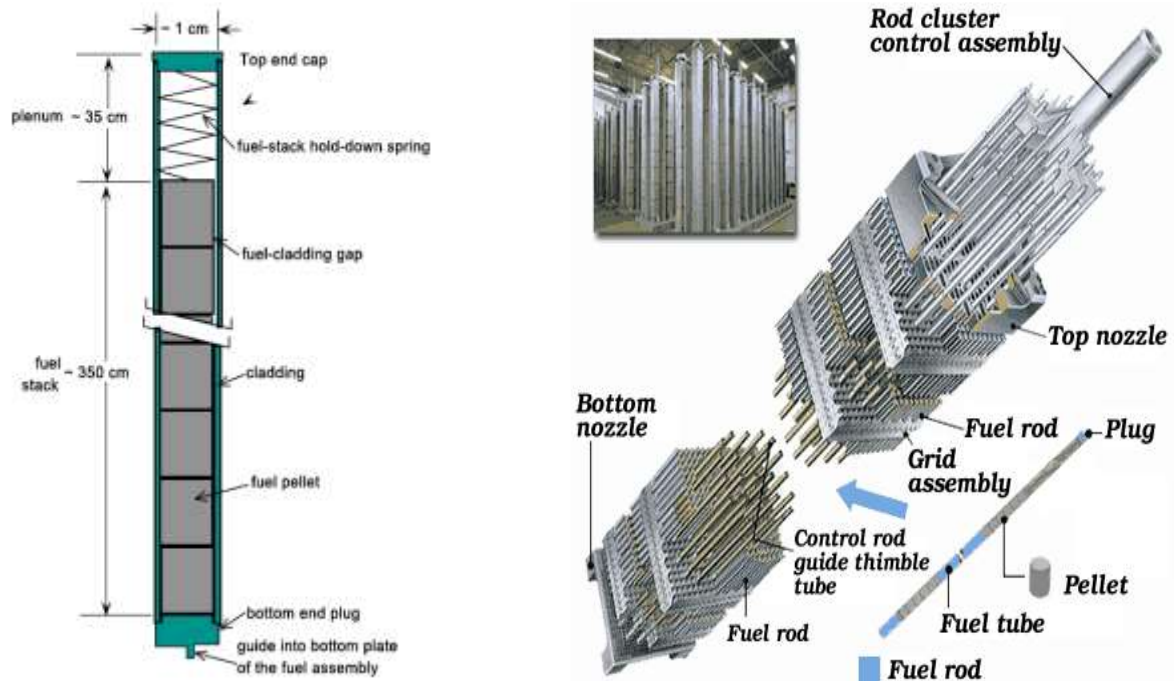


Figure 1: Fuel rod (left, from Olander 2009) and fuel assembly (right, [www.world-nuclear.org](http://www.world-nuclear.org)).

contained in a Zr-based alloy cladding rod (Shoosmith and Johnson 1988). Natural uranium (0.72 %  $^{235}\text{U}$ ) can be used in CANDU and other heavy water moderated reactors, while light water moderated reactors (LWR), require  $\text{UO}_2$  that has been enriched with a fissile nuclide, usually 1-5%  $^{235}\text{U}$ . In MOX fuel,  $\text{UO}_2$  is enriched with 5-15%  $^{239}\text{Pu}$ , originating from fuel reprocessing or atomic weapons programs.

## 3. THE GENERATION OF FISSION PRODUCTS AND HIGHER ACTINIDES IN A NUCLEAR REACTOR-HOW DOES SPENT FUEL GET ITS ACTUAL COMPOSITION.

Spent nuclear fuel is probably one of the most complex solids in the universe, not only because it contains more than 60 chemical elements in different phases, including gas bubbles, metallic particles and solid oxides in solid solution with  $\text{UO}_2$  or as separate phases, but mainly because of the process of in-situ creation of new elements by fission and neutron capture in a nuclear reactor. A short description of how spent fuel gets its actual composition due to several processes which occur simultaneously in a nuclear reactor is given here, more can be found in specialised works (Olander 1976, Bailly et al. 1999). The process of “burning” of the fuel in a nuclear reactor and the generation of the fission products is connected with nuclear fission process, presented schematically for  $^{235}\text{U}$  as:

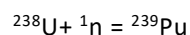


### 3.1.1 Spent Nuclear Fuel; State-of-Knowledge

In this process, the fissile  $^{235}\text{U}$  nucleus when hit by a thermal neutron (neutrons that are in thermal equilibrium with the medium they interact with) produces an unstable  $^{236}\text{U}$  nucleus, which is split in two smaller nuclei called *fission products* (FP) and 2-3 neutrons (which can cause other fissions), as well as gamma photons and a very large amount of energy ( $\sim 200$  MeV). Fission is accompanied with a small mass loss ( $\sim 0.1\%$ ), which is converted to energy according to Einstein's equation,  $E=mc^2$ . Most of this energy ( $\sim 80\%$ ) manifests itself as kinetic energy of the fission fragments, which travel about  $8\ \mu\text{m}$  before being stopped and dissipate the energy as electronic excitations. Throughout this path, referred to as *fission spike*, and across a diameter  $\sim 10$  nm, fuel atoms are very excited and the local temperature may exceed the melting point. The amounts of energy released during fission (or nuclear fuel burning) are  $10^5$ - $10^6$  times higher than the energies of chemical bonds (typical while burning coal or oil in a thermal reactor). This enormous amount of heat needs to be evacuated, first by thermal conductivity from the centre of the fuel rod to its surface-still the temperature difference between the centre of the fuel rod and the surface, only 4-5 mm away, is several hundred degrees. The fuel rods are filled with pressurized He, which facilitates heat transport to the cladding, and high-water flows ( $\text{m}^3/\text{s}$ ) in the reactor evacuate heat to the coolant water. The high flows cause vibrations in the more than 4 m long fuel rods (fretting at the grid spacers is the main cause of cladding damage). The changes in fuel composition caused by fission and neutron capture generally decrease the heat conductivity of the fuel and the same effect is caused by the accumulation of heavier fission gases (Kr and Xe) in the gap between fuel and cladding. The fuel expands thermally and more at the hot centre, which creates stresses, resulting in cracking of the fuel pellets to 10-15 pieces and "fuel bambooning" (Olander 2009). The fission process creates fission products of valences lower than IV, e.g. Nd(III) or Sr(II). Their occupation of the place of a U(IV) results in excess oxygen in the fuel matrix. In this case the neighboring U atom is formally U(V), leading to stronger attraction and shortening of U-O distances. Thus, the lattice parameter of LWR fuels as determined by XRD (X-Ray Diffraction) decreases with increasing burnup at constant O/M (oxygen-to-metal) ratio (Kleykamp 1985, Davies and Ewart 1971, Spino and Papaioanou 2000). Later on, the production of fission gases and solid fission products causes fuel swelling, which together with fuel thermal expansion and cladding creep results in closing of the gap between fuel and cladding. The steep radial temperature gradient from the hot centre to the fuel surface causes thermal diffusion of gaseous and volatile fission products, which migrate from the center of the grain towards grain boundaries and further towards the gap. At any given burnup, the temperature in the centre of the pellets ( $T_c$ ) is roughly proportional to the *linear power rating* (LPR) of the fuel, which is the energy production rate per unit length of the fuel rod. LWR fuel is typically irradiated at lifetime-average linear powers of 15-25 kW/m ( $800\ \text{°C} < T_c < 1200\ \text{°C}$ ). The temperature in the fuel determines the thermally activated diffusion and has thus a considerable significance in the Fission Gas Release (FGR), the migration of volatile or other segregated fission products, and the microstructural characteristics of the fuel (grain size, gas bubbles etc.). Cs, Rb, Te, I are often called "volatile FP", because both in elemental state and a part of their compounds are gaseous at reactor temperatures (Bailly et al. 1999, Ferry et al. 2005).

Extensive measurements have shown that the atomic mobility in operating nuclear fuels is effectively athermal below 1200 K (from about mid-radius to pellet surface); it is instead proportional to the fission rate (Matzke 1980, 1987). This radiation enhanced diffusion arises from thermal spike and pressure gradient effects along the fission tracks (Matzke 1982, Ronchi and Wiss 2002).

Fission can occur also spontaneously for heavy nuclides and in this case, it is a type of radioactive decay. Besides fission, in a nuclear reactor neutron capture in the  $^{238}\text{U}$  nucleus also occurs and produces higher actinides:



$^{239}\text{Pu}$  is fissile, like  $^{235}\text{U}$ . On the other hand,  $^{239}\text{Pu}$  itself is susceptible to further neutron capture which leads to the formation of  $^{240}\text{Pu}$ . Due to the in-growth of  $^{239}\text{Pu}$  and  $^{240}\text{Pu}$  during irradiation, Pu is the heavy metal element with the second highest concentration in spent nuclear fuel after U. Neutron capture occurs also in lighter nuclei e.g.  $^{59}\text{Co} + {}^1_0\text{n} = {}^{60}\text{Co}$  in atoms present in the metallic structure of fuel assemblies or in impurity atoms such as  $^{35}\text{Cl}$ ,  $^{14}\text{N}$  present in the fresh fuel. This neutron activated inventory needs to be accounted for in the overall radionuclide inventory (see section 7).

Besides linear power rating, *burnup* (BU) is the other major irradiation parameter affecting fuel characteristics. It is usually expressed in units of megawatt days per kilogram uranium (MWd / kg U) or GWd / t U. For Mixed Oxide (MOX) fuel, the burnup is expressed in MWd/kg HM, where HM stands for

### 3.1.1 Spent Nuclear Fuel; State-of-Knowledge

Heavy Metal, i.e., U and Pu. Burnup can also be expressed as fraction of fuel atoms that underwent fission, in % FIMA (Fissions per Initial Metal Atom). The average discharge burnup of spent fuel has been increasing over the years due to requirements of better fuel utilisation and improvements in reactor operation technology. A rule of thumb is that ~10 MWd/kg U is produced by 1%  $^{235}\text{U}$ . The explanation to how burnups of 70 or 80 MWd/kg U can be achieved with fuel of only 4 % enrichment is that a significant fraction of all fissions in the lifetime of the discharged fuel occurs in  $^{239}\text{Pu}$ ; depending on the initial enrichment and burnup of individual fuel rods, it may even be higher than the cumulative fissions in  $^{235}\text{U}$ .

The breeding of  $^{239}\text{Pu}$  is largely due to resonance epithermal neutron capture in  $^{238}\text{U}$ . Due to the high cross section for the resonance capture, this event primarily occurs at the outer rim of the fuel pellet (the interior of the pellet being shielded from incoming neutrons of the right energy by  $^{238}\text{U}$  atoms at the outside of the pellet). The higher rate of production of  $^{239}\text{Pu}$  at the outer rim of the pellet in turn leads to a higher fission rate and a local burnup 2-3 times higher than the pellet average (Matzke and Spino 1997). In  $\text{UO}_2$  fuel at local burnup above 50 MWd/kg U and temperatures below 1000-1100 °C, a transformed microstructure called *High Burnup Structure* (HBS) is formed, consisting of small grains of submicron size and a high concentration of 1-2  $\mu\text{m}$  pores (Rondinella and Wiss 2010) containing fission gas at extremely high pressures. The fuel matrix at the rim is depleted of Xe and Kr, which collect at the pores during the restructuring, but Cs remains in the matrix, because it is liquid at these temperatures (Walker et al. 1996). The HBS structure is also observed in MOX fuel, in the Pu-rich islands, where fission density and the corresponding local burn-up exceed the HBS formation threshold. The mechanism leading to the subdivision of fuel grains from the original ~10  $\mu\text{m}$  to ~10<sup>4</sup> grains of 0.1-0.3  $\mu\text{m}$  is probably due to polygonization (reorganisation of dislocations in “sub-boundary” domains) (Rondinella and Wiss 2010).

MOX fuel has slightly lower thermal conductivity and operates at higher  $T_c$ , which results in higher FGR than  $\text{UO}_2$  fuel, but this difference decreases with a homogeneous Pu-distribution (Masih 2006, IAEA 2003b). The burnup of CANDU fuel is lower (6-12 MWd/kg U), but it is operated at higher linear power ratings 20-50 kW/m (800 °C <  $T_c$  < 1700 °C) than LWR fuel (Johnson and Shoesmith 1988). AGR fuel has generally lower burnups than LWR (up to ~40 MWd/kg U) and has typically low FGR (up to 1% at 40 MWd/kg U), unless carbonaceous deposits cause increased FGR (Cowper et al. 2016).

## 4. THE CHEMICAL STATE OF THE FISSION PRODUCTS AND ACTINIDES IN SNF.

The chemical state of the fission products has been analysed thoroughly in several early publications (Kleykamp 1985, Kleykamp et al. 1979, 1993, Imoto 1986, Cordfunke 1988). According to Kleykamp (1985), the most significant chemical property of oxide fuels, e.g.,  $\text{UO}_2$  and MOX, is the equilibrium pressure of oxygen in the gas phase of the fuel rod. The relative partial molar Gibbs free energy of oxygen, or the *oxygen potential* of the fuel, has a major influence in the chemical state of the fission products and on the oxidation of the cladding.

Another important factor affecting the chemical state of the fuel is the *compositional change* during irradiation resulting from the fission process. Fission products are generated in large numbers, with typical distributions depending on the fissile nuclide and the neutron energy. The fission yields for  $^{235}\text{U}$  and  $^{239}\text{Pu}$  with thermal neutrons are shown in Figure 2, together with a schematic view of cracked spent fuel pellets, pellet-cladding gap and grain boundaries (right).

### 3.1.1 Spent Nuclear Fuel; State-of-Knowledge

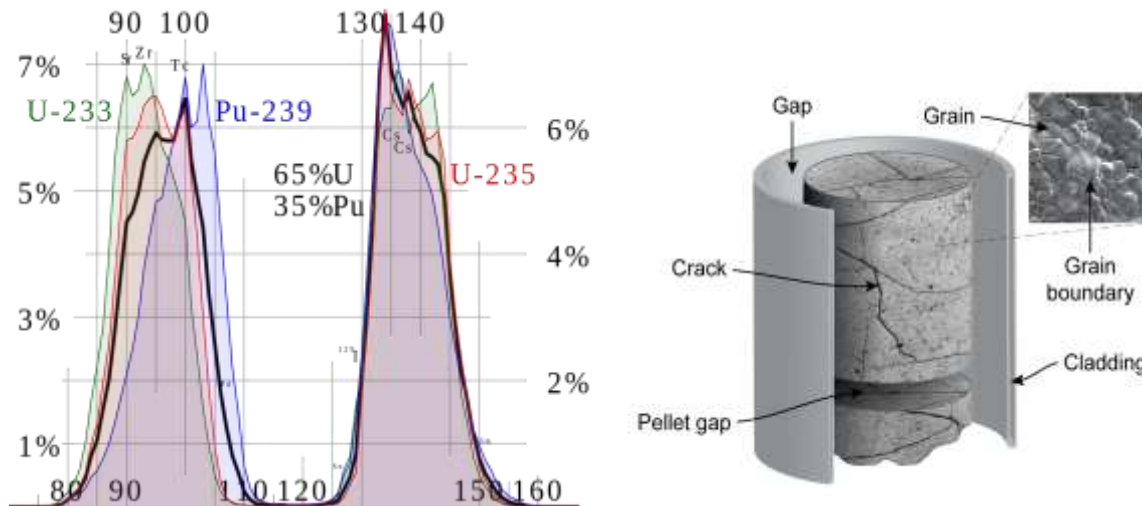


Figure 2: Fission yields (in % per fission) of various fission products as function of the mass number for the thermal fission of  $^{235}\text{U}$ ,  $^{239}\text{Pu}$  and  $^{233}\text{U}$ . Left figure: [https://en.wikipedia.org/wiki/Fission\\_product\\_yield](https://en.wikipedia.org/wiki/Fission_product_yield), right figure: Fors (2009).

As seen from the figure, the thermal neutron fission of  $^{235}\text{U}$  has two maxima around the masses  $95 \pm 15$  and  $135 \pm 15$ , which explains e.g., the high fission yields of  $^{90}\text{Sr}$ ,  $^{129}\text{I}$  and  $^{137}\text{Cs}$  and other isotopes with mass numbers near the maxima.

The chemistry of the fuel-fission product system during and after the irradiation is characterised by several phenomena: a) the fission product concentrations increase gradually during the irradiation process, b) the  $\beta$ -active fission products change their chemical properties due to the decay during and after the irradiation process, c) the oxygen-to-metal ratio (O/M,  $M = \text{U} + \text{Pu}$ ) and the oxygen potential of the fuel change during burnup with an increase of the O/M ratio of the fuel, d) axial and radial temperature gradients in the fuel rod result in material transport phenomena and thermal diffusion processes which cause compositional gradients. At higher inner clad temperatures, the reaction behaviour of cladding has also to be considered with regard to the mass balance of the fuel-fission product system. Finally, in the case of failed fuel rods the coolant is involved through reactions with the fuel and the fission products (see 6.1).

The binding of the various cations in an oxide fuel is realized through oxygen atoms. The chemical state of the fission products and actinides in the fuel can be predicted by calculating the total number of the cations of fission product elements produced and coupling them with oxygen in the order of chemical stability. The most common way of representing such data is through an Ellingham diagram (Ellingham 1944), a plot of the partial molar Gibbs energy of oxygen ( $\Delta \bar{G}_{\text{O}_2}$ ) against temperature. The chemical stability of an oxide at a given temperature can be estimated by the equilibrium partial pressure of oxygen or the oxygen potential. Stable oxides, such as uranium dioxide, have strong metal-oxygen bonds and low oxygen potentials. Other metals, such as Pd, have relatively high oxygen potentials because they don't bind oxygen strongly, see Figure 3.

As seen in Figure 3, which is an Ellingham diagram for spent fuel, the equilibrium lines for Ag, Pd, Rh, Ru, Te, Tc with their corresponding oxides are much higher than the line for  $\text{U}/\text{UO}_2$ , hence these fission products cannot bind to oxygen in the spent fuel matrix. Their oxides would dissociate at the oxygen potential of the fuel and they segregate from the spent fuel matrix in the form of  $\epsilon$ -particles (or 4d-element metallic particles or white inclusions). On the other hand, uranium and other actinides, as well as some fission products, such as the lanthanide ions and e.g., Zr, Sr and Ba bind oxygen much stronger, as indicated by their low equilibrium oxygen potentials, hence they remain dissolved in the  $\text{UO}_2$  matrix. This doping of the  $\text{UO}_2$  matrix with cations of lower valence (e.g.,  $\text{Sr}^{+2}$ ,  $\text{Eu}^{+3}$ ) or tetravalent cations ( $\text{Zr}^{4+}$ ,  $\text{Pu}^{4+}$ ) which cannot be oxidized higher in solid state has important consequences for fuel dissolution (see section 11).

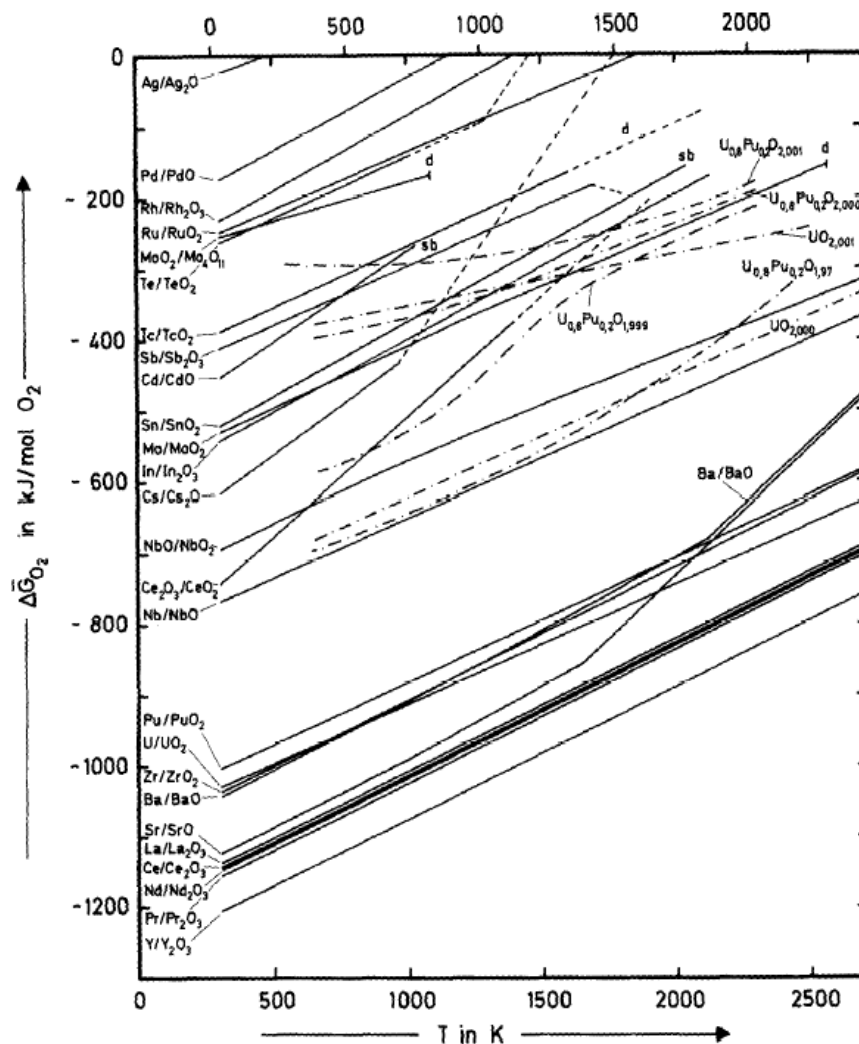


Figure 3: Relative partial molar Gibbs free energies of oxygen of the fission product oxides and of  $UO_{2+x}$  and  $U_{0.8}Pu_{0.2}O_{2+x}$ . d: oxide decomposes sb: oxide sublimes. From (Kleykamp 1985).

The oxygen potential of the fuel increases during burnup, but very little. No oxidation as increased  $x$  in  $UO_{2+x}$  is observed and the oxygen potential is buffered around the values for  $Mo(s)+O_2=MoO_2(s)$  equilibrium. At the end of the irradiation, the fuel is nearly stoichiometric and the oxygen potential is slightly lower at the rim than in the center of the fuel pellet (Matzke 1994, 1995). At high temperatures, Zr of the cladding also acts as excess oxygen getter, forming  $ZrO_2(s)$  (Kleykamp 1979, Matzke 1995). For a more detailed description of the oxygen balance in used fuel see e.g. (Olander 2009). Later, direct measurements of the oxygen potential of low (Une et al. 1991) and high burnup (Matzke 1994) fuels by the solid electrolyte technique confirmed the absence of fuel oxidation. The excess oxygen created during fission is fully neutralized by the oxidation of Mo in the metallic precipitates (Kleykamp 1985) and the inner surface of Zr cladding (Matzke 1995, Kleykamp 1979, 1990).

Kleykamp (1985) classifies the fission products in four groups (in parenthesis are given other elements added to the group by Ferry et al (2005)):

1. Volatile and gaseous fission products: Kr, Xe, Br, I; (Cs, Rb, Te)
2. Fission products forming metallic precipitates: Mo, Tc, Ru, Rh, Pd, Ag, Cd, In, Sn, Sb, Se, Te;
3. Fission products forming oxide precipitates: Rb, Cs, Ba, Zr, Nb, Mo, Se, Te;
4. Fission products dissolved as oxides in the  $UO_2$  matrix: Sr, Zr, Nb, Y, La, Ce, Pr, Nd, Pm, Sm, Eu and the actinides; (Ra)

### 3.1.1 Spent Nuclear Fuel; State-of-Knowledge

There are continuous transitions between group (2) and (3) due to similar oxygen potentials of some fission product oxides and the fuel (Figure 3), which changes its composition during the fission process. Elements which readily substitute for uranium in the uraninite structure, like the other actinides and rare earths (group 4 in the above classification), are expected to remain atomically dispersed within the host matrix (Kleykamp 1985, Hocking et al. 1994, Johnson and Shoosmith 1988). Another term frequently used is that actinide and lanthanide oxides form solid solutions with  $UO_2$ .

An important factor to consider is the solubility of the newly formed oxides in  $UO_2(s)$ . Thus,  $Ln_2O_3$  oxides (REE-oxides) are usually very soluble in  $UO_2(s)$  even at high content, so the lanthanides are always in solid solution with  $UO_2$  and do not segregate (Kleykamp 1993, 1985). These properties, i.e. the low oxygen potential and the large solubility in  $UO_2$  assure that the lanthanide ions will be homogeneously mixed in the spent fuel matrix and can be released only through fuel matrix dissolution.

This is not the case for fission products that have limited solubility in  $UO_2$ : they tend to segregate to grain boundaries and ultimately be excluded to the void spaces within the fuel rod. Sr is predominantly dissolved in  $UO_2$ , while only a small fraction of Ba-oxide is dissolved in  $UO_2$ ; the majority of Ba is precipitated in “grey phases”, which are *perovskite type oxides* of general formula  $(Ba_{1-x-y} Sr_x Cs_y)(U, Pu, Zr, Mo, RE)O_3$ . Grey phases are typical for fuel which has experienced very high temperatures, they are usually not observed in standard LWR fuel.

Several other processes, such as radiation damage, should be considered while making thermodynamic predictions for the chemical state of fission products in fuel (Konashi et al. 1996). Thus, CsI is rarely observed in spent fuel, even though it should form according to thermodynamic data and predictions. The same holds for  $Cs_2(U, Pu)O_4$ , predicted by phase studies in the Cs-U-O system, but never observed as a ternary oxide in LWR spent fuel.

**Metallic particles.** As mentioned before, certain metal/oxide systems, as Ag, Pd, Rh, Ru, Te, Tc, Sb, Cd, In and Sn have oxygen potentials which are higher than that of  $UO_2$  containing various amounts of Pu. These fission products are then expected to exist in metallic form in the fuel matrix. The atoms of these fission products are produced in fission events and through thermal diffusion meet other atoms which also are in metallic form and form metallic alloy particles. The diffusion is more intense in zones with high temperature, thus in the central part of the fuel pellet the metallic particles are larger, while at the rim of the pellet, where the temperature is lower, they are extremely small. The metallic precipitates formed in fuel are usually a hexagonal  $\epsilon$ -phase alloy containing mainly Mo, Ru, Tc, Rh, Pd (Kleykamp et al. 1985, Cui et al. 2012, Buck 2015). They are called  $\epsilon$ -particles, metallic particles, d-element alloy particles or white inclusions. The particle sizes detected by TEM are 1-8 nm at the rim (Thomas et al. 1989, Matzke et al. 1989, Ray et al. 1992). At the rim of the fuel pellet, differences in metal particle composition due to the different Pu fission yields are also reported (Cui et al. 2012, Adachi et al. 1990). With increased burnup, the yield of the components of metallic particles increases and the number of metallic particles also increases. From the yield of fission metal particles during nitric acid dissolution (Adachi 1990), it can be deduced that a large part of these particles is extremely small (a few atoms), hence easily dissolved by the acid.

Other phases occur in the gap between fuel and cladding by condensation of volatile fission products and by chemical interaction of fission products with cladding (e.g.  $ZrI_4(s)$  or  $ZrH_x(s)$ ).

**To summarize:** after irradiation in the reactor, the pellet is cracked to 10-15 pieces and the majority of the fission products (~95%) and actinides are homogeneously distributed in the fuel matrix at the place they are created by fission. A certain percentage of gaseous and volatile fission products (Cs, Rb, I, Te) have migrated to the gap, to cracks in the pellet or to grain boundaries, while other fission products are segregated in  $\epsilon$ -particles or segregated oxide phases.

## 5. INTERIM STORAGE OF SPENT NUCLEAR FUEL, WET AND DRY.

After discharge from the reactor, the spent fuel is stored in pools at the reactor site for 1-3 years or more to allow for the decay of the very short-lived nuclides. Afterwards the fuel is transferred to wet or dry long term interim storage. The number of dry storage casks increases globally, anyhow about 80% of all discharged fuel is stored in wet cooling ponds (IAEA 2013). Due to the absence of operational repositories for spent nuclear fuel today, an extended interim storage is necessary. To maintain retrievability and

### 3.1.1 Spent Nuclear Fuel; State-of-Knowledge

transportability may become more challenging over extended storage periods (IAEA 2020). Even though spent fuel is able to withstand long-term interim storage without major modification of its disposal relevant properties, some potential effects need further consideration.

During **dry interim storage**, high priority items are the stress corrosion cracking (SCC) of welded stainless-steel canisters and the hydride effects (reorientation and embrittlement) of high burnup fuel cladding and its relation with the Ductile to Brittle Transition Temperature (DBTT), which is a key parameter regarding the transport after dry storage (Billone et al. 2013, Grambow 2021).

The transport of spent fuel and the dry interim storage require spent fuel drying before its storage in inert gas atmosphere (He, Ar). The presence of water in dry storage canisters is undesirable, because  $\gamma$ -radiolysis of water vapor produces oxygen, which can oxidize spent fuel with damaged cladding at the relatively high temperatures of dry storage (Jung et al. 2013, Shukla et al. 2019, Bryan et al. 2019). Oxidation of spent fuel by oxygen has been thoroughly studied as function of temperature (Hanson et al. 2008). The spent fuel is oxidized to  $U_4O_{9+x}$  (usually up to  $UO_{2.4}$ ) at temperatures below 230-250 °C and relative humidity below 40 %, based on the data of (Hanson 1998, Einziger et al. 1992, Thomas et al. 1989, Thomas et al. 1993). This is due to the increased stability of the cubic structure of  $U_4O_9(s)$  by the presence of the fission products and the oxidation proceeds to  $U_4O_{9+x}$ , up to  $\sim UO_{2.4}$ . The formation of  $U_3O_7(s)$  phase, typical during oxidation of  $UO_2$  in air, is not observed for spent fuel (Hanson 1998, Thomas et al. 1993). Temperatures higher than 230 °C are needed to form  $U_3O_8(s)$  (Einziger and Cook 1985, Einziger and Strain 1986), a transformation which is accompanied with volume increase ( $\sim 36\%$ ), due to the passage from a cubic to a tetragonal phase (Taylor 1989). This can cause cladding rupture due to fuel swelling, also called unzipping (Einziger and Strain 1986, Hanson 2000). The rate law for fuel oxidation to  $U_4O_9$  is not valid for CANDU fuel (Hanson et al. 2008), given its much lower doping and burnup than LWR fuel.

**Wet interim storage** poses less problems to the cladding and the fuel (IAEA 1998, 2006, 2013), but requires radionuclide separation from the cooling water and increases waste production. Breached fuel rods (if present) are leached through processes similar to these discussed later for fuel dissolution under oxidic conditions, see section 11.

## 6. DAMAGED FUEL RODS

**Fuel cladding.** During irradiation in reactor the spent fuel is separated from the coolant by the cladding, usually a  $\sim 0.6$ - $0.7$  mm thick Zircaloy tube, which is very corrosion resistant. Due to the high coolant temperature, a layer of  $\sim 30$ - $100$   $\mu m$   $ZrO_2$  is formed in contact with water and the excess oxygen during fission causes a  $\sim 5$ - $10$   $\mu m$  thick  $ZrO_2$  layer on the inside (Gras 2014). The atomic hydrogen produced during zirconium corrosion in water is partially (10-20 %) dissolved in the metal and can form zirconium hydrides ( $ZrH_x$ ) at lower temperatures, when the solubility of hydrogen in the metal decreases. On the surface of fuel rods deposition of CRUD (Chalk River Unidentified Deposits) is observed. CRUD investigations have shown that it consists mainly of particles of corrosion products of the metallic parts in the reactor primary circuit (hematite  $Fe_2O_3$  or Ni-Fe-Cr mixed oxides or spinel's) and includes adsorbed nuclides as well (IAEA 2011, Chen 2006). Estimations of the radionuclide inventory in CRUD are not simple and are usually based on measurements at the reactor site during prolonged periods (SKB 2010b, Betova et al. 2012).

The frequency of cladding damaged rods per year in the reactor has decreased from about 1% in the early nuclear power reactors to about  $10^{-5}$  (or 0.001%) today (Olander 2009, IAEA 2016). The mechanical damage (fretting) represents the majority of cladding damages (IAEA 2003b, IAEA 2010, IAEA 2016), other mechanisms include damage by debris in the coolant, hydrogen embrittlement, pellet-cladding interaction (PCI) (Cox 1990), delayed hydride cracking (DHC) (IAEA 2010, Motta et al. 2019).

### 6.1 Oxidation of damaged fuel in reactor and during wet interim storage.

Given the high temperatures in the reactor, water vapor oxidizes the fuel in the breached rod according to:  $UO_2 + xH_2O = UO_{2+x} + xH_2$ . The oxygen potential is determined also by the equilibrium  $H_2O = H_2 + \frac{1}{2} O_2$  at the given temperature. Hydrogen from fuel oxidation by water and especially from internal cladding corrosion by water vapor limits the oxidation to only  $\sim UO_{2.02}$  in the part of the rod away from the defect

### 3.1.1 Spent Nuclear Fuel; State-of-Knowledge

where H<sub>2</sub> accumulates, while at the defect itself and especially for a large one, the oxidation can be more pronounced (up to UO<sub>2.06</sub>, Une et al. 1995). More on fuel oxidation in the reactor, the influence of radiolysis (Li and Olander 1999) etc. can be found in specialized references (Olander et al 1999, 1997, Olander 1986, 1998 Abrefah et al. 1994).

The damaged fuel rods pose problems, because their radiolytically promoted oxidation-dissolution continues during wet interim storage, until they are dried and packed in hermetic vessels under inert gas. The inventory released in the reactor (given the high flows, most of the fuel loss in reactor at a large defect is due to fuel washout) and the one in wet storage are difficult to evaluate, thus usually the complete inventory of the rod is assumed present in the repository. It is not straightforward to evaluate the behavior of pre-oxidized fuel in the repository as compared to undamaged fuel. A few tests under hydrogen with pre-oxidized fuel through several years leaching under oxic conditions indicate massive U precipitation and formation of U(IV)-particles after test start. The concentrations of actinides are about one order of magnitude higher than the solubility of the tetravalent oxides and measurable releases of Cs and Sr occur during at least one year (Puranen et al. 2017, Cowper et al. 2019, Fidalgo et al. 2020). Anyhow, the releases seem to be very limited after this initial period. This is an area where more research efforts will be needed.

## 7. FUEL INVENTORY AND REPOSITORY IMPORTANT PARAMETERS RELATED TO IT.

In safety assessments of nuclear fuel repositories, the boundary conditions are governed by the radiotoxicological impact of individually released radionuclides rather than by the total amount of released elements. It is therefore important to understand the amounts, types and levels of radionuclides in the total inventory in order to make long-term predictions of the SNF behavior in a deep underground repository. Usually, in every safety assessment, a selection of *dose relevant nuclides* (Hemel 2017, SKB 2010d) is made, which excludes radionuclides in very low concentrations or very short lives. For all nuclides in this list, speciation, solubility products, sorption and diffusion coefficients in bentonite near field and sorption and diffusion coefficients in the far field are needed.

Out of 977 fission products listed in databases, many have very short half-lives, in the range of msec (30%), sec (28%) or min (16%). Fission products with cumulative fission yields >0.001% for both U and Pu are: 7 long lived FP (<sup>79</sup>Se, <sup>93</sup>Zr, <sup>99</sup>Tc, <sup>107</sup>Pd, <sup>126</sup>Sn, <sup>129</sup>I, <sup>135</sup>Cs) and 7 medium-lived (<sup>3</sup>H, <sup>85</sup>Kr, <sup>90</sup>Sr, <sup>121m</sup>Sn, <sup>137</sup>Cs, <sup>151</sup>Sm, <sup>155</sup>Eu)-these are generic candidates for dose relevant nuclides. <sup>10</sup>Be, <sup>14</sup>C and <sup>113m</sup>Cd are not important as FP (low yields), but are produced also by neutron activation in the reactor. Some nuclides with half-lives longer than 100 years and sufficient production are: <sup>10</sup>Be, <sup>14</sup>C, <sup>36</sup>Cl, <sup>41</sup>Ca, <sup>59</sup>Ni, <sup>63</sup>Ni, <sup>79</sup>Se, <sup>93</sup>Zr, <sup>94</sup>Nb, <sup>93</sup>Mo, <sup>108m</sup>Ag, <sup>166m</sup>Ho. Actinides and some of their decay products with half-lives higher than 100 days are potentially dose relevant, i.e. <sup>231</sup>Pa, <sup>228</sup>Th, <sup>229</sup>Th, <sup>230</sup>Th, <sup>227</sup>Ac, <sup>226</sup>Ra, <sup>228</sup>Ra, <sup>210</sup>Po, <sup>210</sup>Pb.

Radionuclide inventories, their evolution with time due to decay, heat generation and the radiation field of spent fuel are typically calculated using code packages like SCALE (Standardized Computer Analysis for Licensing Evaluation) (Rearden and Jessee, 2018, Wieselquist et al. 2020). The neutron flux during fuel burning depends on the irradiation history (fuel loading pattern, core operating parameters, control rod sequence, cycle length etc.), which is important to be acquired from reactor operators in order to calculate burnup, fission gas release, residual heat and also the content of fissile material needed e.g., in criticality calculations. The computer program ORIGEN (Oak Ridge Isotope GENERation) used for calculating the isotopic concentrations, decay heat and radiation source terms in spent fuel is developed as part of the code package SCALE (Rearden and Jessee, 2018, Wieselquist et al. 2020). Uncertainties in the calculated inventory can be about 2% for U and Pu contents, 7% for fission products and 11% for minor actinides (SKB 2010a, IAEA 2001). Uncertainties in activation product impurities (<sup>14</sup>C, <sup>36</sup>Cl) contents can be much higher, as often no measurements on their initial content are available and upper bounding values from material specifications for inactive trace impurities are used instead.

### 3.1.1 Spent Nuclear Fuel; State-of-Knowledge

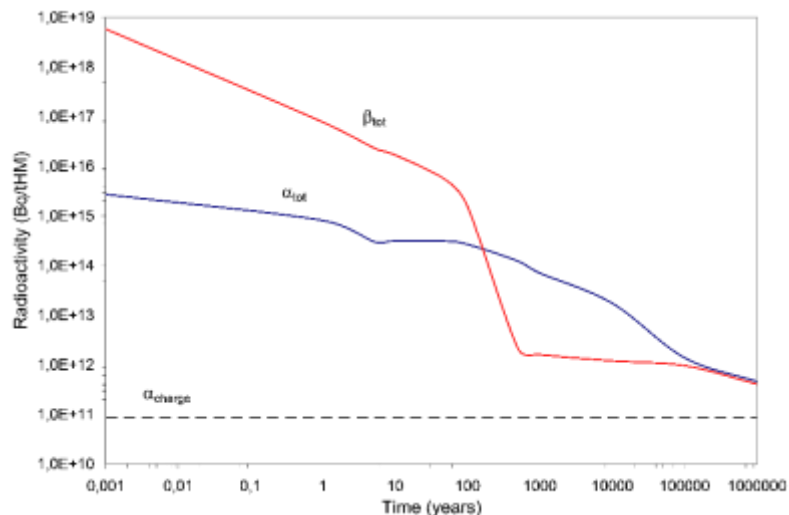


Figure 4: Radioactivity, divided in total number of  $\alpha$ - and  $\beta$ -emissions, in  $\text{UO}_2$  fuel with a burn-up of 40 GWd/THM as a function of cooling time. The lower line indicates the  $\alpha$ -activity in the  $\text{UO}_2$  fuel before irradiation in the pressurized water reactor (From Carbol et al. 2020).

The decay of short-lived fission products will lead to a change over thousands of years in composition, radioactivity and heat production (Carbol et al. 2020). For equal burnup, residual heat generation is higher for MOX fuel than for UOX fuel and cooling remains necessary even after 200 years of decay (Grambow 2021). Radioactive decay of fission products and actinides affects the properties of the nuclear fuel over time, such as the residual heat production discussed above and the nature and intensity of the radiation field surrounding the fuel. This governs shielding requirements during extended storage, radiolysis effects during disposal and radiotoxicity evolution over millions of years.

The majority of fission products decay by  $\beta$ -emission. Most of the fission products have relatively short half-lives in comparison with the actinides and decay within a few hundred years. The first years after discharge the  $\beta(\gamma)$  activity is about 1000 times higher than the  $\alpha$ -activity (Carbol et al. 2020) (see Figure 4).

Low energy  $\alpha$ -emitters are generally much more long-lived than  $\beta(\gamma)$  emitters. This results in a gradual change in the radiation field of the spent fuel: already after 300-500 years in the repository most of the  $\beta(\gamma)$ -emitters have decayed and  $\alpha$ -radiation dominates the energy deposition to the surrounding material. The initial  $\alpha$ -activity mainly originates from the decay of  $^{242,244}\text{Cm}$ ,  $^{238}\text{Pu}$  and  $^{241}\text{Am}$ , whereas the late decrease is caused by the decay of long-lived  $\alpha$ -emitters such as  $^{239,240}\text{Pu}$  and  $^{243}\text{Am}$ .

## 8. INVENTORY OF METALLIC PARTS OF FUEL ASSEMBLIES, CORROSION RELEASE FRACTION.

The cladding tubes for the fuel are made of Zircaloy. Other structural elements of the fuel assemblies are made of stainless steel, Inconel, Incoloy or Zircaloy. The PWR control rods, made of an alloy containing 80% Ag, 15% In and 5% Cd, can also be encapsulated together with the PWR fuel elements.

Some of the radioactivity in the fuel assembly is present in the cladding tubes and other metal parts as neutron activation products of alloying elements and impurities present in the as-fabricated materials. This activation product inventory is calculated e.g., with Scale (Bearden and Jessee 2018, Wieselquist 2020), using as input material composition and the neutron flux based on data from irradiation history in the reactor. If water enters the canister, the metal parts will corrode. It is generally assumed that the activation products are released with the rate with which the metal corrodes. It is then important to revise literature data for corrosion rates of Zircaloy, stainless steel (usually types 304 and 316) and nickel alloys such as Inconel under repository conditions. Recent reviews on corrosion of Zircaloy and steel are given in State-of-the-Art Reports of EC-Project [CAST](#) (Gras 2014, Swanton et al. 2015). The proposed corrosion rates for Zr are either 1-2 nm/y (Gras 2014) or 5 nm/y (Shoosmith and Zagidulin 2011). These and other data on material corrosion should be reviewed in order to obtain corrosion rates for use in the PA model.

### 3.1.1 Spent Nuclear Fuel; State-of-Knowledge

The whole radionuclide inventory contained in CRUD is usually assumed to be released instantaneously upon water contact, i.e., is part of IRF (section 10). Silver in the control rods is a noble metal and is not expected to corrode in anoxic groundwaters, unless dissolved sulphide is present (McNeil and Little 1992), forming very insoluble silver sulphides. Experimental data for silver alloy control rods leaching indicate that if there is a release of Ag-108m, it is below detection limit of the gamma counter (less than ppt-levels) (Roth et al. 2015).

## 9. POST-CLOSURE CRITICALITY.

Neutrons from radioactive disintegrations can cause nuclear fission in fissile isotopes in the fuel. As long as the canister is intact, the great majority of neutrons generated by these disintegrations will pass out of the fuel without causing fission and the process can be neglected. In the case of  $^{235}\text{U}$  and  $^{239}\text{Pu}$  in particular, the efficiency of the fission process increases if the neutrons are moderated (slowed down) to lower energies by collisions with light atomic nuclei. This could occur if water penetrates a failed canister. New neutrons are released by the fissions, and if more neutrons are formed than are consumed, the process can become self-sustaining. The system is then said to be critical and large quantities of energy can be liberated. This process has been utilised under controlled form in the nuclear reactors for energy production.

In the repository, the spent fuel normal criteria for safety against criticality must apply. This means that the effective neutron multiplication factor<sup>1</sup>  $k_{\text{eff}}$ , including all uncertainties, must not exceed 0.95. Usually, a calculation of  $k_{\text{eff}}$  for a canister in the repository carried out with the most reactive assembly type and fresh fuel shows that the reactivity criteria cannot be met with the conservative assumption that the fuel is fresh, especially for PWR fuel (Agrenius 2010). Taking credit in criticality assessment for the reduction in spent fuel nuclear reactivity as a result of irradiation, i.e., burnup credit, is a complex issue. It requires highly sophisticated methodologies for calculating the isotopic inventory of the irradiated fuel for which burnup credit is taken. This knowledge is gained by using depletion codes. The uncertainty of a depletion code is controlled and established through verification of that code, usually by comparison with suitable and appropriate experiments. In-core reactor measurement data are important for verifications of depletion codes (IAEA 2001, IAEA 1998). Calculations using state-of-the-art methods and a reasonable assessment of the uncertainties show that by taking credit for the burn-up of the fuel, the criterion  $k_{\text{eff}} \leq 0.95$  can be met for both BWR and PWR fuel of a given burnup, i.e. criticality safety can be demonstrated. Loading curves show what minimum average fuel assembly burnup is required for a given initial fuel enrichment of fresh fuel assemblies to ensure that the effective neutron multiplication factor,  $k_{\text{eff}}$ , of the canister would comply with the imposed criticality safety criterion (Vasiliev et al. 2019, Agrenius 2002). They are called so, because fuel assemblies which comply with enrichment-burnup criteria of the loading curve can be loaded in the canister without risk for criticality.

In Radioactive Waste Management (RWM) organisations which are in charge of spent fuel handling, criticality analysis is done routinely for interim storage, encapsulation plant and transport from the encapsulation plant to the repository and will not be discussed here. Specific for the repository is the very long analysis times, of the order of  $10^6$  years, which requires a calculation of the reactivity variation during the whole analysis time. Large changes in reactivity are noted for MOX fuel (Herrero et al. 2017) and reactivities higher than the initial one result at several thousand years decay; for  $\text{UO}_2$  fuel the variation of reactivity with time has much smaller amplitudes (Agrenius 2010). A specific case of the criticality in the repository concerns salt repositories, in which the high concentration of  $^{35}\text{Cl}$  in brines, a good neutron absorber, decreases much the reactivity of the canister (Kilger et al. 2013, Sobes et al. 2015).

The corrosion of the canister materials and the changes in geometry (Fe corrosion products have higher molar volume than Fe) and material composition (Fe is converted to  $\text{Fe}_3\text{O}_4$ ) occurring after a canister is breached may affect the reactivity in the long term and need to be accounted for. Recent analysis of this issue for a canister in a repository setup (Agrenius and Spahiu 2016) has shown that a small increase in the burnup is necessary to compensate for the increase in reactivity caused by these long-term material and geometry changes. Several UK studies discuss the Rapid Transient (RT) and Quasi Steady State (QSS)

---

<sup>1</sup>  $k_{\text{eff}}$  is the ratio of neutrons produced from fission in one generation to the number of neutrons lost through absorption and leakage in the preceding generation.

### 3.1.1 Spent Nuclear Fuel; State-of-Knowledge

criticality and their relevance for the repository (Baldwin et al. 2015, Hicks et al. 2018) as well as the likelihood and consequences of post-closure criticality in a generic way, given the lack of Deep Geological Repository (DGR) site (Winsley et al. 2015, Hicks et al. 2018, Mason et al. 2014) with satisfactory results.

Another repository specific issue is the potential criticality outside the canister due to accumulation of fissile material (Bowman and Venneri 1994, Van Konyneburg 1996). Several studies have demonstrated that criticality outside the canister has a vanishingly small probability, requiring several highly improbable events, even when oxidative fuel dissolution was assumed (Oversby 2006, Beherez and Hannertz 1978, Nicot 2008). In the case of European repository concepts with very limited releases of actinides from the canister (section 14), it is more straightforward to demonstrate that this is a very improbable event.

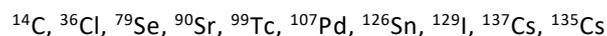
Finally, consequences of residual scenarios of assumed criticality in the repository have been published recently (Hedin et al. 2013) and generic cases have also been treated in (Mason et al. 2015, Winsley et al. 2015, Hicks et al. 2018). In SKB's case (Hedin et al. 2013) it is shown that the temperature of the critical canister is limited by the boiling point of groundwater at the given depth (264 °C at 5 MPa)-a higher temperature would cause water evaporation and subcriticality. The power developed by the critical canister at this temperature (~14 kW) is limited by the capacity of the rock to transport away the generated heat. It was also shown that the critical event causes a limited temperature increase in the neighbouring canisters (up to 60 °C), hence without consequences for their bentonite properties.

## 10. INSTANT RELEASE FRACTION.

When spent fuel comes into contact with groundwater, radionuclides are released from the gap between the fuel and the cladding, from cracks, from water accessible grain boundaries and from the fuel matrix itself with various rates. Traditionally radionuclide releases from such a heterogeneous material have been treated with only two sources of release: the fuel matrix and the Instant Release Fraction, IRF, representing everything released faster than the matrix. As discussed in the previous section, during irradiation in reactor, a certain percentage of the volatile radionuclide inventory has segregated to the gap between the fuel and the cladding, to cracks and also to grain boundaries. The radionuclide fractions released to the fuel/cladding gap, cracks and grain boundaries are referred to as "Instant Release Fraction", IRF. They are released fast (weeks to months) after water contact, but for performance assessment purposes, they are treated as instant release.

The behaviour of fission gases is best known out of these radionuclides and a number of studies on Fission Gas Release (FGR) have been published (Johnson and Tait 1997 and references therein, Johnson et al. 2005, OECD-NEA 2002, Blair et al. 2006, Gonzales-Robles et al. 2016, Wareing et al. 2012). FGR is more strongly correlated to the linear heat rating than to the burnup of the fuel (Kamimura 1992). Anyhow, at very high burnup (60-100 MWd/kg U), the FGR increases exponentially with burnup and HBS thickness (Brémier et al. 2000).

The radionuclides considered as part of the Instant Release Fraction (IRF) include:



(Johnson and Tait 1997, Johnson and MacGinness 2002, Johnson et al. 2004, Ferry et al. 2005, Werme et al. 2004, Ferry et al. 2008, Johnson 2014). A closer look at this list shows that  $^{14}\text{C}$  and  $^{36}\text{Cl}$  originate from neutron activation of nitrogen and chlorine impurities in the fuel, while Cs, Rb, I and Te correspond to volatile fission products, because both the elements and part of their compounds are gaseous at reactor temperatures (Bailly et al. 1999). Most of the other isotopes correspond to segregated fission products (Tc, Pd, Sn, (Ag) in the metallic particles, Sr in grey phases), often with relatively high vapour pressures at reactor temperatures (Cubiccioti and Sanecki 1978). A thorough discussion of segregation is given in Hocking et al. (1994), while volatility is discussed in Cubiccioti and Sanecki (1978).

It is generally assumed that the fission gas release and the release of segregated and volatile nuclides such as Cs and I are related. This is a reasonable assumption for LWR fuels with a few percent FGR, since gas phase diffusion determines both these amounts. The releases of Cs and I are generally lower than FGR. A ratio of 1:1 with FGR is used for I, given the similar diffusion rates with Xe under reactor operating conditions (Lewis et al. 1990), while the diffusion coefficient of Cs is ~1/3 of that of Xe (Lassman et al. 2002, Walker and Lassman 1986), hence a ratio of 1:√3 with FGR is used for Cs releases (Johnson et al. 2012).

### 3.1.1 Spent Nuclear Fuel; State-of-Knowledge

The estimation of IRF is important for a safety assessment, both because of the pulse of their release immediately after canister breach, but also because of the presence of typically mobile radionuclides such as  $^{14}\text{C}$ ,  $^{36}\text{Cl}$ ,  $^{129}\text{I}$  or  $^{79}\text{Se}$ . Usually anions are considered mobile, because most mineral surfaces are negatively charged at near neutral pH, hence do not adsorb anions.

During the period 2000-2006, the assumption of nuclide migration due to ASIED (Alpha Self-Irradiation Enhanced Diffusion-see section 17), together with the inclusion of the inventory in rim porosity led to relatively high values of IRF for spent fuel (Johnson et al. 2004, Johnson et al. 2005, Ferry et al. 2005). Later studies showed that ASIED had negligible effect in nuclide migration (see section 17) and no contribution of the rim inventory to IRF was observed in several studies (Roudil et al. 2007, Roudil et al. 2009, Johnson et al. 2012, Serrano-Purroy 2012, Fors et al., 2009). The same absence of accelerated diffusion from the HBU zone (the Pu islands) is observed for MOX fuel (Carbol et al. 2009a, Johnson et al. 2012).

A large number of studies carried out lately (Roudil et al. 2007, Roudil et al. 2009, Zwicky et al. 2011, Königsberger et al. 2021) and during the EC-project [FIRST- Nuclides](#) (Lemmens et al. 2017, Kienzler et al. 2017, Roth et al. 2019, Gonzales-Robles et al. 2015, Serrano-Purroy et al. 2012, Johnson et al. 2012) improved the database of IRF studies for LWR fuels. In the EC project [FIRST-Nuclides](#) the instant release fraction (IRF) of I and Cs was investigated as a function of burnup and linear power rating (Lemmens et al. 2016). It was shown that above a linear power rating of 25 kW/m, there was a stronger correlation between IRF (Cs and I) and linear power rating than between IRF (Cs and I) and fuel burnup. There already existed a good number of IRF studies for CANDU fuel (Stroess-Gascoyne et al. 1994, Stroess-Gascoyne et al. 1996, Tait et al. 1997 etc.) and recently an IRF and matrix dissolution study for AGR fuel has been published (Cowper et al. 2016), indicating similar behavior to LWR fuel.

Most of the studies connected to IRF estimation have been carried out in presence of air. Recent results from fuel leaching under hydrogen (Ekeroth 2020, Spahiu 2019) show that the concentrations of isotopes typical for metallic particles (Tc, Mo, Ru, Rh, Pd) remain practically constant at very low levels ( $\sim 10^{-10}$  M) during more than 2 yearlong experiments, indicating an absence of IRF behaviour under such conditions. The same concerns the discussion of the grain boundary fraction: if the grain boundaries are attacked preferentially when fuel comes into contact with water, the segregated fraction of nuclides there will be released (Kienzler et al. 2014). In many tests under hydrogen, the constancy of Cs levels in solution is used to judge absence of fuel dissolution (Carbol et al. 2005, Carbol et al. 2009a, Fors et al. 2009, Spahiu et al. 2000, 2002, 2004), hence the preferential leaching of grain boundaries under such conditions seems to be inhibited. Further, relatively low grain boundary inventories of I, Cs and Sr have been reported for LWR fuels (Gray 1999, Gray et al. 1992, Rudil et al. 2007, Roudil et al. 2009, Roth et al. 2019); see discussion in Roth et al. 2019 for some high iodine grain boundary values in Gray (1999).

The leaching behaviour and the chemical state of Se in the  $\text{UO}_2$  matrix were studied in the [FIRST-Nuclides](#) EC-project. It was found that the estimated very low fractional release of Se (<0.22%) from the below detection limit values (Johnson et al. 2012) is likely due to the direct chemical bonding of Se to U atoms as Se(II) (selenide) ion, probably replacing oxygen in the cubic  $\text{UO}_2$  lattice (Curti et al. 2014, 2015). The inclusion of Se in the IRF is based on its assumed migration as  $\text{Cs}_2\text{Se}$  in reactor, similar to  $\text{Cs}_2\text{Te}$  and  $\text{CsI}$  (Cubicciotti and Sanecki 1978, Hocking et al. 1994).

In recent examples of performance assessments (SKB 2010b, SKB 2010d, Johnson 2014), an estimation of FGR for the whole fuel inventory is carried out by calculating it first for all rods in equilibrium cores, varying core parameters within wide ranges and using certified programs applied for licensing fuel use in reactor (Nordström 2009, Oldberg 2009). Then appropriate relationships for typical values of linear heat rate and burnups are established, through which FGR for the whole fuel inventory can be estimated (SKB 2010b). For other segregated nuclides such as these in the metallic particles, or activation products of impurities ( $^{36}\text{Cl}$ ,  $^{14}\text{C}$ ), values based on experimental leaching data are discussed and used (Johnson 2014, Werme et al. 2004, Posiva 2021).

## 11. RADIOLYTICALLY PROMOTED FUEL DISSOLUTION IN PRESENCE OF AIR.

**Radiolysis.** The spent fuel generates a complex radiation field ( $\alpha$ ,  $\beta$  and  $\gamma$ ) with broad energy spectra due to the decay of unstable nuclides. Spent fuel in contact with water will produce very reactive radicals ( $\text{OH}\cdot$ ,  $\text{H}\cdot$ ,  $\text{OOH}\cdot$ ,  $e_{\text{aq}}^-$ ) and molecules ( $\text{H}_2\text{O}_2$ ,  $\text{H}_2$ ,  $\text{O}_2$ ) due to radiolysis of water (Spinks and Woods 1990). Although oxidizing and reducing radiolytic species are produced in equivalent amounts, the lower reactivity of the molecular reducing species (mainly  $\text{H}_2$ ) will lead to locally oxidizing conditions near the fuel surface. The effects of  $\alpha$ -radiolysis are considered as dominating, both because of the much longer time periods of its presence in the repository, and because of the short range from the fuel surface in which the energy is deposited. Radiolysis of water has been thoroughly studied by both experiments and modelling. Low LET (Linear Energy Transfer) radiation, such as  $\gamma$ -radiation, does not produce any detectable amounts of the stable species  $\text{H}_2$  and  $\text{H}_2\text{O}_2$  in pure de-aerated water (Allen 1961, Jegou et al. 2005), because they react via  $\text{OH}\cdot$  and  $\text{H}\cdot$  radicals in a chemical chain reaction to reform  $\text{H}_2\text{O}$ . In aerated water, virtually all the hydrated electrons and  $\text{H}\cdot$  radicals formed are oxidised by  $\text{O}_2$ , and the main products of low LET water radiolysis in a system open to air are a steady state concentration of  $\text{H}_2\text{O}_2$  with constant releases of  $\text{H}_2$  and  $\text{O}_2$  (Spinks and Woods 1990). Alpha particles have high LET (Linear Transfer Energy) and a very short range. They can cause radiolysis of a thin layer of water ( $\sim 35\mu\text{m}$ ) near the fuel surface and produce mainly the molecular radiolysis products  $\text{H}_2\text{O}_2$  and  $\text{H}_2$ , because most of the radicals recombine in the  $\alpha$ -track. The oxidants produced by radiolysis ( $\text{OH}\cdot$ ,  $\text{OOH}\cdot$ ,  $\text{H}_2\text{O}_2$ ,  $\text{O}_2$ ) oxidize U atoms in the fuel matrix surface to U(VI), which is then released in solution, especially if carbonate is present in solution, due to the formation of strong U(VI)-carbonate complexes. The rate of this oxidative dissolution is much higher than that of non-oxidative dissolution (Röllin 2001) and U(VI) hydrated oxides (schoepite) are several orders of magnitude more soluble than  $\text{UO}_2(\text{s})$ .

**Fuel leaching studies.** The first studies of spent nuclear fuel radiolysis promoted dissolution were undertaken in the late 1970s (Katayama 1976, Eklund and Forsyth 1978, Johnson 1982) and were carried out in hot cell atmosphere. Already in the first studies it was observed that the release rates were higher for some nuclides such as Cs and they generally decreased with time (Katayama 1976), but were relatively insensitive to temperature (Johnson 1982). These studies were relatively simple, given the need to operate with manipulators inside the hot cell and consisted in contacting the spent fuel (fragments, or 1-2 pellets together with cladding) with the leaching solution during a given time interval, then analyzing the solution for the released radionuclides by radiochemical methods, and later by ICP-MS. Already in the beginning of 1990'ies there were more than 30 such studies (Forsyth and Werme 1992) and a forum for discussing them (Spent Fuel Workshop) was established since 1983. Methods used in geochemistry to study dissolution rates of minerals, often reported in  $\text{mg m}^{-2}\text{d}^{-1}$ , were also attempted, obtaining rates of the order of a few  $\text{mg m}^{-2}\text{d}^{-1}$ . Anyhow, spent fuel surface area is a difficult parameter to assess (methods such as BET (Brunauer et al. 1938), based on adsorption of inert gases at low temperature, are usually not successful) and estimations of geometric surface area using a roughness factor were most often used. An extensive discussion of this issue and estimated spent fuel surface areas are given in Grambow et al. (2010). Much more commonly used in spent fuel studies is the Fraction of the Inventory in the Aqueous Phase (FIAP) for a nuclide, which is the ratio of the activity (or mass) of the nuclide released in solution divided by its activity(mass) in the solid fuel sample. This requires knowledge of the fuel inventory for each nuclide ( $\mu\text{g/g}$  fuel or  $\text{Bq/g}$  fuel), determined by dissolving an adjacent pellet to the one studied or calculated. Fractional Release Rates (FRR) during a time interval are expressed through the increase of FIAP per unit time (day or year) (Grambow et al. 1996, Jegou et al. 2004, Ekeroth et al. 2020). A discussion of the different ways of expressing fuel dissolution rates and their advantages/disadvantages is given in Hanson and Stout (2004). Usually, the concentration of U is reported, given that a variety of U(VI) solid phases may form after a few months of leaching, depending on the composition of the leaching solution. Fractional release rates for fission products such as Sr are usually used to estimate the fuel matrix dissolution rate. Based on the results of several studies in a variety of groundwaters typical for different repository concepts, including salt brines, long-term Sr release rates were  $\sim 10^{-7}\text{ d}^{-1}$  under oxidizing conditions, i.e., in presence of air (Loida et al. 2012). Leaching studies with MOX fuel under oxidizing conditions (Loida et al. 1998, Glatz et al. 2001, Jegou et al. 2001, Jegou et al. 2004) show  $\sim 7$  times higher release rates than  $\text{UO}_2$  fuel of similar burnup (Grambow 2021, Jegou 2004). The fractional rates measured under much lower oxygen levels were about an order of magnitude lower (Forsyth et al. 1986, Johnson 1982, Johnson and Shoemsmith 1988, Loida et al. 1996). Based on all the fuel dissolution studies available until 2000, the EC-project [SPA](#)

### 3.1.1 Spent Nuclear Fuel; State-of-Knowledge

(Spent fuel Performance Assessment) (Baudoin et al. 2000) estimated fuel matrix dissolution rates to be in the interval  $10^{-4} \text{ a}^{-1}$  to  $10^{-7} \text{ a}^{-1}$ , with a best estimate rate of  $10^{-6} \text{ a}^{-1}$ .

Due to lack of space, mainly fuel dissolution studies are discussed in this report. Anyhow much of our understanding for the mechanism of radiolytically promoted fuel dissolution was obtained in studies with  $\text{UO}_2$ , SIMFUEL (Lucuta et al. 1996) and other fuel analogues, such as  $\text{UO}_2$  doped with inactive or  $\alpha$ -emitting isotopes. Another major achievement was the compilation of the NEA-TDB high quality thermodynamic databases for actinides and the most important fission products (Grenthe et al. 1992, Silva et al. 1995, Rard et al. 1999, Guillaumont et al. 2003, Olin et al. 2005 etc.), making thermodynamic modelling and interpretation of the leaching data possible. The influence of the various molecular oxidants, such as  $\text{O}_2$ ,  $\text{H}_2\text{O}_2$  and that of other solution parameters such as pH and carbonate on the oxidative dissolution of both spent fuel and  $\text{UO}_2(\text{s})$  was investigated. The role of Ca-ions and of silica in suppressing fuel corrosion rate was also investigated (Tait and Luht 1997, Santos 2006a, Santos 2006b). Electrochemical studies with  $\text{UO}_2$  and SIMFUEL electrodes, in which the corrosion current density (corresponding to the corrosion rate) is measured as function of the corrosion potential, accompanied with thorough investigation of the electrode surfaces by various spectroscopic techniques contributed to an increased understanding of the mechanism of  $\text{UO}_2$  oxidative dissolution and the construction of electrochemical fuel dissolution models (Shoesmith et al. 2003). It was established quite early based on electrochemical measurements that  $\text{H}_2\text{O}_2$  was 200 times faster than  $\text{O}_2$  in oxidizing the  $\text{UO}_2$  surface (Shoesmith et al. 1985, Shoesmith 2000). The  $\epsilon$ -particles in spent fuel (section 4) can act as catalysts for reactions involving  $\text{H}_2\text{O}_2$  or  $\text{O}_2$  (which would accelerate fuel corrosion) and  $\text{H}_2$  (which would suppress corrosion, see next section) (Broczkowski et al. 2005, 2010). A review of the studies concerning oxidative dissolution of  $\text{UO}_2$  and spent fuel, discussing the mechanism for molecular oxidant reduction, the influence of  $\alpha$ - and  $\beta$ ,  $\gamma$ -radiolysis and of the pH, temperature and various components of the groundwater is given in Shoesmith (2000).

**Studies to obtain modeling parameters.** Many other studies in the last 20 years were undertaken in order to obtain various parameters needed in the modelling of the oxidative dissolution of  $\text{UO}_2(\text{s})$  (section 16). Rate constants for interfacial reactions were determined in experiments with  $\text{UO}_2$  particle suspensions where the surface was in excess, resulting in pseudo first order reactions. By plotting the pseudo first order rate constant against the solid surface area to solution volume ratio, the second order rate constant is obtained from the slope (Ekeroth and Jonsson 2003, Roth and Jonsson 2008, Jonsson et al. 2007). The oxidation process was shown to be kinetically limited by the first one-electron transfer step from  $\text{UO}_2$  to the oxidant, also for multielectron oxidants ( $\text{O}_2$  and  $\text{H}_2\text{O}_2$ ). Further, the rate constant for the elementary reaction was shown to depend on the one-electron reduction potential of the oxidant (Ekeroth and Jonsson 2003). This made possible to evaluate oxidation rate constants for reaction with  $\text{UO}_2$  surface for all radical and molecular oxidants (Roth and Jonsson 2008). The role of carbonate in the mechanism of  $\text{UO}_2$  oxidative dissolution by  $\text{H}_2\text{O}_2$  was investigated and dissolution rates for oxidized U as function of carbonate concentration were determined. It was also shown that the oxidation of  $\text{UO}_2$  by  $\text{H}_2\text{O}_2$  is the rate determining step in the oxidative dissolution of  $\text{UO}_2$  in aqueous systems containing  $\geq 1 \text{ mM HCO}_3^-$  and the oxidation rate was determined (Hossain et al. 2006). The density of  $\text{UO}_2$  surface sites for oxidation was determined (Hossain et al. 2006, Hossain and Jonsson 2008). Another important simplification was the classification of oxidants according to their importance for fuel oxidation, by noting that the rate of fuel oxidation is given by the product of rate constant times oxidant concentration ( $r_i = k_i \times c_i$ ). It follows that for radicals that have large rate constants ( $k_i$ ), but concentrations ( $c_i$ ) many orders of magnitude lower than molecular oxidants, the product, and hence their relative importance, is much smaller. The main oxidant of the fuel matrix, with a contribution  $>99.9 \%$  under anoxic conditions and  $\alpha$ -radiation, was found to be  $\text{H}_2\text{O}_2$  (Ekeroth et al. 2006). In tests with  $\text{UO}_2$  powder, the oxidative dissolution yield of  $\text{H}_2\text{O}_2$  (the ratio of the amount of produced U(VI) to the amount of consumed  $\text{H}_2\text{O}_2$ ) was  $\sim 80 \%$ , the remaining 20% decomposed to  $\text{H}_2\text{O}$  and  $\text{O}_2$  (Ekeroth and Jonsson 2003). This yield was 14% for a  $\text{UO}_2$  pellet and less than 0,2% for SIMFUEL (Nilsson and Jonsson 2011, Bauhn et al. 2018). The impact of the various oxidants was revised later, accounting also for the redox reactivity of the materials (Lousada et al. 2013), see further in this section.

**Recent fuel studies.** Finally, a few recent spent fuel dissolution studies under oxidizing conditions concerning specific issues, such as the influence of high burnup or of  $\gamma$ -radiation from neighbouring rods in wet interim storage will be discussed.

The rim of the fuel pellet has higher actinide and fission product concentrations than the inside of the pellet, as well as smaller grains due to the high burnup structure (Rondinella and Wiss 2010). This means

### 3.1.1 Spent Nuclear Fuel; State-of-Knowledge

that the production of  $\alpha$ ,  $\beta$ ,  $\gamma$  radiolytic products will be higher at the rim as compared to a grain on the inside of the pellet. As shown by three systematic leaching studies of fuels with variable burnup (Ekeroth et al. 2009 and references therein, Jegou et al. 2004, Hanson 2008), the high doping level at the pellet rim both with actinides (such as Pu) and fission products makes the fuel matrix less prone to oxidation and counteracts successfully both the higher surface area and the higher radiation field. This means that fuel dissolution rates determined with average burnup fuel are valid also for high burnup fuel.

The increased redox stability of the doped  $\text{UO}_2$  matrix was confirmed later in studies comparing the redox reactivity of  $\text{UO}_2$  pellets with Y-doped  $\text{UO}_2$  or SIMFUEL (Trummer et al. 2010, Pehrman et al. 2012, Barreiro-Fidalgo and Jonsson 2019). The rate constants for oxidation by molecular oxidants  $\text{H}_2\text{O}_2$  or  $\text{O}_2$  were 2 respectively 4 orders of magnitude lower for SIMFUEL than for  $\text{UO}_2$  pellets, while no difference was observed for strong oxidants such as radicals (Pehrman et al. 2012). This was not due to the ability of the surface to decompose  $\text{H}_2\text{O}_2$ , which was quite similar ( $\sim 30\%$  difference) for all solids tested (Pehrman 2012), but to the lower redox reactivity of doped  $\text{UO}_2$ . Preliminary evidence that rare-earth doping suppresses the corrosion of  $\text{UO}_2$  under aqueous conditions results also from electrochemical studies (He et al. 2012, Razdan et al. 2014, Liu et al. 2017a, Liu et al. 2017b). In a study of Gd-doped  $\text{UO}_2$ , a substantial decrease in the dissolution rates was observed with increasing dopant concentration (Casella et al. 2012). Much lower U releases from Gd-doped pellets were observed also under  $\gamma$ -radiation (Barreiro-Fidalgo and Jonsson 2019), i.e., in presence of radicals. Serrano-Purroy et al. (2012) found lower releases from the part containing the rim as compared to the centre of the spent fuel pellet. Thermochemical measurements of  $\text{UO}_{2+x}$  solid solutions with two and three valent oxides (Mazeina et al. 2008), indicate that they are more resistant to oxidation and oxidative leaching than  $\text{UO}_2$  because of the additional stability resulting from the energetic contribution of the dopants. Similar increased stability towards oxidative dissolution is observed for the Pu-aggregates in spent (Carbol et al. 2009a, Jegou et al. 2010) or fresh (Odorowski et al. 2016) MOX fuel.

The influence of external  $\gamma$ -radiation from neighboring rods in wet interim storage to fuel dissolution from damaged rods was investigated in a series of studies of both  $\text{UO}_2$  and heterogeneous MIMAS (Micronised MASTer blend)-MOX fuel (Jegou et al. 2007, 2010). For  $\text{UO}_2$  fuel, U and  $\text{H}_2\text{O}_2$  concentrations were higher in the tests carried out with external  $\gamma$ -irradiation or added  $\text{H}_2\text{O}_2$  and uranyl peroxide (studtite) was detected on the fuel surface, but the releases rates of Sr and Cs were quite similar to the fuel leached without external  $\gamma$ -irradiation, in which no studtite could be observed (Jegou et al. 2007). For MOX fuel similar increased U and  $\text{H}_2\text{O}_2$  concentrations were observed with external  $\gamma$ -radiation, but also a 2-3 times increase in the release rates of Sr and Cs. Raman spectroscopy analysis demonstrated that the surrounding  $\text{UO}_2$  matrix was much more sensitive to oxidation than Pu-aggregates (Jegou et al. 2010).

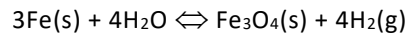
## 12. SPENT FUEL DISSOLUTION IN DEEP REPOSITORY: CANISTER EFFECTS.

### 12.1. Redox conditions in a failed canister.

If the spent fuel comes into contact with water, the release of actinides and most of the fission products will depend on  $\text{UO}_2(\text{s})$  matrix dissolution rate, since the great majority of fission products ( $>95\%$ , Ferry et al. 2005) are preserved there. The rate depends on many parameters, both intrinsic (fuel burnup, surface area etc.) and environmental (temperature, pH, groundwater composition etc.). However, the most important ones are the redox conditions on the fuel surface. Within a few years after repository closure, all the oxygen present will be consumed by reducing minerals (Earth was formed in absence of  $\text{O}_2$ ), bacteria or canister material, resulting in an  $\text{O}_2$ -free and reducing environment (Puigdomenech et al. 2001, Wersin et al. 1994, Kolar and King 1996). Such repository redox conditions assure low solubility and strong sorption for reduced forms of nuclides (e.g. 3+ and 4+ states of actinides). They are very difficult to realize in a laboratory; the redox conditions in an Ar-flushed glove box with 1 or 0.01 ppm  $\text{O}_2$  are shown between the dotted lines in Figure 5, while these relevant for a European repository concept are much more reducing. This is why such studies are difficult; even traces of  $\text{O}_2$  would oxidize U(IV) to U(VI) or Pu(IV) to Pu(V). The use of a strong reductant in solution (as actinide chemists do (Rai et al. 2003)) to fight radiolytic oxidants cannot be done, if they are present in the near field. As shown below, both dissolved  $\text{H}_2$  and Fe(II)

### 3.1.1 Spent Nuclear Fuel; State-of-Knowledge

can create such conditions. In all European deep repository concepts, relatively large amounts of dissolved hydrogen will be present during long time periods (Johnson 2005, Bonin et al. 2000). A major hydrogen source is the anoxic corrosion of the massive iron containers:



The equilibrium pressure of hydrogen for this reaction is very high, of the order of several hundred atmospheres (Garrels and Christ 1965). Another hydrogen source is  $\alpha$ -,  $\beta$ - and  $\gamma$ - radiolysis of the groundwater by the radiation of spent fuel. In the Swedish and Finish concepts

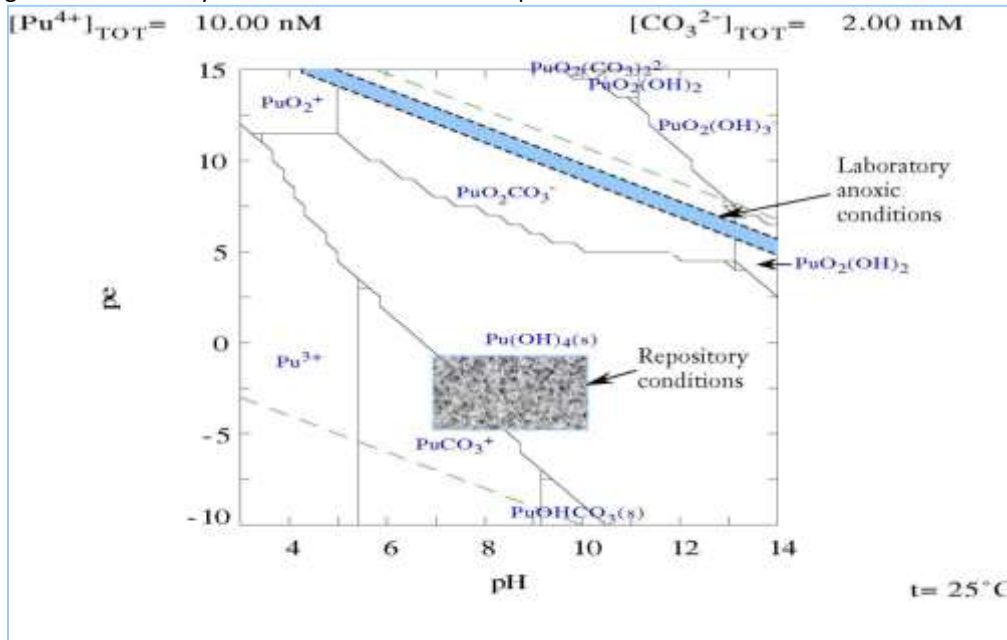


Figure 5: Redox conditions in a glovebox with 1 ppm (upper line) or 0.01 ppm  $\text{O}_2$  (lower line), as compared to repository conditions, shown in a Eh-pH diagram for Pu (Eh (mV) = 59.16 pe).

with a massive cast-iron insert. In the case of a limited canister defect and groundwater intrusion, the anoxic corrosion of iron gives rise to the production of hydrogen at a higher rate than its diffusive mass transport away from the canister. The concentration of dissolved  $\text{H}_2$  in the solution inside the canister is expected to quickly exceed its solubility in groundwater (Liu and Neretniks 2002, Sellin 2002). Gas phase formation occurs when the pressure of the hydrogen equals at least the hydrostatic pressure, around 5 MPa at 500 meters depth. For this reason, several studies of spent fuel leaching in the presence of hydrogen at pressures up to 5 MPa ( $[\text{H}_2]_{\text{diss}} \sim 40 \text{ mM}$ ) or in the presence of metallic iron have been carried out recently.

## 12.2. Spent fuel dissolution under reducing conditions.

The results of several published studies during the last 20 years show a large impact of the presence of dissolved hydrogen (added or produced in situ by anoxic corrosion of Fe) in suppressing effectively the radiolytic fuel oxidation/dissolution process. For this reason, these tests are referred to as tests carried out under "reducing conditions". As will be discussed below, the reducing conditions do not refer to the redox potential of the bulk solution, rather to complex interfacial phenomena occurring at the very surface of the spent fuel or  $\alpha$ -emitting actinide oxide surfaces.

It is therefore important to present arguments in support of a fuel oxidative dissolution below detection limit from various studies of fuel leaching with  $[\text{H}_2] > 0.8 \text{ mM}$  or in presence of Fe(s) and from similar tests with  $\alpha$ -doped  $\text{UO}_2$ . Such arguments are:

Instead of increasing as in the case of oxidative fuel dissolution, the concentrations of U, Pu, Np and other redox sensitive nuclides usually decrease during the first samplings. In all published fuel dissolution tests in dilute carbonate solutions, including MOX fuel which has a much stronger alpha field (Spahiu et al. 2000, Albinsson et al. 2003, Ollila et al. 2003, Spahiu et al. 2004, Carbol et al. 2005, Carbol et al. 2009, Fors et al.

### 3.1.1 Spent Nuclear Fuel; State-of-Knowledge

2009, Ekeroth et al. 2020, Puranen et al. 2020) the concentration of U decreases in the first days to weeks. Similar behavior is observed in 5 M NaCl solutions (Loida et al. 2001, Loida et al. 2005, Carbol et al 2005) or in high pH solutions (Loida et al. 2012). Given the relatively low initial concentrations, this decrease is due to the reduction by hydrogen of the oxidized forms present in an initial pre-oxidized fuel surface layer. An acidification of the solution, which accompanies uranyl reduction by H<sub>2</sub> was observed in un-buffered 5 M NaCl solutions (Loida et al. 2001, Carbol et al. 2005). Then the U levels remain constant for months to years near  $3 \times 10^{-9}$  M, that coincides very well with the solubility of UO<sub>2</sub>(am) (Guillamont et al. 2003) (see Figure 6, left). As discussed by Ekeroth et al. (2020), this rules out any presence of U(VI) solid phases. At the same time, this low U levels indicate complete absence of radiolytic oxidants (O<sub>2</sub>, H<sub>2</sub>O<sub>2</sub>), given the extreme ease with which they oxidize U(IV) at near neutral pH (Baker and Newton 1961, Newton 1975, Elliot et al. 1986) resulting in a fast increase by orders of magnitude of the U concentration.

The same holds for Np and Pu, which are present at levels even lower than the solubilities of their corresponding tetravalent oxides (Cui et al. 2008, Fors et al. 2009, Ekeroth et al. 2020, Puranen et al. 2020). This suggests that co-precipitation of neptunium and plutonium with uranium may have occurred, producing a solid solution with actinide content U:Pu:Np  $\sim 1:10^{-2}:10^{-3}$ , i.e. as their inventory in spent fuel or in the solution before reductive precipitation.

A decrease of the molybdate level, a stable tetrahedral oxo-anion, was observed only in the tests with MOX fuel (Carbol et al. 2005) or in the presence of metallic Fe (Albinsson et al. 2003, Puranen et al. 2020).

This reductive precipitation of U(VI) and other nuclides from the pre-oxidized layer apparently occurs on the fuel surface itself, since very low levels of radionuclides were found in the vessel rinse (Albinsson et al. 2003). More than 99% of the uranium was precipitated on the surface of the spent fuel itself (Ollila et al. 2003).

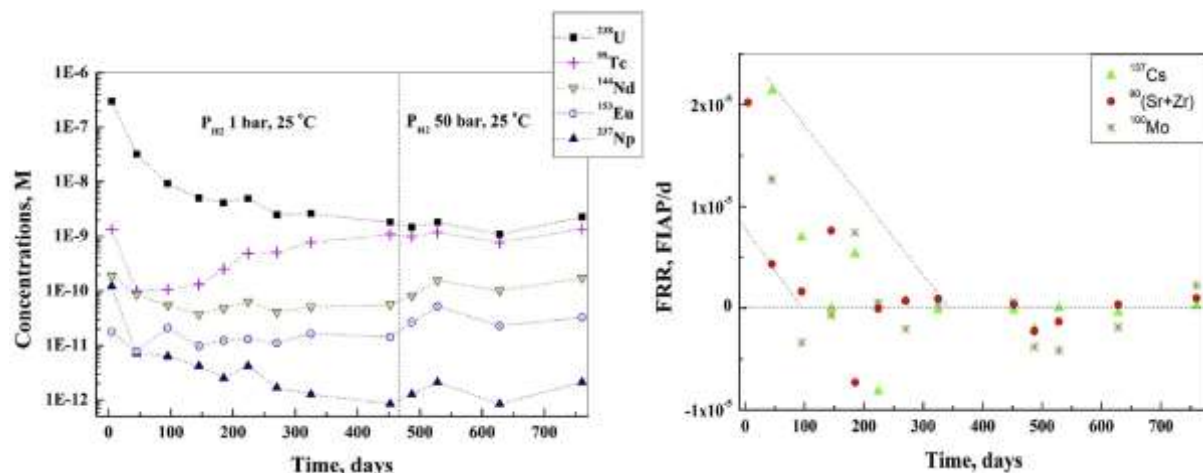


Figure 6: Evolution of concentrations of actinides, lanthanides and Tc (left) and fractional release rates (right) during fuel powder (0.25-0.5 mm) leaching under 1 bar H<sub>2</sub>, 25 °C. Ekeroth et al. 2020.

Another indication of negligible U(VI) levels in bulk solution comes from tests of fuel leaching in the presence of metallic iron (Grambow et al. 1996a, Carbol et al 2005, Puranen et al. 2017, Puranen et al. 2020). It is well known that U(VI) is reduced to U(IV) and sorbed or precipitated on the surface of metallic iron, both from studies on ZVI (Zero Valent Iron) barriers (Fiedor et al. 1998, Gu et al. 1998, Farrell et al. 1999, Morrison et al. 2001) and in our field (Grambow et al. 1996b, Cui and Spahiu 2002). Under anoxic conditions, magnetite reduces U(VI) to U(IV) (Scott et al. 2005), while green rust on iron surfaces precipitates UO<sub>2</sub>(s) (Cui and Spahiu 2002). Thus, if U(VI) would be present in solution due to oxidative fuel dissolution, it would get reduced and precipitate on the iron surface. During the co-dissolution of fuel and iron, both oxidants and U(VI) were scavenged on the fuel surface and very little, if at all, on the iron surface. No accumulation of U on iron was reported in these tests, only U levels corresponding to adsorption of U(IV) on iron corrosion products (Grambow et al. 1996a, Carbol et al. 2005, Puranen et al. 2020, Odorowski et al. 2017).

The reductive capacity of the fuel surface under such conditions can be estimated best by tests carried out at KIT-INE, adding 0.1 or 1 mM Br to the 5 M NaCl solutions in the presence of various amounts of dissolved hydrogen (Metz et al. 2007, Loida et al. 2007). Bromide is a known OH-radical scavenger, which reacts with

### 3.1.1 Spent Nuclear Fuel; State-of-Knowledge

the OH-radical about 250 times faster than molecular hydrogen (Zehavi and Rabani 1972) and cancels any beneficial effect of molecular hydrogen in bulk solution, even under radical rich  $\beta$ ,  $\gamma$ -radiations. Separate tests in 5 M NaCl solutions with added bromide in presence of  $H_2$  showed extensive production of molecular radiolytic oxidants under external  $\gamma$ -radiation and the oxidation of an added  $UO_2$  pellet (Metz et al. 2007). However, in tests with spent fuel in Br-containing solutions, where the intrinsic  $\gamma$ -radiation has apparently created the same oxidizing conditions in the bulk solution, the measurements show absence of molecular oxidants in the autoclave, as well as low and decreasing concentrations of U or Pu (Loida et al. 2007). In this case, only surface mediated processes can be responsible for the consumption of the molecular oxidants produced near the fuel surface by  $\alpha$ -radiation and in the bulk solution by intrinsic  $\gamma$ - or  $\beta$ -radiation.

Besides the absence of U(VI) in bulk solution, *the oxidation state of the solid surface* has been analyzed with various methods in some studies. An electrochemical study indicated irreversible reduction of  $UO_2$  electrode surfaces in the presence of  $\gamma$ -radiation and 50 bar  $H_2$  (King et al. 1999). A reduction of the  $UO_2$  surface placed at 30  $\mu m$  distance from an alpha source in presence of  $H_2$  bubbling was observed at 100 °C, while surface oxidation was observed by XPS (X-ray Photoelectron Spectroscopy) under Ar atmosphere (Sunder et al. 1990). The thermal activation of hydrogen at 100 °C cannot be ruled out, but similar XPS results were recently obtained at room temperature (Hansson et al. 2021). XPS studies of the spent fuel surface before and after leaching under 1 bar  $H_2$  indicate a partially oxidized surface before start and a completely reduced surface after the test (Ekeroth et al. 2020). XPS analysis of a 10%  $^{233}U$  doped pellet after long-term leaching under  $H_2$  showed a fully reduced ( $UO_{2.00}$ ) surface (Carbol et al. 2009b).

Even though the increase of U levels due to U(VI) formation is the best indicator of oxidative dissolution, the presence of non-redox-sensitive fission products in real fuel, such as Sr and Cs, make it possible to judge on fuel dissolution rate via their releases. A systematic reduction by more than two orders of magnitude of the released fraction of Sr or Cs during successive time intervals is observed and alternative intervals with positive and negative rates result after only a few weeks (Ekeroth et al. 2020) (see Figure 6, right). The same trend was observed in experiments lasting over one-year in the presence of a hydrogen atmosphere (Carbol et al. 2005, Puranen et al. 2020) and only at very long leaching times Cs or Sr releases are below detection limit (Spahiu 2002, Carbol et al. 2005, Cui et al. 2008). It should be kept in mind that extremely low levels of radionuclides are analysed in these tests, e.g., the  $^{90}Sr$  concentration during more than one-year long tests under hydrogen varied between 0.15-0.23 ppb (Spahiu et al. 2004), an amount which is less than the amount of  $^{90}Sr$  in a monolayer of fuel. The case of some tests carried out with a whole clad fuel pellet, where a continuous release of Cs and Sr was observed together with decreasing U levels is discussed in (Ekeroth et al. 2020). There are much more radionuclide data which could be used as proof of negligible matrix dissolution in  $H_2$  tests, such as the extremely low and constant concentrations of the lanthanides or components of the metallic particles (Ekeroth et al. 2020). As recognised by Shoesmith (2013), commonly no corrosion (oxidative dissolution) rates can be measured in presence of  $H_2$ .

## 13. ALPHA DOPED $UO_2$ LEACHING UNDER ANOXIC AND REDUCING CONDITIONS.

The majority of the spent nuclear fuel in a geologic repository is not expected to be exposed to groundwater before storage times of the order of a thousand years have elapsed. As discussed in section 7, already after a few hundred years of storage,  $\alpha$ -radiation will dominate the radiation field of the spent nuclear fuel. In order to mimic the radiation field of a few thousand-year-old fuel,  $UO_2$  containing different fractions of short-lived  $\alpha$ -emitters, the so-called  *$\alpha$ -doped  $UO_2$* , can be used to study the effects of  $\alpha$ -radiolysis on the corrosion behaviour of aged spent fuel exposed to groundwater in a geologic repository. Usually, the doping level is reported as content of the  $\alpha$ -emitter (wt%  $^{233}U$ ) or as specific activity (MBq/g). By using the calculated activity decay in the spent fuel of a certain burn-up with time,  $\alpha$ -doped samples are also referred to as “3000 y old fuel”, equivalent to 33 MBq/g or 10wt%  $^{233}U$ . It should be kept in mind that  $\alpha$ -doped  $UO_2$  does not simulate the composition and structure of the spent fuel, only the radiation field.

#### 13.1. Anoxic conditions and old fuel -Threshold of specific $\alpha$ -activity.

The results of the static batch experiments under Ar flushing (Rondinella et al. 2004) in carbonate-containing solutions indicated that  $\alpha$ -radiolysis enhances uranium dissolution for pellets doped with 10wt%  $^{233}\text{U}$ , while in the case of lower doping levels such as 1wt%  $^{233}\text{U}$ , corresponding to 3.3 MBq/g, it is difficult to observe any effect of the  $\alpha$ -radiolysis on the increase of the U concentrations with time. The  $\alpha$ -radiolysis of a few tens of microns thick water layer near the  $\text{UO}_2$  surface is expected to produce mainly molecular radiolytic products as  $\text{H}_2\text{O}_2$  and hydrogen (Spinks and Woods 1990). As already discussed, U(IV) ions in solution or in the  $\text{UO}_2$  solid are oxidized very quickly by traces of oxidants such as  $\text{H}_2\text{O}_2$  and  $\text{O}_2$  (Baker and Newton 1961, Newton 1975, Elliot et al. 1986). Any oxidized U(VI) contributes to the increase of U concentrations due to the presence of bicarbonate ions, which form strong complexes with U(VI). In spite of the relatively sensitive measurement methods for low uranium concentrations and the absence of any other reductants than radiolytic  $\text{H}_2$ , no detectable increases were observed during the whole duration of the experiment (Rondinella et al. 2004). The authors proposed a *threshold of  $\alpha$ -activity* between 3.3 and 33 MBq/g, below which no effect of  $\alpha$ -radiolysis could be observed. The results of Muzeau et al. (2009) with  $^{238}\text{Pu}$ -doped pellets of specific alpha activity 18 MBq/g were similar, and the authors proposed this new specific activity level as the lower limit for detecting  $\alpha$ -radiolysis enhanced dissolution.

#### 13.2. Alpha doped $\text{UO}_2$ leaching under reducing conditions.

The tests carried out by Ollila (2006) indicate clearly that the presence of a small amount of sulphide and strict anoxic conditions are sufficient to cancel any oxidising effect due to  $\alpha$ -radiolysis from a few thousand-year-old fuel. In most tests with  $^{233}\text{U}$ -doped  $\text{UO}_2$  (0, 5 and 10wt%) under reducing (Fe(s) presence) conditions, very low total uranium concentrations were measured ( $<10^{-10}$  M). The results showed no evidence for enhanced dissolution of samples containing  $^{233}\text{U}$  over those that contained only normal levels of  $^{235}\text{U}$  and  $^{238}\text{U}$  (Ollila et al. 2003, Ollila and Oversby 2006). The experiments were thoroughly analysed for the location of precipitated uranium. Negligible amounts were found on the corroding iron (Ollila and Oversby 2005). The release of  $^{238}\text{U}$  from the samples, especially during the first year or so of testing, appeared to be dominated either by high energy surface sites formed by crushing of the samples or by high-energy interior sites at grain boundaries or associated with crystal imperfections. According to Grambow et al. (2017), the observed continuous isotopic exchange on  $\text{UO}_2$  surfaces despite solubility equilibrium (Ollila, 2008) cannot be used as proof that there is a significant solid-state transformation despite  $\text{UO}_2$  saturation, as it may only involve restructuration of a few surface sites on  $\text{UO}_2$ , given that less than a mono-layer is involved in this exchange.

During the EC-project [SFS](#), three tests with 10wt%  $^{233}\text{U}$  doped  $\text{UO}_2$  were carried out under various hydrogen concentrations (Carbol et al. 2005). In the autoclave experiment with a 10%  $^{233}\text{U}$  doped pellet extremely low U concentrations were measured, even when  $\text{H}_2$  was substituted with Ar, while XPS analysis of the pellet surface after test indicated  $\text{UO}_{2.00}$  (Carbol et al. 2009b). In spite of these results, a clear observation of any influence of hydrogen is complicated by the very limited effects of  $\alpha$ -radiolysis, even for pellets doped with 10wt%  $^{233}\text{U}$  (Rondinella et al. 2004), see previous section on threshold of  $\alpha$ -activity.

A  $\text{UO}_2$  pellet with a much higher doping level (385 MBq/g corresponding to 50 years old fuel) was tested by Muzeau et al. (2009), and a very clear effect of  $\alpha$ -radiolysis was observed under Ar atmosphere, with U concentrations increasing quickly with time in carbonate solutions. The same system, tested under a 1 bar  $\text{H}_2$  atmosphere, showed a slight decrease, not increase, of U concentrations. Recently Odorowski et al. (2017) tested the same highly doped pellets (385 MBq/g) in Callovo-Oxfordian simulated groundwater and in the presence of metallic Fe foil under Ar atmosphere from start. The results of the more than one year test showed very low uranium concentrations in solution ( $4 \times 10^{-10}$  –  $4 \times 10^{-9}$  M), corresponding to the solubility of  $\text{UO}_2 \cdot x\text{H}_2\text{O}$ . The analysis of the uranium sorbed or precipitated during the test through autoclave and iron foil acid stripping indicated that very little total U was released during the whole test ( $\sim 10 \mu\text{mol}$ ). Most of it was sorbed on the Ti walls of the autoclave (7.6  $\mu\text{mol}$ ), corresponding to the calculated values with  $K_d$  for sorption of U(IV) on  $\text{TiO}_2$ . The authors conclude that Fe(II) produced by iron corrosion completely cancels the oxidative dissolution of the highly doped pellets. In her Ph. D. thesis, Odorowski (2015) reports similar data for the leaching of an unirradiated MOX pellet with alpha activity  $1.3 \times 10^9$  Bq/g, i.e., with a very high alpha dose rate, in the presence of an iron foil. The strong effect of

### 3.1.1 Spent Nuclear Fuel; State-of-Knowledge

Fe(II) in these tests is probably due to formation of hydroxo-carbonates as Fe corrosion products, not magnetite, leading to high Fe(II) concentrations ( $10^{-4}$ - $10^{-3}$  M) in solution. The same unirradiated MOX pellet dissolved relatively fast in air or Ar atmosphere (Odorowski et al. 2016).

During surface catalytic decomposition,  $H_2O_2$  is split in a first step into two OH-radicals adsorbed at the surface (Hiroki and LaVerne 2005). Further reaction of OH-radicals with  $H_2O_2$  produces the peroxide radical  $HOO\cdot$  and water. Finally, two peroxide radicals give  $H_2O_2$  and  $O_2$ , with an overall stoichiometric reaction  $H_2O_2 = H_2O + \frac{1}{2} O_2$ . The similarity of the constants for the reactions in bulk solution:



makes it possible for hydrogen present in solution to react with the surface bound hydroxyl radicals according to reaction (2). Using deuterium ( $D_2$ ) as a tracer of reaction (2), Bauhn et al. (2018a, b) showed that HDO was indeed produced both on a SIMFUEL surface and  $\alpha$ -doped  $UO_2$ , supporting the conclusion that a large part of radiolytic  $H_2O_2$ , instead of oxidizing uranium, reacts with the hydrogen in the system to give water.

## 14. FUEL DISSOLUTION RATES UNDER REDUCING CONDITIONS.

From this discussion of the experimental data presented above, it is evident that the choice of a rate for fuel dissolution is not simple. First, it is important to keep in mind that  $UO_2(s)$  can dissolve in absence of oxidants and release U(IV) ions (green in solution), or undergo oxidative dissolution (corrosion) in presence of oxidants and release uranyl ions ( $UO_2^{2+}$ , yellow in solution). The non-oxidative (or chemical) dissolution continues from the time of water contact until the concentration of U(IV) reaches the  $UO_2(s)$  solubility limit, hence is not important for the very low flow rates or quasi stationary conditions at the repository (Ekeroth et al. 2020, Grambow et al. 2010). It may become important for embedded radionuclide release only in case U(IV) is transported away adsorbed in a clay slurry (SKB 2011). Second, if a low oxidative fuel fractional dissolution rate is chosen, e.g.  $10^{-7} a^{-1}$ , the release of U(VI) and other redox sensitive species e.g. Pu(V), Tc(VII), Mo(VI) etc. should be considered in the radionuclide transport modelling.

Another factor to be considered is that it is quite difficult to determine such low rates based on accurate measurements of sub-ppb concentrations of all nuclides in tests under reducing conditions. Thus, an ICP-MS error of 20% (Röllin et al. 2001, Johnson et al. 2012, Ekeroth et al. 2020) means that in a leach test with 1 g fuel leached in 100 ml groundwater, in spite of an ideally constant U concentration of 1 ppb during one year, a dissolution rates of  $4 \times 10^{-9} a^{-1}$  can be obtained by the slope of the line passing from the lower point of the error bar for the sampling at day 1 and the higher point of the error bar of the sampling at day 365. Slight deviations from ideal constancy (1 ppb) indicate that the lowest measurable rates are of the order of  $\sim 10^{-8} a^{-1}$ . Alternatively, a dissolution rate of  $10^{-8} a^{-1}$  means that the release of the most abundant nuclide in spent fuel, U, from 2 g fuel used in a typical autoclave experiment with  $\sim 800$  ml solution, should cause an increase of U concentration of  $9.2 \times 10^{-11}$  M (or 0.023 ppb) in one year. For this reason, it seems reasonable to assume that  $10^{-8} a^{-1}$  is the lowest detectable limit of oxidative dissolution (corrosion) rate. Such low dissolution rates are not too different from a solubility limited model (Johnson 2014). As the higher limit the rate selected in the EC-project SPA ( $10^{-6} a^{-1}$ ), based mainly on experimental data obtained in the presence of various dissolved oxygen levels, may be used (Baudoin et al. 2000). If a low corrosion rate is selected, the arguments presented in the two previous sections and others, such as the decrease of the alpha field at the expected time of canister breach, should be discussed - it is not convincing to use just a number and a reference. For a discussion of parameter ranges for which the fuel matrix dissolution model is valid, see e.g. (SKB 2011, Posiva 2021). Critical  $H_2$  concentrations, which completely cancel oxidative fuel dissolution are above 0.8 mM for fresh fuel (Ekeroth et al. 2020). Critical  $H_2$  concentrations as a function of fuel age can be found in (Trummer and Jonsson 2010, Liu et al. 2016).

The influence of hydrogen is successfully modelled (see section 15) based on  $H_2$  catalysis on  $\epsilon$ -particles of spent fuel, while a mechanism for the threshold of alpha activity is not yet available. Such a mechanism, based e.g., on oxygen vacancies created on fuel surface by  $\alpha$ -recoil atoms, as suggested in (Carbol et al. 2005, Cui et al. 2008, Shoesmith 2013), would be very valuable to confirm by tests or modelling. The results of Bauhn et al. (2018a, b) indicate consumption of a large part of radiolytic  $H_2O_2$  by hydrogen and by

### 3.1.1 Spent Nuclear Fuel; State-of-Knowledge

catalytic decomposition at the fuel surface to water and oxygen, which is a much slower oxidant. It should be kept in mind that the  $\alpha$ -doped pellets in the real case (old fuel) will contain metallic  $\epsilon$ -particles.

## 15. POTENTIAL CATALYST (E-PARTICLE) POISONING.

Due to their high content of noble metals,  $\epsilon$ -particles are resistant to water corrosion. The release of the various metal components under oxidative leaching was reported to be proportional to the metal's oxidation potentials, i.e. Mo>Tc>Ru>Rh>Pd (Cui et al. 2001), while no releases could be observed under 1 bar H<sub>2</sub> (Ekeröth et al. 2020).

It is well known that noble metal catalysts, such as e.g., Pd, are *poisoned* by sulphide ions of the groundwater, which form strong surface complexes with the metal surface (Chaplin et al. 2012, Angeles-Welder et al. 2010). The effect of sulphide ions on radiation-induced dissolution of spent fuel has been investigated by the use of simplified model systems (Yang et al. 2013). The reaction between sulphide and H<sub>2</sub>O<sub>2</sub> is rapid; and 3 to 4 H<sub>2</sub>O<sub>2</sub> molecules are consumed per oxidized sulphide. Experiments with  $\gamma$ -radiolysis in the presence of sulphide show that release of radiolytically oxidized uranium decreases with the concentration of sulphide in solution. Sulphide also reduces uranium (VI) in anoxic solutions (Hua et al. 2006). No poisoning of the palladium catalyst could be detected in the presence of relatively high concentrations of sulphide (1 mM). According to Yang et al. (2013), this is due to the high concentration of dissolved hydrogen, which causes desorption of sulphide from the Pd surface.

The fact that sulphide reacts quickly with H<sub>2</sub>O<sub>2</sub> also means that the small quantities of sulphide ions that may remain in the groundwater after its contact with copper and/or iron surfaces of the canister cannot reach the fuel surface as long as it is producing H<sub>2</sub>O<sub>2</sub>. This is the case assumed in a model with an oxidative dissolution rate in the interval 10<sup>-8</sup> to 10<sup>-6</sup>/year. However, most of the experimental data show no evidence of oxidative dissolution and in case all peroxide and other radiolytic oxidants are neutralized by hydrogen, sulphide ions can reach the fuel surface, thus poisoning  $\epsilon$ -particles by building a Pd-sulphide layer. Extensive sulphide-arsenide corrosion has been observed in metallic particles from the Oklo site in Gabon (Utsonomiya and Ewing 2006), which occurred probably after radioactivity decay. Further, H<sub>2</sub>O<sub>2</sub> or hypochlorite are used to regenerate Pd-catalysts poisoned by sulphide in industrial practice (Schüth et al. 2004, Wang et al. 2004, Munakata and Reinard 2007, Chen and Huang 2013). In case the radiation field of spent fuel is still high and some sulphide poisoning of the  $\epsilon$ -particles occurs, and if no other mechanisms contribute to hydrogen activation, the produced radiolytic oxidants should create oxidizing conditions at the surface. This implies that all sulphide will be consumed by H<sub>2</sub>O<sub>2</sub> and the catalyst surface will be regenerated.

## 16. FUEL DISSOLUTION MODELLING

Since the first studies of spent fuel dissolution, efforts to model the radiolytically promoted fuel dissolution in more or less detailed mechanistic approaches were also undertaken. The driving force is the required mechanistic understanding of the radionuclide release processes in the applications for licensing SNF disposals. A short description of the published and most frequently used mechanistic models will be given in this section; more details can be found in e.g. Eriksen et al. 2012, Roth and Jonsson 2008, Carbol et al. 2020, Grambow 2021.

The development of a radiolytic model for fuel dissolution needs to consider radiolytic oxidant production, homogeneous reactions in bulk solution, diffusive transport and heterogeneous reactions on the fuel surface. The homogeneous water radiolysis caused by  $\alpha$ -,  $\beta$ - and  $\gamma$ - radiation is a thoroughly investigated field, due to the needs of nuclear industry. High quality databases with experimental values for reaction rates between various radiolytic species and the radiolytic yields (or G-values) exist, as well as computer programs such as Maxima Chemist (Carver et al. 1996) and Chemsimul (Kirkegaard et al. 2008), which basically solve a system of differential equations of the type  $dC_i/dt = k C_i$  and calculate the concentrations of all species  $i$  as a function of time. The dose rate emitted from the fuel surface is used together with the radiolytic yields (G-values) to calculate the rate of production of all species in solution. For alpha radiolysis, sometimes an average dose rate is used to calculate the production of e.g., H<sub>2</sub>O<sub>2</sub> as:  $R = D_\alpha \times \rho_w \times G_{H_2O_2}$ , where  $D_\alpha$  is the average  $\alpha$ -dose rate,  $\rho_w$ -density of water,  $G_{H_2O_2}$ -radiolytic yield for the given species. Several works have treated the calculation of  $\alpha$ -dose rate profiles at the fuel surface using various approaches e.g., the ratio between the specific stopping power values in water and in UO<sub>2</sub> (Sunder 1994),

### 3.1.1 Spent Nuclear Fuel; State-of-Knowledge

other approximations (Nielsen and Jonsson 2006), Bethe-Block equation, (Cachoir et al. 2005, Poulesquen et al. 2006), as well as SRIM and ASTAR stopping power databases (Hansson et al. 2020).

In the first fuel models (Christensen et al 1994, Christensen 1998), given the absence of kinetic data for fuel surface reactions with oxidants, it was assumed that the first layer of fuel in contact with water was dissolved, in order to use kinetic equations for homogeneous reactions in the model. Reactions involving both radical and molecular species with the first fuel layer, based on available data for oxidation of other metal ions than U were used and the constants were adjusted based on electrochemical data for  $\text{UO}_2$  oxidation and dissolution. Similar homogeneous kinetics for the reaction of the first fuel layer was assumed in the models of Kelm and Bohnert (2004), Traramo (Lundström 2003) and Poulesquen et al. (2006).

The Matrix alteration model (MAM) was developed during the [SFS](#), [NF-PRO](#) and [MICADO](#) EC-projects by Amphos21, CIEMAT and ENRESA, considering water radiolysis and the kinetics of fuel oxidation by molecular and radical species, as well as dissolution reactions for surface species (Merino et al. 2005). By expressing the concentration of surface species as the product of surface site density (Clarens et al. 2004) and surface to volume ratio, homogeneous kinetics codes could be used (Quinones et al. 2006). The constants were derived by calibrating the multistep oxidation-surface complexation-dissolution mechanism with experimental data on  $\text{UO}_2$  dissolution (de Pablo et al. 2004, de Pablo et al. 1999, Bruno et al. 1991). The model was applied on  $\alpha$ -doped  $\text{UO}_2$  and spent fuel dissolution (Merino et al. 2005, Riba et al. 2020). The effect of hydrogen on spent fuel dissolution rates by  $\epsilon$ -particle catalysis was also included (Duro et al. 2013).

The model of SUBATECH (Grambow et al. 2011) considers water radiolysis and diffusion of radiolytic species with the radiolytic transport code Traramo (Lundström 2003), as well as dose gradients at the fuel surface. The water radiolysis model and electrochemical surface reactions are coupled. The effect of  $\text{H}_2$  is described by an effect on the corrosion potential.

The Fuel Matrix Dissolution Model (FMDM) is an electrochemical reaction/diffusion model (Jerden et al. 2015), based on previous mixed potential models (King and Kolar 1999, Shoesmith et al. 2003), but has included  $\epsilon$ -particles on the fuel surface, which catalyse both reactions with oxidants and with hydrogen. Account is taken for the change in threshold for oxidative dissolution with pH and the model accounts also for temperature influence, precipitates on the fuel surface, etc..

The steady state model was developed by KTH (Royal Institute of Technology, Stockholm) group (Jonsson et al. 2007, Roth and Jonsson 2008) and it is called so because in a system with constant radiation dose rate, the concentrations of the oxidants at the surface reach relatively fast (seconds to minutes) a steady state. This occurs when the rate of oxidant production by radiolysis equals that of oxidant consumption by fuel oxidation. This group introduced the study of the heterogeneous kinetics by determining elementary oxidation rate constants (section 11), but also kinetic constants for other important interfacial reaction rates, especially these occurring on  $\epsilon$ -particles (simulated by Pd), such as the reaction of  $\text{H}_2$  with  $\text{H}_2\text{O}_2$  (Nilsson and Jonsson 2008a) or  $\text{H}_2$  with  $\text{U(VI)}$  in solution (Nilsson and Jonsson 2008b). However, the main effect from the presence of  $\epsilon$ -particles and  $\text{H}_2$  was found to be solid phase reduction of oxidized  $\text{UO}_2$  on the surface of the spent nuclear fuel. Electrochemical measurements of very low corrosion potentials for SIMFUEL electrodes in presence of hydrogen (Broczkowski et al. 2005) indicate that the  $\epsilon$ -particles are galvanically coupled to the  $\text{UO}_2$  matrix. Studies of the catalytic effect of pure Pd-particles on the reaction between  $\text{H}_2\text{O}_2$  and  $\text{H}_2$  had shown that the second order rate constant with respect to  $\text{H}_2\text{O}_2$  and Pd is virtually diffusion controlled (i.e.very fast) for  $\text{H}_2$  pressures higher than 1 bar (Nilsson and Jonsson 2008a) (see Figure 7). The efficiency and dynamics of the solid phase reduction process was confirmed in experiments using  $\text{UO}_2$  pellets doped with Pd particles (Trummer et al. 2008, 2009) and in long-term fuel leaching

### 3.1.1 Spent Nuclear Fuel; State-of-Knowledge

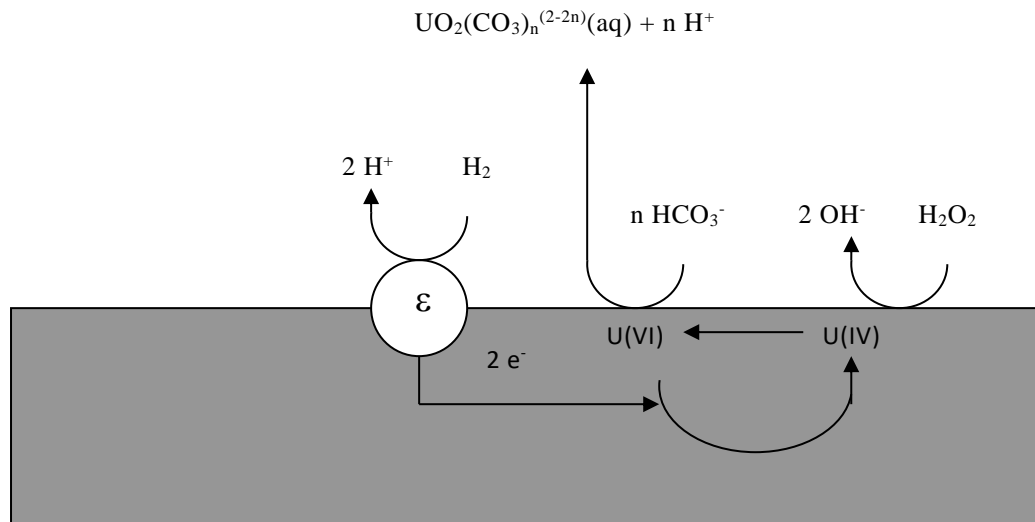


Figure 7: Elementary processes for fuel dissolution by radiolytic oxidants in presence of H<sub>2</sub>. From Eriksen et al. 2008.

experiments in sealed glass ampoules (Cera et al. 2006, Eriksen et al. 2008), which indicate that the rate of fuel dissolution approaches zero when the concentration of radiolytically produced H<sub>2</sub> is in the range of 10<sup>-5</sup> to 10<sup>-4</sup> mol dm<sup>-3</sup>. The influence of Fe(II) in bulk solution was introduced by considering an appropriate function of the rate constant that reduces the H<sub>2</sub>O<sub>2</sub> concentration at the fuel surface, estimated from simulations (Nielsen et al. 2008). The model considers water radiolysis, diffusion of species and heterogeneous kinetics at the spent fuel surface, considering that only H<sub>2</sub>O<sub>2</sub> production leads to spent fuel oxidation, since its contribution is ~ 99.9% of the total (Ekeroth et al. 2006). All oxidized spent fuel is considered to be dissolved for [HCO<sub>3</sub><sup>-</sup>] > 1 mM. The model predicts that only 0.1 bar H<sub>2</sub> will effectively inhibit the dissolution of the spent fuel aged 100 years or more, while in the presence of 1 μM Fe<sup>2+</sup>, even 0.01 bar H<sub>2</sub> will be sufficient to stop oxidative fuel dissolution (Jonson et al. 2007).

The model of UWO (University of Western Ontario, Canada) first used a one-dimensional model with diffusion-reaction expressions solved numerically by finite element methods (Wu et al. 2012). It took into account the α-radiolysis of water, the reaction of H<sub>2</sub>O<sub>2</sub> with UO<sub>2</sub> (see right hand part of Figure 7), selecting a high constant to compensate for the galvanic coupling with noble metal particles, the reaction with H<sub>2</sub> via galvanic coupling (electrons from H<sub>2</sub> catalysed on ε-particles reduce U atoms oxidized by H<sub>2</sub>O<sub>2</sub>, which otherwise would be released as soluble uranyl carbonate complexes), and the consumption of H<sub>2</sub>O<sub>2</sub> by Fe(II) in bulk solution. The dominant redox control agent was found to be H<sub>2</sub>. Later, (Wu et al. 2014a) considered a full α-radiolysis scheme (instead of only H<sub>2</sub>O<sub>2</sub>) and reaction-diffusion expressions were solved for a two-dimensional model. The interaction of H<sub>2</sub>O<sub>2</sub> with metallic particles was introduced explicitly. The 2-D model was used also to model corrosion in fuel fractures (Wu et al. 2014b). Liu et al. (2016) modified the 2-D model to determine the separate effects of radiolytic H<sub>2</sub> (internal to a fracture) from that produced by iron corrosion (external) on the suppression of spent fuel corrosion for different fracture geometries, α-radiation dose rates and concentrations of external H<sub>2</sub>. Later, the model was successfully tested with experimental data on α-doped UO<sub>2</sub> dissolution and investigated also the influence of oxygen from H<sub>2</sub>O<sub>2</sub> decomposition and radiolytic H<sub>2</sub> accumulation in a closed system on fuel dissolution (Liu et al. 2017c).

Mechanistic models attempt normally to describe the results of individual dissolution experiments using UO<sub>2</sub> or SIMFUEL and external α- or γ-irradiation, α-doped UO<sub>2</sub> or spent fuel. The simpler radionuclide release models for spent nuclear fuel, applied by the waste management organisations in their safety assessment codes to calculate radionuclide release from a breached canister in the repository select a fractional release rate interval for the fuel, based on the analysis of all available data for the given repository conditions and discuss also for which environmental parameter ranges the model is valid. The cases of irregular fuel (fuel damaged in reactor, fuel residues, experimental reactor fuel, etc.) are handled separately. In these radionuclide release models, the IRF as percent of the total inventory is estimated and is released immediately upon water contact. Usually, fractional release rates for activation products from metallic parts of fuel assemblies as the metals corrode are also estimated based on available corrosion

### 3.1.1 Spent Nuclear Fuel; State-of-Knowledge

data. Examples of safety assessment release models estimating: (1) release of activation products from Zircaloy and other metal parts of the fuel assemblies through corrosion, (2) IRF (Instant Release Fraction) for all relevant nuclides and (3) fuel matrix fractional dissolution rate, can be found in Johnson (2014), Werme et al. (2004) (only IRF and matrix dissolution) or Posiva source term report (Posiva 2021).

## 17. LONG-TIME STRUCTURAL STABILITY OF THE FUEL MATRIX.

The time at which the fuel will contact water is estimated to be in the range of thousands to millions of years after disposal. The effects of radioactive decay, mainly alpha decay and build-up of helium could possibly change the microstructure of the fuel over these long time periods. During long term storage in the repository as long as the canister is not breached, no consequences of radiation damage are expected in this mixed oxide waste form (Matzke 1982). This is because both component oxides ( $\text{UO}_2$ ,  $\text{PuO}_2$ ) in MOX or  $\text{UO}_2$  fuel are of the fluorite type structure, which are not susceptible to radiation induced amorphization (at least for temperatures above 5 K for  $\text{UO}_2$ ) (Weber et al. 1998). This is an enormous advantage of the high symmetry of the fluorite structures, which usually have less than 1% swelling, an increase of the lattice parameter (up to 0.6%) and an increase of Vickers hardness due to radiation damage (Wiss et al 2014), but do not become amorphous even for relatively high dpa (displacement per atom) values.

Alpha Self Irradiation Enhanced Diffusion (ASIED), similar to athermal diffusion observed in the reactor caused by fission fragments, was suggested in the beginning of 2000 to cause mobility of fission products in the long term. Various models were proposed to estimate this alpha self-irradiation enhanced diffusion (Ferry et al. 2005). An upper estimate was based on the extrapolation of the measured athermal diffusion coefficient of uranium atoms during reactor operation by assuming proportionality of the diffusion coefficient ( $D_\alpha$ ,  $\text{m}^2/\text{s}$ ) with the alpha activity per volume ( $A_\alpha$ ,  $\text{Bq}/\text{m}^3$ ). Further research showed that this effect was negligible. Ferry et al. (2008) describe an experimental study where heavy ion bombardment of iodine implanted  $\text{UO}_2$  was used to simulate the effect of alpha irradiation on iodine mobility in  $\text{UO}_2$  fuel. No measurable displacement of iodine could be detected (less than 50 nm), which is consistent with a diffusion coefficient of about  $10^{-28}$   $\text{m}^2/\text{s}$ . Ferry et al. (2008) concluded that the athermal diffusion process would make a negligible contribution to the IRF. They stated: "Based on theoretical models supported by experiments simulating  $\alpha$ -decay effects on atom mobility in spent fuel, the release of fission products to grain-boundaries should not be significant even on the long-term". These conclusions are supported also by the modelling works of Van Brutzel and Crocombette (2007) and Martin et al. (2009).

The large number of alpha decays in spent fuel (see Figure 4) results in He atom bubbles, which start forming in conventional spent fuel after several thousand years; however, in MOX fuels, they could begin forming within 1000 years (Wiss et al., 2014). Ferry et al. (2008) analysed the effect of helium build-up in the central and intermediate zones, as well as in the rim structure of the fuel pellet. The calculated amount of helium accumulated in bubbles prior to  $10^4$  years, based on the conservative assumption that all He atoms are trapped in bubbles, is much lower than the critical values derived from rupture criteria. Using the data presented by Ferry et al. (2008), one can conclude that the helium produced by alpha-decay is not sufficient to produce micro-cracking of grains in  $\text{UO}_2$  fuel for several hundred thousand years (SKB 2010p). The operational model presented in Ferry et al (2008) was improved further (Ferry et al. 2010) concerning the calculation of the pressure in highly compressed gas and the rupture criteria. Extremely high pressures have been estimated in fission gas bubbles, where Xe has the density of the solid Xe (Thomas 1991, Nogita and Une 1998). The authors recognise that observations on He-implanted  $\text{UO}_2$ ,  $\alpha$ -doped  $\text{UO}_2$  pellets and natural analogues evidence a macroscopic damage for He concentrations that are more than an order of magnitude higher than their calculated helium critical concentrations (Ferry et al 2016).

A sample of natural uranium dioxide (pitchblende) from Pen Ar Ran mine in France was studied by (Roudil et al. 2008). The sample was 320 Ma old and had not been subjected to any single events that could have caused helium loss. The samples had retained less than 5% (2.1% on average) of the total amount of radiogenic helium formed and the damage level due to  $\alpha$ -decays was also very high (about 180 dpa). No macroscopic damage, such as opening of grain boundaries or intra-granular fractures, was observed. The authors deduced a He diffusion coefficient that is nine orders of magnitude higher than that expected in  $\text{UO}_2$  nuclear fuel. According to Ferry et al. (2010), the high release of He may be due to bubble coalescence and percolation, without creating any other damage in the material.

## REFERENCES

- Abrefah, J., de Aguiar Braid, A., Wang, W., Khalil, Y., Olander D.R., 1994. High temperature oxidation of UO<sub>2</sub> in steam-hydrogen mixtures, *J. Nucl. Mater.* 208, pp. 98 - 110.
- Adachi, T., Ohnuki, M., Yoshida, N., Sonobe, T., Kawamura, W., Takeishi, H., Gunji, K., Kimura, T., Suzuki, T., Nakahara, Y., Muromura, T., Kobayashi, Y., Okashita, H. 1990. Dissolution study of spent PWR fuel: Dissolution behavior and chemical properties of insoluble residues, *J. Nucl. Mater.* 174, p. 60-71.
- Agrenius, L. 2002. Criticality safety calculations of storage canisters, SKB Technical Report TR-02-17, Svensk Kärnbränslehantering AB.
- Agrenius, L. 2010. Criticality safety calculations of disposal canisters, SKBdoc 1193244, Version 4.0, Svensk Kärnbränslehantering AB.
- Agrenius, L., Spahiu, K. 2016. Criticality effects on long-term changes in material compositions and geometry in disposal canisters, SKB Technical Report TR-16-06, Svensk Kärnbränslehantering AB.
- Albinsson, Y., Ödegaard-Jensen, A., Oversby, V.M., Werme, L., 2003. Leaching of spent fuel under anaerobic and reducing conditions. *Mat Res Soc Symp. Proc* 757, pp. 407–413.
- Allen, A.O., 1961. *The Radiation Chemistry of Water and Aqueous Solutions*, Princeton, N.J. Van Nostrand, 1961.
- Angeles-Wedler, D., Mackenzie, K., Kopinke, F-D., 2010. Palladium-catalyzed hydrodechlorination for water remediation: catalyst deactivation and regeneration, *Int. J. Civil & Env. Eng.* 2, pp. 49-52.
- Bailly, H., Ménessier, D., Prunier, C., eds., 1999. *The nuclear fuel of pressurized water reactor and fast neutron reactors*, Lavoisier Publishing, Paris.
- Baker, F.B., Newton, T.W. 1961. The reaction of U(IV) with hydrogen peroxide. *J. Phys. Chem.* 65, pp.1897-1899.
- Baldwin, T.D., Mason, R., Hicks, T.W., 2016. Types of critical systems and the credibility of rapid transient criticality in a geological disposal facility, Galson Sciences/Amec Report No. 1541-1, version 2.1.
- Barreiro-Fidalgo, A., Jonsson M. 2019. Radiation induced dissolution of (U, Gd) O<sub>2</sub> pellets in aqueous solution - A comparison to standard UO<sub>2</sub> pellets. *J. Nucl. Mater.* 514, pp. 216-223.
- Barreiro-Fidalgo, A., Roth, O., Puranen, A., Evins, L.Z., Spahiu, K. 2020. Aqueous leaching of ADOPT and standard UO<sub>2</sub> spent nuclear fuel under H<sub>2</sub> atmosphere, *Proc. 3rd Annual Meeting EC-project Disco*, pp. 37-43.
- Baudoin, P., Gay, D., Certes, C., Serres, C., Lührmann, L., Martens, K-H., Dold, D., Mariovet, J., Vieno, T., 2000. Final report of SPA (Spent fuel disposal Performance Assessment) EC-project, EUR 19132 EN, Brussels, European Community.
- Bauhn, L., Ekberg, C., Fors, P., Spahiu, K. 2018a. The fate of hydroxyl radicals produced during H<sub>2</sub>O<sub>2</sub> decomposition on the SIMFUEL surface in the presence of dissolved hydrogen, *J. Nucl. Mater.* 507 pp. 38-43.

### 3.1.1 Spent Nuclear Fuel; State-of-Knowledge

Bahn, L., Hansson, N., Ekberg, C., Fors, P., Delville, R., Spahiu, K. 2018b. The interaction of molecular hydrogen with  $\alpha$ -radiolytic oxidants on a (U,Pu)O<sub>2</sub> surface. *J. Nucl. Mater.* 505, pp. 54-61.

Beharentz P, Hannertz K, 1978. Criticality in a spent fuel repository in wet crystalline rock, SKB report KBS-TR-108, Svensk Kärnbränslehantering.

Betova, I., Bojinov, M., Saario, T. 2012. Start-up and shut-down water chemistries in pressurized water reactors, Report VTT-R-00699-12, VTT, Finland.

Billone, M.C., Burtseva, T.A., Einziger, R.E. Ductile to brittle transition temperature for high-burnup cladding alloys exposed to simulated drying-storage conditions, *J. Nucl. Mater.* 433, pp. 431-448.

Blair, P. Romano, A., Hellwig, Ch., Chawla, R. 2006. Calculations of fission gas behaviour in high burnup structure, *J. Nucl. Mater.* 350 pp. 232-239.

Bonin, B., Colin, A., Dutfoy, A., 2000. Pressure building during early stages of gas production in a radioactive waste repository, *J. Nucl. Mater.*, 281 p. 1-14.

Bowman C D, Venneri F, 1994. Underground supercriticality from plutonium and other fissile material. LA-UR-94-4022A, Los Alamos National Laboratory. (Also published in *Science and Global Security*, 5, pp 279–320).

Bémier, S., Walker, C.T., Manzel, R., 2002. Fission gas release and fuel swelling at burn-ups higher than 50 MWd/kg U, OECD-NEA Symp. Proc. "Fission Gas Behaviour in Water Reactor Fuels", Cadarache, France, September 2000, pp. 93-106.

Broczkowski, M., Noël, J., Shoesmith, D. 2005. The inhibiting effects of hydrogen on the corrosion of uranium dioxide under nuclear waste disposal conditions. *J. Nucl. Mater.* 346, pp. 16-23.

Broczkowski, M., Zagidulin, D., Shoesmith, D.W., 2010. The role of dissolved hydrogen on the corrosion/dissolution of spent nuclear fuel, In "Nuclear Energy and the Environment", ACS Symposium Proceedings, Vol.1046, Chapter 26, pp. 349-380.

Brunauer, S., Emmett, P., Teller, E. 1938. Adsorption of gases in multimolecular layers, *J. Am. Chem. Soc.* 60, pp. 309-319.

Bruno, J., Casas, I., Puigdomenech, I. 1991. The kinetics of dissolution of UO<sub>2</sub> under reducing conditions and the influence of an oxidized surface layer, *Geochim. Cosmochim. Acta*, 55, pp. 647-658.

Bryan, C.R., Durbin, S.G., Lindgren, E., Ilgen, A.G., Montoya, T.J., Dewers, T., Fascitelli, D. 2019. SNL contribution: Consequence analysis for moisture remaining in dry storage canisters after drying, Report SAND2019-8532 R, Sandia National Laboratory, USA.

Buck, E.C., Mausolf, E.J., McNamara, B.K., Soderquist, C.Z., Schwantes J.M. 2015. Nanostructure of metallic particles in light water reactor used nuclear fuel. *J. Nucl. Mater.* 461 pp. 236-243.

Cachoir, C., Glatz, J-P., Grambow, B., Lemmens, K., Martínez-Esparza, A., Mennecart, T., Rondinella, V., Spahiu, K., Wegen, D. 2005. Effect of alpha irradiation field on long term corrosion rates of spent fuel. ITU Report JRC-ITU-SCA-2005/01, Institute for Transuranium Elements, Karlsruhe.

Carbol, P., Cobos-Sabate, J., Glatz, J-P., Grambow, B., Kienzler, B., Loida, A., Martinez-Esparza, A., Metz, V., Quiñones, J., Ronchi, C., Rondinella, V., Spahiu, K. (Eds), Wegen, D.H., Wiss, T. 2005. The effect of dissolved hydrogen on the dissolution of 233U doped

### 3.1.1 Spent Nuclear Fuel; State-of-Knowledge

UO<sub>2</sub>(s), high burn-up spent fuel and MOX fuel. SKB TR-05-09, Svensk Kärnbränslehantering AB.

Carbol, P., Fors P, Gouder T, Spahiu K, 2009b. Hydrogen suppresses nuclear waste corrosion, *Geochim. Cosmochim. Acta* 73, pp. 4366-4375.

Carbol, P., Fors, P., Van Winckel, S., Spahiu, K. 2009a. Corrosion of irradiated MOX fuel in presence of dissolved H<sub>2</sub>. *J. Nucl. Mater.* 392, 45–54. <https://doi.org/10.1016/j.jnucmat.2009.03.044>.

Carbol, P., Wegen, D.H., Wiss, T., Fors, P., Jegou, C., Spahiu, K. 2020, Spent fuel as waste material, Chapter 6.13, pp. 347-386 in “Comprehensive Nuclear Materials” Eds. in chief Konings R.J.M, Stoller R.E., Elsevier, <https://doi.org/10.1016/B978-0-12-803581-8.10374-1>.

Carver M.B., Hanley D.V., and Chaplin K.R., 1979. Maksima-Chemist: A Program for Mass Action Kinetics Simulation by Automatic Chemical Equation Manipulation and Automatic Integration Using Stiff Techniques,” AECL-6413, Atomic Energy of Canada Ltd.

Casella, A., Hanson. B., Miller, W., 2012. The effect of fuel chemistry on UO<sub>2</sub> dissolution. *J. Nucl. Mater.* 476, pp 45–55.

Cera, E., Bruno. J., Duro, L., Eriksen, T., 2006. Experimental determination and chemical modelling of radiolytic processes at the spent fuel/water interface. Long contact time experiments, SKB Technical Report TR-06-07, Svensk Kärnbränslehantering AB.

Chaplin, B., Reinhard, M., Schneider, W., Schüth, C., Shapley, J., Strathmann, T., Werth, C., 2012. Critical review of Pd-based catalytic treatment of priority contaminants in water, *Environ. Sci&Techn.* 46, pp. 3655-3670.

Chen, J-C., Huang, J-J., 2013. Regeneration of spent fuel catalysts by H<sub>2</sub>O<sub>2</sub> chemical treatment. *APCBEE Procedia* 5, pp. 107-111.

Chen, X. 2000. On the interaction between fuel Crud and water chemistry in nuclear power plants, SKI Report 2000:05, Statens Kärnkraftinspektion, Sweden.

Christensen, H., 1998. Calculations simulating spent fuel leaching experiments, *Nucl. Technol.* 124, pp. 165–174.

Christensen, H., Sunder, S., Shoesmith, D.W., 1994. Oxidation of nuclear fuel (UO<sub>2</sub>) by the products of water radiolysis: development of a kinetic model. *J. Alloys Compd.* 213–214, pp.93–99.

Clarens, F., de Pablo, J., Casas, I., Gimenez, J., Rovira, M. 2004. Surface site densities of uranium oxides: UO<sub>2</sub>, U<sub>3</sub>O<sub>8</sub>, *Mat. Res. Soc. Symp. Proc.* 807, pp. 71-76.

Cordfunke, E.H.P., Konings R.J.M. 1988. Chemical interactions in water cooled nuclear fuel, *J. Nucl. Mater.* 152, pp. 301-309.

Cowper, M., Askeljung, C., Puranen, A., Granfors, M., Jädemäs, D. 2016. Scoping Studies of the Matrix Dissolution Rate and Instant Release Fractions of Spent AGR Fuel, AMEC-FW report 103583-01 issue 3.

Cowper, M., Askeljung, C., Puranen, A., Granfors, M., Jädemäs, D. 2019. Scoping Studies of the Matrix Dissolution Rate and Instant Release Fractions of Spent AGR Fuel, AMEC-FW report 103583-01 issue 9.

Cox, B. 1990. Pellet cladding interactions (PCI) of zirconium alloy fuel cladding-A review, *J. Nucl. Mater.* 172, pp. 249-292.

### 3.1.1 Spent Nuclear Fuel; State-of-Knowledge

Cubiccioti D., Sanecki, J.E., 1978. Characterisation of deposits on the inside surfaces of LWR cladding, *J. Nucl. Mater.* Pp.96-111.

Cui, D. and Spahiu, K. 2002. The reduction of U(VI) on corroded iron under anoxic conditions, *Radiochim. Acta* 90, pp. 623–628.

Cui, D., Ekeroth, E. Fors, P., Spahiu K. 2008. Surface mediated process in the interaction of spent fuel or  $\alpha$ -doped UO<sub>2</sub> with H<sub>2</sub>. *MRS Symp. Proc.* 1104, pp. 87-99.

Cui, D., Eriksen, T., Eklund, U-B. 2001. On metal aggregates in spent fuel, synthesis and leaching of Mo-Ru-Pd-Rh alloy, *MRS Symp. Proc.* 663 pp. 427-434.

Cui, D., Rondinella, V.V., Fortner, J.A., Kropf, A.J., Eriksson, L., Wronkiewicz, D.J., Spahiu, K. 2012. Characterisation of metallic particles extracted from spent nuclear fuel, *J. Nucl. Materials*, 420 p. 328-333.

Curti, E., Froideval-Zumbiehl, A., Günther-Leopold, I., Martin, M., Bullmer, A., Linder, H., Borca, C.N., Grolimund, D., 2014. Selenium redox speciation in high-burnup UO<sub>2</sub> fuel; Consequences for the release of <sup>79</sup>Se in a deep underground repository, *J. Nucl. Mater.* 453, pp. 98-106.

Curti, E., Puranen, A., Grolimund, D., Jädernas, D., Sheptyakova, D., Mesbah, A., 2015. Characterization of selenium in UO<sub>2</sub> spent nuclear fuel by micro X-ray absorption spectroscopy and its thermodynamic stability. *Environmental Science: Processes and Impacts*, 17, 1760.

Davies, J.H., Ewart, F.T. 1971. The chemical effect of composition changes in irradiated oxide fuel materials, *J. Nucl. Mater.*, 41, pp. 143-155.

de Pablo, J., Casas, I., Gimenez, J., Clarens, F., Duro, L, Bruno, J. 2004. The oxidative dissolution mechanism of uranium dioxide. The effect of pH and oxygen partial pressure, *Mat. Res. Soc. Symp. Proc.* 807, pp. 83-88.

de Pablo, J., Casas, I., Gimenez, J., Molera, M. Rovira, M., Duro, L., Bruno, J. 1999. The oxidative dissolution of uranium dioxide I. The effect of temperatura in hydrogen carbonate media, *Geochim. Cosmochim. Acta*, 63, pp. 3097-3103.

Duro, L., Riba, O., Martínez-Esparza, A., Bruno, J. 2013. Modelling the activation of H<sub>2</sub> on spent fuel surface and inhibiting effect of UO<sub>2</sub> dissolution. *MRS Proceedings*, 1518, 133.

Einzig R E, Cook J A, 1985. Behavior of breached light water reactor spent fuel rods in air and inert atmosphere at 229 °C, *Nucl. Techn.* 69, pp. 51-71.

Einzig R E, Strain R V, 1986. Behavior of breached pressurized water reactor spent fuel rods in air atmosphere between 250 and 360 °C, *Nucl. Techn.* 75, pp. 82-95.

Einzig R E, Thomas L E, Buchanan H C, Stout R B, 1992. Oxidation of spent fuel in air at 175 to 195 °C, *J. Nucl. Mat.* 190, pp. 53-60.

Ekeroth E, Roth O, Jonsson M, 2006. The relative impact of radiolysis products in radiation induced oxidative dissolution of UO<sub>2</sub>, *J. Nucl. Mater.* 2006, 355, 38-46.

Ekeroth E., Jonsson M. 2003. Oxidation of UO<sub>2</sub> by radiolytic oxidants. *J. Nucl. Mater.* 322, pp. 242-248.

Ekeroth, E., Granfors, M., Schild, D., Spahiu, K. 2020. The effect of temperature and fuel surface area on spent nuclear fuel dissolution kinetics under H<sub>2</sub> atmosphere, *J. Nucl. Mater.* 531, id. 151081.

### 3.1.1 Spent Nuclear Fuel; State-of-Knowledge

- Ekeroth, E., Low, J., Zwicky, H-U., Spahiu, K. 2009. Corrosion studies with high burn-up LWR fuel in simulated groundwater". MRS Symp. Proc. 1124, pp. Q02-07.
- Eklund, U.B., Forsyth, R.S., 1978. Leaching of irradiated UO<sub>2</sub> fuel, SKB Report KBS-TR-70, Svensk Kärnbränslehantering AB.
- Ellingham, H.J.T. 1944. Reducibility of oxides and sulphides in metallurgical processes. J. Soc. Chem. Ind. 63, pp. 125-160.
- Elliot, A.J., Padamshi, S., Pika, J. 1986. Free radical redox reactions of uranium ions in sulphuric acid solutions, Canad. J. Chem. 64 pp. 314-320.
- Eriksen, T. E., Jonsson, M., Merino, J., 2008. Modelling time resolved and long contact time dissolution studies of spent nuclear fuel in 10 mM carbonate solution-A comparison between two models and experimental data, J. Nucl. Mater. 375, pp. 331-339.
- Eriksen, T.E., Shoesmith, D.W., Jonsson, M. 2012. Radiation induced dissolution of UO<sub>2</sub> based nuclear fuel – A critical review of predictive modelling approaches. J. Nucl. Mater. 420, 409–423. <https://doi.org/10.1016/j.jnucmat.2011.10.027>
- Evins, L.Z., Valls, A., Duro, L. 2020. Proceedings of the 3rd Annual Meeting of EC-project DisCo (Modern spent fuel dissolution and chemistry in failed container conditions), Deliverable D1.20.
- Farrel, J., Bostick, W.D., Jarabek, R., Fiedor N, 1999. Uranium removal from ground water using zero valent iron media. Ground Water 37 pp. 618-624.
- Ferry C, Radwan J, Palancher H, 2016. Review about the effect of He on the microstructure of spent nuclear fuel in a repository, MRS Advances. Vol.1(62), p. 4147-4156.
- Ferry, C., Piron, J-P., Ambard, A. 2010. Effect of helium on the microstructure of spent fuel in the repository, J. Nucl. Mater. 407, p. 100-109.
- Ferry, C., Piron, J-P., Poulesquen, A., Poinssot, C. 2008. Radionuclides release from spent fuel under disposal conditions: re-evaluation of the Instant Release Fraction, MRS Symp. Proc. 1107, pp 447–454.
- Ferry, C., Poinssot, C., Broudic, V., Cappelaere, C., Desgranges, L., Garcia, P., Jegou, C., Lovera, P., Marimbeau, P., Piron, J.-P., Poulesquen, A., Roudil, D., Gras, J.-M, Bouffieux P. 2005. Synthesis on the spent fuel long term evolution. Report CEA-R-6084, Commissariat à l'Énergie Atomique, Saclay, France.
- Fiedor, J.N., Bostick, W.D., Jarabek R.J., Farrell J. 1998. Understanding the mechanism of uranium removal from groundwater by zero-valent iron using X-ray photoelectron spectroscopy. Environ. Sci. Technol. 32, pp. 1466-1473.
- Fors, P., Carbol, P., Van Winckel, S., Spahiu, K. 2009. Corrosion of high burn-up structured UO<sub>2</sub> fuel in presence of dissolved H<sub>2</sub>. J. Nucl. Mater. 394, 1–8. <https://doi.org/10.1016/j.jnucmat.2009.07.004>.
- Fors, P., 2009. The effect of dissolved hydrogen on spent nuclear fuel corrosion, Ph. D. Thesis, Chalmers University of Technology, Gothenburg, Sweden.
- Forsyth, R.S., Werme, L.O. 1992. Spent fuel corrosion and dissolution, J. Nucl. Mater. 190, pp 3-19.
- Forsyth, R.S., Werme, L.O., Bruno, J., 1986. The corrosion of spent UO<sub>2</sub> fuel in synthetic groundwater. J. Nucl. Mater. 138, 1–15.

### 3.1.1 Spent Nuclear Fuel; State-of-Knowledge

Garrels, R.M. Christ, C.L. 1965. Solutions, Minerals, and Equilibria, Harper & Row, New York.

Glatz, J-P., Carbol, P., Cobos-Sabate, J., Gouder, T., Miserque, F., Gimenez, J., Wegen, D. 2001. Release of radiotoxic elements from high burn-up UO<sub>2</sub> and MOX fuel in the repository, Mat. Res. Soc. Symp. Proc. 663 pp. 33-40.

Gonzales-Robles, E., Metz, V., Wegen, D.W., Herm, M., Papaioannou, D., Bohnert, E., Gretter, R., Müller, N., Nasyrow, R., de Weerd, W., Wiss, T., Kienzler, B. 2016. Determination of fission gas release of spent nuclear fuel in puncturing test and leaching experiments under anoxic conditions, J. Nucl. Mater. 479, pp. 67-75.

Gonzales-Robles, E., Serrano-Purroy, D., Sureda, R., Casas, I., de Pablo, J. 2015. Dissolution experiments of commercial PWR (52 MWd/kg U) and BWR (53 MWd/kg U) spent nuclear fuel clad segments in bicarbonate water under oxidizing conditions. Experimental determination of matrix and instant release fractions, J. Nucl. Mater. 465, pp. 63-70.

Grambow, B. 2021. Spent nuclear fuel long term behaviour and performance, Chapter 6.11 in Encyclopaedia of Materials, Elsevier, Amsterdam.

Grambow, B., Bruno, J., Duro, L., Merino, J., Tamayo, A., Martin, C., Pepin, G., Schumacher, S., Smidt, O., Ferry, C., Jegou, C., Martinez-Esparza, A., Loida, A., Metz, V., Kienzler, B., Bracke, G., Pellegrini, D., Mathieu, G., Wasselin-Turpin, V., Serres, C., Wegen, D., Jonsson, M., Johnson, L., Lemmens, K., Liu, J., Spahiu, K., Ekeroth, E., Casas, I., de Pablo, J., Watsson, C., Robinson, P., Hodgkinson, D. 2010. Final activity report: EU-project MICADO (Model uncertainty for the mechanism of dissolution of spent nuclear fuel in a waste repository), 60 p.

Grambow, B., Ferry, C., Casas, I., Bruno, J., Quinones, J., Johnson, L., 2011. Spent Fuel Waste Disposal: Analyses of Model Uncertainty in the MICADO Project. Energy Procedia 7, pp. 487–494. <https://doi.org/10.1016/j.egypro.2011.06.066>

Grambow, B., Lemmens, K., Minet, Y., Poinssot, C., Spahiu, K., Bosbach, D., Cachoir, C., Casas, I., Clarens, F., Christiansen, B., De Pablo, J., Ferry, C., Gimenez, J., Gin S, Glatz, J.P., Gago, J., Gonzalez Robles, E., Hyatt, N.C., Iglesias, E., Kienzler, B., Luckscheiter, B., Martinez Esparza Valiente, A., Metz, V., Ödegaard-Jensen, Ollila, K., Quinones, J., Rey, A., Ribet, S., Rondinella, V., Skarnemark, G., Wegen, D., Serrano-Purroy, D., Wiss, T., 2008. NF-PRO: Final synthesis report RTD component 1: Dissolution and release from the waste matrix (No. Deliverable D.1.6.3). European Commission, Bruxelles, Belgium.

Grambow, B., Loida, A., Dressler, P., Geckeis, H., Gago, J., Casas, I., de Pablo, J., Gimenez, J., Torrero, M.E. 1996a. Long-term safety of radioactive waste disposal: chemical reaction of fabricated and high burnup spent UO<sub>2</sub> fuel with saline brines. Final report. Wissenschaftliche Berichte FZKA 5702, Forschungszentrum Karlsruhe.

Grambow, B., Loida, A., Martinez-Esparza, A., Diaz-Arcoas, P., De Pablo, J., Paul, J-L., Marx, G., Glatz, J-P., Lemmens, K., Ollila, K., Christensen, H. 2000. Source term for performance assessment of spent fuel as a waste form, European Commission, Nuclear Science and Technology, EUR 19140 EN.

Grambow, B., Smailos, E., Geckeis, H., Muller, R. and Hentschel, H. 1996b. Sorption and reduction of uranium (VI) on iron corrosion products under reducing saline conditions. Radiochim. Acta 74, pp. 149-154.

Grambow, B., Vandenborre, J., Suzuki-Muresan, T., Philippini, V., Abdelouas, A., Deniard, P., Jobic, S., 2017. Solubility equilibrium and surface reactivity at solid/liquid interfaces of relevance to disposal of nuclear waste. J. Chem. Thermodyn. 114, 172–181. <https://doi.org/10.1016/j.jct.2017.05.038>.

### 3.1.1 Spent Nuclear Fuel; State-of-Knowledge

- Gras, J-M 2014. State of the art of 14C in Zircaloy and Zr alloys-14C release from zirconium alloy hulls. D 3.1 of the European Project CAST, <https://www.projectcast.eu/publications>.
- Gray W J, 1999. Inventories of iodine-129 and cesium-137 in the gaps and grain boundaries of LWR spent fuels. MRS Symp. Proc. 556, pp 487–494.
- Gray, W. J., Strachan, D.M., Wilson, C.N., 1992. Gap and grain boundary inventories of Cs, Tc and Sr in spent LWR fuel. MRS Symp. Proc. 257, pp 353–360.
- Grenthe, I., Fuger, J., Konings, R.J.M., Lemire, R., Muller, A.B., Nguen-Trung. C., Wanner, H. 1992. Chemical thermodynamics. Vol. 1. Chemical thermodynamics of uranium. Amsterdam: Elsevier.
- Gu, B., Liang, L., Dickey, M.J., Yin, X., Dai, S. 1998. Reductive precipitation of uranium (VI) by zero-valent iron. Environ. Sci. Technol. 32, pp. 3366-3373.
- Guillamont, R., Fanghänel, T., Grenthe, I., Neck, V., Palmer, D., Rand, M.H., 2003. Update on the chemical thermodynamics of uranium, neptunium, plutonium americium and technetium, OECD-NEA, Chemical Thermodynamics Vol. 5, pp. 182-187, Elsevier.
- Hanson B D, 1998. The burnup dependence of light water reactor spent fuel oxidation, Report PNL-11929, Pacific Northwest National Laboratory, Richland, WA, USA.
- Hanson B D, Daniel R C, Casella A M, Wittman R S, Wu W, MacFarlan P J, Shimskey R W, 2008. Fuel-In-Air, FY07 Summary report, Report PNNL-17275. Pacific Northwest National Laboratory, USA.
- Hanson B. D., 2000. Clad Degradation - Dry Unzipping, Civilian Radioactive Waste Management Service - Management and Operations, ANL-EBS-MD-000013.
- Hanson, B., 2008. Examining the conservatism in dissolution rates of commercial spent nuclear fuel, Proc. 12th Int. High-Level Waste Management Conf., Las Vegas, American Nuclear Society, pp 404-411.
- Hanson, B.D., Stout, R.B., 2004. Re-examining the dissolution of spent fuel: a comparison of different methods for calculating rates. MRS Symp. Proc. 824, pp 89–94.
- Hansson, N., Ekberg, C., Spahiu, K. 2020. Alpha dose rate calculation for UO<sub>2</sub> based materials using stopping power models, Nucl. Mater.&Energy 22, 100734.
- Hansson, N.L, Tam, P.L., Ekberg, C., Spahiu, K. 2021. XPS study of external  $\alpha$ -radiolytic oxidation of UO<sub>2</sub> in the presence of argon or hydrogen, J. Nucl. Mater. 543, paper 152604.
- He, H., Broczkowski, M.M., O’Neil K., Ofori D., Semenikhin O., Shoesmith D.W. 2012. Corrosion of nuclear fuel (UO<sub>2</sub>) inside a failed nuclear waste container. NWMO TR-2012-09, Canada.
- Hedin, A. Evins, L.Z., Spahiu, K. 2013. What if criticality in a final repository, SKBdoc 1417199, Svensk Kärnbränslehantering AB.
- Herrero, J.J., Vasiliev, A., Pechia, M., Rochman, D., Ferroukhi, H., Johnson, L., Caruso, S. 2017. Criticality safety assessment for geological disposal of spent fuel using PSI-BUCSS-R methodology, Nagra Report NAB 17-23, Nagra, Wettingen, Switzerland.
- Hicks, T.W, Doudou S., Walters, W.S. 2018. Demonstrating the criticality safety of the spent fuel disposal, Contractor report to RWM no. GLS-1649-5-V3.1.
- Hiroki, A., LaVerne, J.A. 2005. Decomposition of hydrogen peroxide at water-ceramic oxide interfaces, J. Phys. Chem. B 109, pp. 3364-3370.

### 3.1.1 Spent Nuclear Fuel; State-of-Knowledge

Hocking, W.H., Duclos, A.M., Johnson, L.H., 1994. Study of fission product segregation in used CANDU fuel by X-ray photoelectron spectroscopy, J. Nucl. Mater. 209 pp. 1-26.

Hossain M.M., Jonsson, M., 2008. UO<sub>2</sub> oxidation site densities determined by one- and two-electron oxidants, J. Nucl. Mater. 373, pp. 186-189.

Hossain, M.M., Ekeroth, E., Jonsson, M. 2006. Effects of HCO<sub>3</sub><sup>-</sup> on the kinetics of UO<sub>2</sub> oxidation by H<sub>2</sub>O<sub>2</sub>, J. Nucl. Mater. 358, pp. 202-208.

Hua, B., Xu, H., Terry, J. Deng, B. 2006. Kinetics of U(VI) reduction by hydrogen sulfide in anoxic aqueous systems, Environ. Sci. Technol. 40, pp. 4666-4671.

Hummel, W. 2017. Chemistry of selected dose relevant nuclides, Nagra Technical Report NTB 17-05, NAGRA, Wettingen, Switzerland.

IAEA 1998. Durability of spent nuclear fuels and facility components during wet storage, IAEA-TECDOC- 1012, International Atomic Energy Agency, Vienna, Austria.

IAEA 2001. Implementation of burnup credit in spent fuel management systems, IAEA-TECDOC-1241, International atomic energy agency, Vienna, Austria.

IAEA 2003b. Fuel failures in water reactors: Causes and mitigation, IAEA-TECDOC-1345, International Atomic Energy Agency Vienna, Austria.

IAEA 2003a. Status and advances in MOX fuel technology, Technical Report Series-415, IAEA, Vienna, Austria.

IAEA 2006. Understanding and managing ageing of materials in spent fuel storage facilities. IAEA Technical Reports Series No. 443, International Atomic Energy Agency, Vienna, Austria.

IAEA 2010b. Delayed hydride cracking of zirconium alloy fuel cladding, IAEA-TECDOC-1649, International Atomic Energy Agency Vienna, Austria.

IAEA 2010a. Review of fuel failures in water cooled reactors. IAEA Nuclear Energy Series No. NF-T-2.1, International Atomic Energy Agency Vienna, Austria.

IAEA 2013. Spent fuel storage operation -lessons learned. Report IAEA-TECDOC-1725, International Atomic Energy Agency, Vienna, Austria.

IAEA 2016. Review of fuel failures in water cooled reactors (2006-2015), IAEA Nuclear Energy Series No. NF-T-2.5, International Atomic Energy Agency Vienna, Austria.

IAEA 2020. Storage of Spent Nuclear Fuel, Safety Standards Series No. SSG-15, Rev.1, International atomic energy agency, Vienna, Austria.

IAEA-2011. Optimisation of water chemistry to ensure reliable water reactor fuel performance at high burnup and in ageing plant (FUWAC), IAEA-TECDOC-1666, International Atomic Energy Agency, Vienna, Austria.

Imoto S. 1986. Chemical state of fission products in irradiated UO<sub>2</sub>, J. Nucl. Mater., 140 p. 19-27.

Jegou, C., Caraballo, R., De Bonfils, J., Broudic, V., Peugeot, S., Vercouter, T., Roudil, D. 2010. Oxidizing dissolution of spent MOX<sub>47</sub> fuel subjected to water radiolysis: Solution chemistry and surface characterisation by Raman spectroscopy, J. Nucl. Mater. 399, pp. 68-80.

### 3.1.1 Spent Nuclear Fuel; State-of-Knowledge

- Jegou, C., Muzeau, B., Broudic, V., Peugeot, S., Poulesquen, A., Roudil, D., Corbel, C. 2005. Effect of external gamma irradiation on dissolution of the spent UO<sub>2</sub> fuel matrix, *J. Nucl. Mater.* 341, pp. 62-82.
- Jegou, C., Muzeau, B., Brudic, V., Roudil, D., Deschanel, X. 2007. Spent fuel UO<sub>2</sub> matrix alteration in aqueous media under oxidizing conditions, *Radiochim. Acta*, 95, pp. 513-522.
- Jegou, C., Peugeot, S., Brudic, V., Roudil, D., Deschanel, X., Bart, J.M. 2004. Identification of the mechanism limiting the alteration of clad spent fuel segments in aerated carbonated groundwater, *J. Nucl. Mater.* 326, pp.144-155.
- Jegou, C., Peugeot, S., Lucchini, J.F., Corbel, C., Brudic, V., Bart, J.M. 2001. Effect of spent fuel burnup and composition on the alteration of the U(Pu)O<sub>2</sub> matrix, *MRS Symp. Proc.* 663 pp. 33-40.
- Jerden, J.L., Frey, K., Ebert, W. 2015. A multiphase interfacial model for the dissolution of spent nuclear fuel. *Journal of Nuclear Materials*, 462, 135-146.
- Johnson L.H., Shoesmith, D.W. 1988. Spent fuel. In: *Radioactive Waste Forms for the Future*, Eds.: Lutze, W and Ewing, R. C., North-Holland Physics Publishing, The Netherlands, 1988.
- Johnson, L. H., McGinnes, D. F., 2002. Partitioning of radionuclides in Swiss power reactor fuels. NAGRA Report NTB 02-07, NAGRA, Switzerland.
- Johnson, L. H., Poinssot, C., Ferry, C., Lovera, P., 2004. Estimates of the instant release fraction of UO<sub>2</sub> and MOX fuel at t = 0. NAGRA Report NTB 04-08, NAGRA, Switzerland.
- Johnson, L. H., Tait, J. C., 1997. Release of segregated nuclides from spent fuel. SKB TR 97-18, Swedish Nuclear Fuel and Waste Management Co. (SKB).
- Johnson, L., 2014. A model for radionuclide release from spent UO<sub>2</sub> and MOX fuel, NAGRA report NAB 13-37. NAGRA, Wettingen, Switzerland.
- Johnson, L., Ferry, C., Poinssot, C., Lovera, P. 2005. Spent fuel radionuclide source-term model for assessing spent fuel performance in geological disposal. Part I: Assessment of the instant release fraction. *J. Nucl. Mater.* 346, pp 56–65.
- Johnson, L., Günther-Leopold, I., Kobler, Waldis, J., Linder, H.P., Low, J., Cui, D., Ekeröth, E., Spahiu, K., Evins, L.Z., 2012. Rapid aqueous release of fission products from high burn-up LWR fuel: Experimental results and correlations with fission gas release. *J. Nucl. Mater.* 420, 54–62. <https://doi.org/10.1016/j.jnucmat.2011.09.007>.
- Johnson, L.H. ed., 2005. Spent fuel evolution under disposal conditions, NAGRA Technical Report NTB 04-09, Wettingen Switzerland.
- Johnson, L.H., 1982. The dissolution of irradiated UO<sub>2</sub> fuel in groundwater. Report AECL-6837. Atomic Energy Canada Limited, Pinawa, Manitoba, Canada.
- Jonsson M, Nielsen F, Roth O, Ekeröth E, Nilsson S, Hossain M M, 2007. Radiation induced spent nuclear fuel dissolution under deep repository conditions. *Environ. Sci. & Technol.*, 41, pp 7087–7093.
- Jung H, Shukla P, Ahn T, Tipton L, Das K, He X, Basu D, 2013. Extended storage and transportation: Evaluation of drying adequacy, Center for Nuclear Waste Regulatory Analysis (CNWRA), San Antonio, TX, USA.
- Kamimura, K., 1992. Fission gas release behaviour of high burn-up MOX fuels for thermal reactors. In: *Fission gas release and fuel rod chemistry related to extended burn-up*.

### 3.1.1 Spent Nuclear Fuel; State-of-Knowledge

Proceedings of a Technical Committee Meeting held in Pembroke, Ontario, Canada, 28 April – 1 May 1992. IAEA-TECDOC-697, International Atomic Energy Agency, pp 82–88.

Katayama, Y.B. 1976. Leaching of Irradiated LWR spent fuel pellets in deionized water and typical ground water. Report BNWL 2057 UC-70. Batelle Pacific Northwest Laboratory, Richland, WA, USA.

Kelm, M., Bohnert, E., 2004. A kinetic model for the radiolysis of chloride brine, its sensitivity against model parameters and a comparison with the experiments, Forschungszentrum Karlsruhe, Report FZKA 6977.

Kienzler, B., Duro, L., Lemmens, K., Metz, V., de Pablo, J., Valls, A., Wegen, D., Johnson, L., Spahiu, K. 2017. Summary of the Euratom collaborative project FIRST-Nuclides and conclusions for the safety case, Nucl. Technol. 198, p. 260-276.

Kienzler, B., Gonzales-Robles, E., 2013. State-of-the-Art on Instant Release of Fission Products from Spent Nuclear Fuel, Proc. 15th Int. Conf. on Environ. Remediation and Radioactive Waste Management, ICEM-2013, p. ICEM2013-96044.

Kienzler, B., Metz, V., Valls, A. 2014. Fast/Instant release of safety relevant radionuclides from spent nuclear fuel, First Nuclides, Final Scientific Report, Deliverable No. 5.13. DELIVERABLE (D-N°:XX) (igdtp.eu).

Kienzler, B., Metz, V., Valls, A., 2015. Fast / Instant Release of Safety Relevant Radionuclides from Spent Nuclear Fuel, FIRST-Nuclides - Final Scientific Report, Contract Number: FP7-295722. European Commission.

Kilger, R., Bock, M., Gmal, B., 2013. Exclusion of criticality for a final repository in a saline host rock based on the neutron absorbing properties of Cl-35. In: American Nuclear Society (ANS), Criticality Safety in the Modern Era: Raising the Bar. ANS Topical Meeting of the Nuclear Criticality Safety Department (NCSD), Wilmington, NC, USA, 29 September - 3 Oktober 2013, ANS: La Grange Park, IL, USA.

King, F., Kolar, M. 2003. The Mixed-Potential Model for UO<sub>2</sub> Dissolution MPM, Versions V1.3 and V1.4, Ontario Hydro, Nuclear Waste Management Division, Report No. 06819-REP-01200-10104 R00.

King, F., Quinn, M.J., Miller, H.H. 1999. The effect of hydrogen and gamma radiation on the oxidation of UO<sub>2</sub> in 0.1 mol·dm<sup>-3</sup> NaCl solution, SKB Technical Report TR-99-27. Svensk Kärnbränslehantering AB.

Kirkegaard, P., Bjergbakke, E., Olsen, J.V. 2008. CHEMSIMUL: A chemical kinetics software package. Roskilde: Danmarks Tekniske Universitet, Risø Nationallaboratoriet for Bæredygtig Energi. Denmark. Forskningscenter Risø. Risø-R-1630 EN. <http://orbit.dtu.dk/files/6278806/ris-r-1630.pdf>

Kleykamp H, 1979. The chemical state of LWR high-power rods under radiation, J. Nucl. Mater. 84 p. 109-117.

Kleykamp H, 1993. The solubility of selected fission products in UO<sub>2</sub> and (U, Pu)O<sub>2</sub>. J. Nucl. Mater., 206 p. 82-86.

Kleykamp, H. 1985. The chemical state of the fission products in oxide fuels. J. Nucl. Mater. 131 pp. 221-246.

Kleykamp, H. 1990. Post-irradiation examinations and composition of the residues from nitric acid dissolution experiments of high-burnup LWR fuel, J. Nucl. Mater. 171, p. 181-188.

### 3.1.1 Spent Nuclear Fuel; State-of-Knowledge

Kleykamp, H., Paschoal, J. O., Pejsa, R., Thommler, F. 1985. Composition and structure of fission product precipitates in irradiated oxide fuels: Correlation with phase studies in the Mo-Ru-Rh-Pd and BaO-UO<sub>2</sub>-ZrO<sub>2</sub>-MoO<sub>2</sub> systems, *J. Nucl. Mater.* 130, p. 426-433.

Kolár M, King F, 1996. Modelling the consumption of oxygen by container corrosion and reaction with Fe(II). *MRS Symp. Proc.* 412, pp 547–554.

Konashi, K., Shiokawa, Y., Kayano, H. 1996. Simulation of CsI decomposition in fuel cladding gap, *J. Nucl. Mater.* 232, p. 181-185.

Köningsberger, E., Spahiu, K., Herschend, B. 2021. Thermodynamic study of chlorine content in stainless steel, *Metallurg. Mater. Transac.* 52B pp. 840-853.

Lassman, K.A., Schubert, A., van de Laar, J., Walker, C.T. 2002. On the diffusion coefficient of cesium in UO<sub>2</sub> fuel, In: *OECD-NEA Symp. Proc. "Fission Gas Behaviour in Water Reactor Fuels"*, Cadarache, France, September 2000, pp. 45-52.

Lemmens, K., Gonzalez-Robles, E., Kienzler, B., Curti, E., Serrano-Purroy, D., Sureda, R., Martínez-Torrents, A., Roth, O., Slonszki, E., Mennecart, T., Günther-Leopold, I., Hozer, Z. 2017. Instant release of fission products in leaching experiments with high burnup nuclear fuels in the framework of the Euratom project FIRST- Nuclides. *J. Nucl. Mater.* 484, pp. 307-323.

Lewis, B.J., Hunt, C.E.L., Iglesias, J., 1990. Source term of iodine and noble gas fissions products in the fuel-to-sheath gap of intact operating fuel elements, *J. Nucl. Mater.* 172, pp. 197-205.

Li, C., Olander D.R. 1999. Steam radiolysis by alpha particle irradiation, *Rad. Phys. Chem.* 54, pp. 361-371.

Liu, L., Neretnieks, I. 2002. The effect of hydrogen on oxidative dissolution of spent fuel. *Nucl. Technol.*, 138 pp. 69-77.

Liu, N. Z., He, H.M., Noel, J.J. and Shoesmith D.W. 2017 b. The electrochemical study of Dy<sub>2</sub>O<sub>3</sub> doped UO<sub>2</sub> in slightly alkaline sodium carbonate/bicarbonate and phosphate solutions, *Electrochim. Acta* 235 pp. 654-663.

Liu, N. Z., J. Kim, J. Lee, Y. S. Youn, J. G. Kim, J. Y. Kim, J. J. Noel and D. W. Shoesmith 2017a. Influence of Gd doping on the structure and electrochemical behavior of UO<sub>2</sub>, *Electrochim. Acta* 247 pp. 496-504.

Liu, N., Qin Z., Nöel J.J., Shoesmith, D.W. 2017c. Modelling the radiolytic corrosion of  $\alpha$ -doped UO<sub>2</sub> and spent nuclear fuel. *J. Nucl. Mater.*, 494, pp. 87-94.

Liu, N., Wu L., Qin Z., Shoesmith, D.W. 2016. Roles of radiolytic and externally generated H<sub>2</sub> in the corrosion of fractured spent fuel. *Environ. Sci & Technol.* 50, pp. 12348-12355.

Loida, A., B. Grambow, B., Karsten, G., Dressler P. 1998. Radionuclide release from spent MOX fuel. *MRS Symp. Proc.* 506 pp. 923-924.

Loida, A., Gens, R., Bube, C., Lemmens, K., Cachoir, C., Mennecart, T., Kienzler, B. 2012. Corrosion behavior of spent fuel in high pH solutions-Effect of hydrogen, *MRS Symp. Proc.* 1475 pp. 119-124.

Loida, A., Grambow B., Geckeis, H. 1996. Anoxic corrosion of various high burnup samples, *J. Nucl. Mater* 238, pp.11-22.

Loida, A., Grambow, B., Geckeis, H. 2001. Spent fuel corrosion behaviour in salt solution in the presence of hydrogen overpressure, *Proc. ICM'01, 8th Internat. Conf. on Radioactive Waste Management*, Bruges, Belgium, pp. 711–716.

### 3.1.1 Spent Nuclear Fuel; State-of-Knowledge

- Loida, A., Metz, V., Kienzler, B., Geckeis, H. 2005. Radionuclide release from high burnup spent fuel during corrosion in salt brine in the presence of hydrogen overpressure. *J. Nucl. Mater.* 346 pp. 24-31.
- Loida, A., Metz, V., Kienzler, B. 2007. Alteration behavior of high burnup spent fuel in salt brine under hydrogen overpressure and in presence of bromide MRS. *Symp. Series*, 985 pp. 15-20.
- Lousada, C.M., Trummer, M., Jonsson, M. 2013. Reactivity of H<sub>2</sub>O<sub>2</sub> towards different UO<sub>2</sub>-based materials: The relative impact of radiolysis products revisited. *J. Nucl. Mater.* 434 pp. 434–439.
- Lucuta, P.G., Verrall, R.A., Matzke, H.-J., Palmer, B.J.F. 1991. Microstructural features of SIMFUEL-simulated high burn-up UO<sub>2</sub>-based nuclear fuel, *J. Nucl. Mater.* 178, pp. 48-60.
- Lundström T., 2003. Radiation chemistry of aqueous solutions related to nuclear reactor systems and spent fuel management, PhD-thesis, Linköping University, Dissertation No. 840.
- Martin, G., Maillard, S., Van Brutzel, L., Garcia, P., Dorado, B., Valot, C., 2009. A molecular dynamics study of radiation induced diffusion in uranium dioxide. *J. of Nucl. Mater.* 385, pp 351–357.
- Masih A.H. 2006. Models for MOX fuel behaviour: A selective review, SKI Technical report 2006: 10, Statens Kärnkraftinspektion, Sweden.
- Mason, R.M., Martin, J.K., Smith, P.N., Winsley, R.J. 2015. Consequence modelling of hypothetical post-criticality events for spent fuel disposal, *Min. Mag.* 79, pp. 1505-1513.
- Mason, R.M., Smith, P.N., Holton, D. 2014. Modelling consequences of hypothetical criticality: Synthesis report for post-closure criticality consequence analysis, Report RWM 005140, RWM, UK.
- Matzke H., Spino, J. 1997. Formation of the rim structure in high burnup Fuel, *J. Nucl. Mater.* 248 pp. 170-179.
- Matzke, H. 1980. Gas release mechanisms in UO<sub>2</sub>-A critical review, *Radiat. Eff.*, 53 p. 219-242.
- Matzke, H. 1982. Radiation damage in crystalline insulators, oxides and ceramic nuclear fuels, *Rad. Eff.* 64 p. 3-33.
- Matzke, H. 1987. Atomic transport properties in UO<sub>2</sub> and mixed oxides (U,Pu)O<sub>2</sub>, *J. Chem. Soc. Farad. Trans. II*, 83 pp. 1121-1142.
- Matzke, H., 1994. Oxygen potential in the rim region of high burnup UO<sub>2</sub> fuel, *J. Nucl. Mater.* 208, pp. 18-26.
- Matzke, H., 1995. Oxygen potential measurements in high burnup LWR UO<sub>2</sub> fuel, *J. Nucl. Mater.* 223, pp. 1-5.
- Matzke, H., Blank, H., Coquerelle, M., Lassman, K., Ray, I.L.F, Ronchi, C., Walker, C.T. 1989. Oxide fuel transients, *J. Nucl. Mater.* 166, pp. 165-178.
- Mazeina, L., Navrotsky, A., Greenblatt, M., 2008. Calorimetric determination of energetics of solid solutions of UO<sub>2+x</sub> with CaO and Y<sub>2</sub>O<sub>3</sub>. *Journal of Nuclear Materials*, 373, pp 39-43.
- McNeil M.B., Little, B.J. 1992. Corrosion mechanisms for copper and silver objects in near-surface environments, *J. Am. Inst. Conservation*, 31, pp. 355-366.

### 3.1.1 Spent Nuclear Fuel; State-of-Knowledge

Merino J., Cera E., Bruno J., Quinones J., Casas I., Clarens F., Gimenez J., de Pablo J., Rovira M., Martinez-Esparza A., 2005. *J. Nucl. Mater.* 346 (2005) pp. 40–47.

Metz, V., Bohnert, E., Kelm, M., Schild, D., Reinhardt, J., Kienzler, B., Buchmeiser, M. 2007. Gamma-radiolysis of NaCl brine in the presence of UO<sub>2</sub>(s): Effects of hydrogen and bromide, *MRS. Symp. Proc.* 985, pp. 33-40.

Morrison, S.J., Metzler, D.R., Carpenter, C.E. 2001. Uranium precipitation in a permeable reactive barrier by progressive irreversible dissolution of zero valent iron, *Environ. Sci. Technol.* 35, pp. 385-390.

Motta, A.T., Capolungo, L., Chen, L-Q., Cinbiz, M.N., Daymond, M.R., Koss, D.A., Lacroix, L., Pastore, G., Simon, P.-C.A., Tonks, M.R., Wirth, B.D., Zikry, M.A. 2019. Hydrogen in zirconium alloys: A review, *J. Nucl. Mater.* 518, pp. 440-460.

Munakata, N., Reinhard, M. 2007. Palladium-catalyzed aqueous hydrodehalogenation in column reactors: Modelling of deactivation kinetics with sulphide and comparison of regenerants. *Appl. Catalysis B* 75, pp. 1-10.

Muzeau, B., Jégou, C., Delaunay, F., Broudic, V., Brevet, A., Catalette, H., Simoni, E., Corbel, C., 2009. Radiolytic oxidation of UO<sub>2</sub> pellets doped with alpha emitters (238/239Pu), *J. All. Comp.* 467, pp. 578-589.

Newton T.W. 1975. ERDA Critical Review Series, The kinetics of the oxidation-reduction reactions of uranium, neptunium, plutonium and americium in aqueous solutions, (TID-26506), NTIS, Springfield VA USA.

Nicot J-P, 2008. Methodology for bounding calculations of nuclear criticality of fissile material accumulations external to a waste container at Yucca Mountain, Nevada. *Applied Geochemistry*, 23, pp 2065–2081.

Nielsen F, Jonsson M, 2008. Simulations of H<sub>2</sub>O<sub>2</sub> concentration profiles in the water surrounding spent nuclear fuel taking mixed radiation fields and bulk reactions into account, *J. Nucl. Mater.* 374 pp. 281-285.

Nielsen, F., Jonsson, M. 2006. Geometrical  $\alpha$ - and  $\beta$ -dose distributions and production rates of radiolysis products in water in contact with spent nuclear fuel, *J. Nucl. Mater.* 359, pp. 1-7.

Nilsson S., Jonsson, M. 2011. H<sub>2</sub>O<sub>2</sub> and radiation induced dissolution of UO<sub>2</sub> and SIMFUEL pellets. *J. Nucl. Mater.* 410 pp. 89-93

Nilsson, S., Jonsson, M. 2008a. On the catalytic effect of UO<sub>2</sub>(s) and Pd(s) on the reaction between H<sub>2</sub>O<sub>2</sub> and H<sub>2</sub> in aqueous solution, *J. Nucl. Mater.* 372, pp. 160-163.

Nilsson, S., Jonsson, M. 2008b. On the catalytic effect of Pd(s) on the reduction of UO<sub>2</sub>+ with H<sub>2</sub> in aqueous solution, *J. Nucl. Materials* 374, pp. 290-292.

Nogita, K., Une, K. 1998. High resolution TEM observation and density estimation of Xe bubbles in high burnup UO<sub>2</sub> fuels, *Nucl. Instrum. Methods Phys. Res., Sect. A* 141, pp. 481–486.

Nordström, E. 2009, Fission gas release data for Ringhals PWR, SKB Technical Report TR-09-26, SKB, Sockholm, Sweden.

Odorowski, M., 2015. Etude de l'altération de la matrice (U,Pu)O<sub>2</sub> du combustible irradié en conditions de stockage géologique : Approche expérimentale et modélisation géochimique, Ph. D. Thesis, Mines Paris Tech, France.

### 3.1.1 Spent Nuclear Fuel; State-of-Knowledge

Odorowski, M., Jegou, C., de Windt, L., Broudic, V., Jouan, G., Peugeot, S., Martin, C. 2017. Effect of metallic iron on the oxidative dissolution of UO<sub>2</sub> doped with a radioactive alpha emitter in synthetic Callovo-Oxfordian water, *Geochim. Cosmochim. Acta* 219, pp.1-21.

Odorowski, M., Jegou, C., de Windt, L., Broudic, V., Peugeot, S., Magnin, M., Tribet, M., Martin, C. 2016. Oxidative dissolution of unirradiated Mimas MOX fuel (U/Pu oxide) in carbonated water under oxic and anoxic conditions. *J. Nucl. Mater.* 468 p. 17-25.

OECD-NEA 2002. Symposium Proceedings „Fission Gas Behavior in Water Reactor Fuels”, held in Cadarache, France, September 2000. [https://www.oecd-nea.org/jcms/pl\\_13488](https://www.oecd-nea.org/jcms/pl_13488)

Olander, D. 2009. Nuclear fuels-Present and future, *J. Nucl. Mater.* 389, pp.1-22.

Olander, D.R. 1976. Fundamental Aspects of Nuclear Reactor Fuel Elements, Technical Report TID-26711-P1, California Univ. Berkley, USA. <https://doi.org/10.2172/7343826>.

Olander, D.R. 1986. Oxidation of UO<sub>2</sub> by high pressure steam, *Nucl. Technol.* 74, pp. 215-217.

Olander, D.R. 1998. Mechanistic interpretation of UO<sub>2</sub> oxidation, *J. Nucl. Mater.* 252, pp. 121-130.

Olander, D.R., Kim, Y.S., Wang, W.E., Yagnik, S.K, 1999. Steam oxidation in defective fuel rods, *J. Nucl. Mater.* 270. pp. 11-20.

Olander, D.R., Wang W.E., Kim Y.S., Li C.Y., Lim, S., Yagnik, S. K., 1997. Chemical processes in defective fuel rods, *J. Nucl. Mater.* 248, pp. 214-219.

Oldberg, K. 2009. Distribution of fission gas release in 10x10 fuel, SKB Technical Report TR-09-25, SKB, Sockholm, Sweden.

Olin, Å., Noläng, B., Osadchii, E., Öhman, L. and Rosen, E., 2005. Chemical thermodynamics. Vol. 7. Chemical thermodynamics of selenium. Amsterdam: Elsevier.

Ollila K, 2006. Dissolution of unirradiated UO<sub>2</sub> and UO<sub>2</sub> doped with <sup>233</sup>U in 0.01 M NaCl under anoxic and reducing conditions, Posiva Report 2006-08. 87 p. Posiva Oy, Olkiluoto, Finland.

Ollila K, Albinsson Y, Oversby V, Cowper M, 2003. Dissolution rates of unirradiated UO<sub>2</sub>, UO<sub>2</sub> doped with <sup>233</sup>U, and spent fuel under normal atmospheric conditions and under reducing conditions using an isotope dilution method, SKB TR-03-13, 2003.

Ollila K, Oversby V M, 2005. Dissolution of unirradiated UO<sub>2</sub> and UO<sub>2</sub> doped with <sup>233</sup>U under reducing conditions. SKB TR-05-07, Svensk Kärnbränslehantering AB.

Ollila K, Oversby V, 2006. Testing of uranium dioxide enriched with <sup>233</sup>U under reducing conditions, MRS Symp. Proc. Vol. 932, pp. 167-173.

Ollila, K. 2008. Dissolution of unirradiated UO<sub>2</sub> and UO<sub>2</sub> doped with <sup>233</sup>U in low- and high-ionic-strength NaCl under anoxic and reducing conditions, Posiva Working Report 2008-50. Posiva Oy, Olkiluoto, Finland.

Oversby V M, 1996. Criticality in a high-level waste repository. A review of some important factors and an assessment of the lessons that can be learned from the Oklo reactors. SKB TR- 96-07, Svensk Kärnbränslehantering AB.

Oversby, V.M. 2005. Rates and mechanisms of radionuclide release and retention inside a waste disposal canister (In Can Processes), Final report No. CONTRACT N° FIKW-CT-2000-00019. European Commission, Bruxelles, Belgium.

### 3.1.1 Spent Nuclear Fuel; State-of-Knowledge

Pehrman, R., Trummer M., Lousada C.M., Jonsson M. 2012. On the redox reactivity of doped UO<sub>2</sub> pellets—influence of dopants on the H<sub>2</sub>O<sub>2</sub> decomposition mechanism, *J. Nucl. Mater.* 430, pp. 6–11.

Poinssot, C., Ferry, C., Kelm, M., Grambow, B., Martinez-Esparza, Johnson, L., Andriambololona, Z., Bruno, J., Cacho, C., Cavedon, J.M., Christensen, H., Corbel, C., Jegou, C., Lemmens, K., Loida, A., Lovera, P., Miserque, F., De Pablo, J., Poulesquen, A., Quinones, J., Rondinella, V., Spahiu, K., Wegen, D., 2005. Spent fuel stability under repository conditions, Final Report No. CONTRACT N° FIKW-CT-2001-00192 SFS. European Commission, Bruxelles, Belgium.

Posiva, 2021. Source Terms for the Safety Case in Support of the Operating Licence Application. Working report. Posiva Oy, Eurajoki (in preparation).

Poulesquen, A., Jegou, C., Peugeot, S. 2006. Determination of the alpha dose rate profile at the UO<sub>2</sub>/water interface, *MRS Symp. Proc.*, 932 pp. 505-512.

Puigdomenech I, Trotignon L, Kotelnikova S, Pedersen K, Griffault L, Michaud V, Lartigue J-E, Hama K, Yoshida H, West J, Bateman K, Milodowski A, Banwart S, Rivas Perez J, Tullborg E-L, 2000. O<sub>2</sub> consumption in a granitic environment, *MRS. Symp. Proc.*, 608 pp. 179-184.

Puranen, A., Barreiro-Fidalgo A, Evins, L.Z., Spahiu, K. 2017. Spent fuel leaching in the presence of corroding iron, *MRS Advances, Energy &Sustain.* 2 (12) pp. 681-686.

Puranen, A., Barreiro-Fidalgo, A., Evins, L.Z., Spahiu, K., 2020. Spent fuel leaching and the impact of iron corrosion—the effects of hydrogen generation and formation of iron corrosion products. *J. Nucl. Mater.* 542, paper 152423.

Puranen, A., Granfors, M., Ekeröth, E., Spahiu, K. 2017. Lessons learned from leaching of high burnup UO<sub>2</sub> fuel under H<sub>2</sub> atmosphere, *MRS Advances*, 1(61) pp. 4169 - 4175.

Quiñones, J., Iglesias E., Martinez-Esparza A., Merino A., Cera E., Bruno J., de Pablo J., Casas, I., J. Giménez J., Clarens F., Rovira M., 2006. Modelling of the spent fuel dissolution rate evolution for repository conditions. Matrix Alteration Model results and sensibility analysis. *MRS Symp. Proc.* 932, pp.433-440.

Rai, D., Yui, M., Moore, D.A. 2003. Solubility and solubility product at 22°C of UO<sub>2</sub>(c) precipitated from aqueous U(IV) solutions. *J. Solution. Chem.*, 32, pp 1–17.

Rard, J.A., Rand, M.H., Anderegg, G., Wanner, H., 1999. Chemical thermodynamics. Vol. 3. Chemical thermodynamics of Technetium. Amsterdam: Elsevier.

Ray, I.L.F., Thiele, H., Matzke, H. 1992. Transmission electron microscopy study of fission product behaviour in high burnup UO<sub>2</sub>, *J. Nucl. Mater.* 188, pp. 90-95.

Razdan, M., Shoesmith, D.W. 2014, Influence of trivalent dopants on the structural and electrochemical properties of UO<sub>2</sub>, *J. Electrochem. Soc.* 161, H105-H113.

Rearden, B.T., Jessee, M.A. Eds, 2018. SCALE Code System, Report ORNL/TM-2005/39, version 6.2.3. Oak Ridge National Laboratory, Oak Ridge, Tennessee, USA.

Riba, O., Coene, E., Silva, O. Duro, L. 2020. Spent fuel alteration 1D model integrating water radiolysis and reactive solute transport, Deliverable D.20, Proc. 3d Annual Workshop EC-Project Disco, pp. 95-108.

Röllin, S., Spahiu, K., Eklund, U.B., 2001. Determination of dissolution rates of spent fuel in carbonate solutions under different redox conditions with a flow-through experiment. *J. Nucl. Mater.* 297, 231–243.

### 3.1.1 Spent Nuclear Fuel; State-of-Knowledge

- Ronchi, C., Wiss, T., 2002. Fission fragment spikes in uranium dioxide, *J. Appl. Phys.*, 5837-5848.
- Rondinella V V, Cobos J, Wiss T, 2004. Leaching behaviour of low-activity alpha-doped UO<sub>2</sub>, *MRS Symp. Proc.* 824, pp. 167-173.
- Rondinella, V., Wiss, T., 2010. The high burnup structure in nuclear fuel, *Materials today*, 13 pp. 24-32.
- Roth, O., Cui, D., Askeljung, C., Puranen, A., Evins, L.Z., Spahiu, K. 2019. Leaching of spent nuclear fuels in aerated conditions: Influences of sample preparation on radionuclide release patterns, *J. Nucl. Mater.* 527, paper 151789.
- Roth, O., Granfors, M., Puranen, A., Spahiu, K. 2015. Release of 108mAg from irradiated PWR control rod absorbers under deep repository conditions, *MRS Symp. Proc.* 1744, pp. 217-222.
- Roth, O., Jonsson M., 2008. Oxidation of UO<sub>2</sub>(s) in aqueous solutions, *Centr. Eur. J. Chem.* 6, pp. 1-14.
- Roudil D, Jégou C, Broudic V, Muzeau B, Peugeot S, Deschanel X, 2007. Gap and grain boundary inventories from pressurized water reactor spent fuels. *J. Nucl. Mater.*, 362 pp. 411–415.
- Roudil, D., Bonhoure, J., Pik, R., Cuney, M., Jégou, C., Gauthier-Lafaye, F. 2008. Diffusion of radiogenic helium in natural uranium oxides. *J. Nucl. Mater.* 378, pp 70–78.
- Roudil, D., Jégou, C., Broudic, V., Muzeau, B., Peugeot, S., Deschanel, X., 2009. Rim instant release radionuclide inventory from French high burnup spent UOX fuel, *MRS Symp. Proc.* 1193, pp. 627-633.
- Santos, B.G., Noel, J.J., Shoesmith, D.W. 2006a. The influence of calcium ions on the development of acidity in corrosion products deposits on SIMFUEL, UO<sub>2</sub>, *J. Nucl. Mater.* 350 pp. 320-331.
- Santos, B.G., Noel, J.J., Shoesmith, D.W. 2006b. The influence of silica on the development of acidity in corrosion products deposits on SIMFUEL(UO<sub>2</sub>), *Corr. Sci.* 48 pp. 3852-3868.
- Schüth, C., Kummer, N-A., Weidenthaler, C., Schad, H., 2004. Field application of a tailored catalyst for dechlorinating chlorinated hydrocarbon contaminants in groundwater, *Appl. Catalysis B* 52, pp. 179-203.
- Scott, T.B., Allen, G.C., Heard, P.J., Randel, M.G. 2005. Reduction of U(VI) to U(IV) on the surface of magnetite. *Geochim. Cosmochim. Acta*, 69, pp 5639–5646.
- Sellin, P. 2002. SR 97: Hydromechanical evolution in a defective canister, *MRS Symp. Proc.* 663 pp. 755-763.
- Serrano-Purroy, D., Clarens, F., González-Robles, E., Glatz, J.P., Wegen, D.H., de Pablo, J., Casas, I., Giménez J., Martínez-Esparza A., 2012. Instant release fraction and matrix release of high burn-up UO<sub>2</sub> spent nuclear fuel: Effect of high burn-up structure and leaching solution composition. *J. Nucl. Mater.* 427, pp. 249–258.
- Shoesmith 2013. The chemistry/electrochemistry of spent nuclear fuel as a waste form, Chapter 11 in: Burns, P.C., Simon, G.E. (Eds.), "Uranium: Cradle to Grave", Mineralogical Society of Canada, Quebec.
- Shoesmith, D. W. 2000. Fuel corrosion processes under waste disposal conditions. *J. Nucl. Mater.* 282 pp. 1-31.

### 3.1.1 Spent Nuclear Fuel; State-of-Knowledge

Shoesmith, D.W., Kolar, M., King, F. 2003. A mixed-potential model to predict fuel (uranium dioxide) corrosion within a failed nuclear waste container, *Corrosion* 59, pp. 802-816.

Shoesmith, D.W., Sunder S., Johnson L.H., Bailey M.G., 1985. Oxidation of CANDU fuel by the alpha radiolysis products of water, *MRS. Symp. Proc.* 50, pp. 309-316.

Shoesmith, D.W., Zagidulin, D. 2011. The corrosion of zirconium under deep geologic repository conditions. *J. Nucl. Mater.* 418, pp. 292-306.

Shukla P, Sindelar R, Lam P-S, 2019. Consequence analysis of residual water in a storage canister, Report SRNL-STI-2019-00495, Savannah River National Laboratory, USA.

Silva, R.J., Bidoglio, G., Rand, M.H., Robouch, P.B., Wanner, H., Puigdomenech, I., 1995. *Chemical thermodynamics. Vol. 2. Chemical thermodynamics of Americium.* Amsterdam: Elsevier.

SKB 2010b. Spent nuclear fuel for disposal in the KBS-3 repository, SKB Technical Report TR 10-13, Svensk Kärnbränslehantering AB.

SKB 2010d. Data report for the safety assessment SR-Site. SKB Technical Report TR-10-52. Svensk Kärnbränslehantering AB.

SKB 2010p. Fuel and canister process report for the safety assessment SR-Site, SKB Technical Report TR-10-46, Svensk Kärnbränslehantering.

SKB, 2011. Long-term safety for the final repository for spent nuclear fuel at Forsmark. Main report of the SR-Site project. SKB TR-11-01, Svensk Kärnbränslehantering AB.

Sobes, V., Scaglione J.M., Wagner J.C, Dunn M.E., 2015. Validation study for crediting chlorine in criticality analyses for spent nuclear fuel, International Conference on Nuclear Criticality, September 13, 2015, Charlotte, NC, USA.

Spahiu, K., Cui, D., Lundström, M., 2004. The fate of radiolytic oxidants during spent fuel leaching in the presence of dissolved near field hydrogen, *Radiochim. Acta*, 92 pp. 625-629.

Spahiu, K., Eklund, U.-B., Cui, D., Lundstrom, M. 2002. The influence of near field redox conditions on spent fuel leaching, *MRS. Symp. Proc.* 713 pp. 633-638.

Spahiu, K., Werme, L., Eklund, U-B. 2000. The influence of near field hydrogen on actinide solubilities and spent fuel leaching, *Radiochim. Acta* 88 pp. 507-511.

Spinks J.W.T., Woods R. J.1990. *An introduction to radiation chemistry.* Third edition, New York: John Wiley & Sons Inc.

Spino, J., Papaioanou, D. 2000. Lattice parameter changes associated with the rim-structure formation in high burn-up UO<sub>2</sub> fuels by micro x-ray diffraction, *J. Nucl. Mater.* 281, pp. 146-162.

Stroes-Gascoyne S, 1996. Measurements of instant-release source terms for <sup>137</sup>Cs, <sup>90</sup>Sr, <sup>99</sup>Tc, <sup>129</sup>I and <sup>14</sup>C in used CANDU fuels. *J. Nucl. Mater.* 238, pp 264–277.

Stroes-Gascoyne S, Tait J C, Porth R J, McConnel J L, Lincoln W J, 1994. Release of <sup>14</sup>C from the gap and grain-boundary regions of used CANDU fuels to aqueous solutions, *Waste Management*, 14, p. 385-392.

Sunder, S., Boyer, G.D., Miller, N.H. 1990. XPS studies of UO<sub>2</sub> oxidation by alpha radiolysis of water at 100 °C, *J. Nucl. Mater.*, 175, pp. 163-169."

### 3.1.1 Spent Nuclear Fuel; State-of-Knowledge

Sunder S. 1998. Calculation of radiation dose rates in a water layer in contact with used Candu UO<sub>2</sub> fuel, Nucl. Technol. 122, pp. 211-221.

Swanton S W, Baston G M N, Smart N R, 2015. Rates of steel corrosion and carbon-14 release from irradiated steels-State of the art review, D 2.1 of the EC Project CAST.

Tait, J.C., Cornett, R.J.J., Chant, L.A., Jirovec, J., McConnell, J., Wilkin, D.L., 1997. Determination of Cl impurities and <sup>36</sup>Cl instant release from used CANDU fuels, MRS Symp. Proc. 465, pp. 503-510.

Tait, J.C., Luht, J.M., 1997. Dissolution rates of uranium from unirradiated UO<sub>2</sub> and uranium and radionuclides from used CANDU fuel using a single pass flow-through apparatus, Ontario Hydro Report No. 06819-REP-01200-006-ROO.

Taylor, P., Wood, D.D., Duclos, A.M., Owen, D.G., 1989. Formation of uranium trioxide hydrates on UO<sub>2</sub> fuel in air-steam mixtures near 200 °C, J. Nucl. Mater., 166, pp. 70–75.

Thomas, L. E., Einziger, R. E., Buchanan, R. E., 1993. Effect of fission products on air oxidation of LWR spent fuel, J. Nucl. Mater. 201, pp. 310-319.

Thomas, L.E., Einziger, R.E., Woodley, R.E., 1989. Microstructural examination of oxidized spent PWR fuel by transmission electron microscopy, J. Nucl. Mater. 166, pp. 243-251.

Thomas L.E. 1991. Condensed-phase xenon and krypton in UO<sub>2</sub> spent fuel, in: S.E. Donnelly, J.H. Evans (Eds.), Fundamental Aspects of Inert Gases in Solids, Plenum Press, NewYork, 1991, pp. 431–441.

Trummer, M., Nilsson, S., Jonsson, M. 2008. On the effects of fission product noble metal inclusions on the kinetics of radiation induced dissolution of spent nuclear fuel, J. Nucl. Mater. 378, pp. 55-59.

Trummer, M., B. Dahlgren, Jonsson M. 2010a. The effect of Y<sub>2</sub>O<sub>3</sub> on the dynamics of oxidative dissolution of UO<sub>2</sub>. J. Nucl. Mater. 407, pp. 195-199.

Trummer, M., Jonsson, M., 2010b. Resolving the H<sub>2</sub> effect on radiation induced dissolution of UO<sub>2</sub>-based spent nuclear fuel. J. Nucl. Mater. 396, 163–169. <https://doi.org/10.1016/j.jnucmat.2009.10.067>

Trummer, M., Roth, O., Jonsson, M. 2009. H<sub>2</sub> inhibition of radiation induced oxidative dissolution of spent fuel, J. Nucl. Mater. 383 pp. 226-230.

Une, K., Imamura, M., Amaya, M., Korei, Y., 1995. Fuel oxidation and irradiation behaviours of defective BWR fuel rods. J. Nucl. Mater., 223, pp.40-50.

Une, K., Tominaga, Y., Kashibe, S. 1991. Oxygen potentials and lattice parameter of irradiated BWR fuels, J. Nucl. Sci.Technol. 28 pp. 409-417.

Utsonomiya, S., Ewing, R.C. 2006. The fate of the epsilon phase (Mo-Ru-Pd-Tc-Rh) in the UO<sub>2</sub> of the Oklo natural fission reactors, Radiochim. Acta, 94, pp. 749-753.

Van Brutzel, L., Crocombette, J-P. 2007. Atomic scale modelling of the primary damage state of irradiated UO<sub>2</sub> matrix. In: Aktaa, J., Samaras, M., Serrano de Caro, M., Victoria, M., Wirth, B. (eds). Structural and Refractory Materials for Fusion and Fission Technologies. Warrendale, PA: Materials Research Society. Materials Research Society Symposium Proceedings 981E, JJ01-01.

Van Konyneburg, R.A. 1996. Comments on the draft paper “Underground supercriticality from plutonium and other fissile material” by C.D. Bowman and F. Venneri, Science and Global Security, 5 pp. 303-322.

### 3.1.1 Spent Nuclear Fuel; State-of-Knowledge

- Vasiliev, A., Herrero, J., Pecchia, M., Rochman, D., Ferroukhi, H., Caruso, S. 2019. Preliminary assessment of criticality safety constraints for Swiss spent nuclear fuel loading in disposal canisters. *Materials*, 12, 494. <https://doi.org/10.3390/ma12030494>.
- Walker, C.T., Lassmann, K., 1986. Fission gas and caesium gradients in single grains of transient tested UO<sub>2</sub> fuel: Results of an EPMA investigation. *J. Nucl. Mater.* 138, 155–161. [https://doi.org/10.1016/0022-3115\(86\)90001-2](https://doi.org/10.1016/0022-3115(86)90001-2).
- Walker, C.T., Bagger C., Mogensen M., 1996. Observations on the release of cesium from UO<sub>2</sub> fuel, *J. Nucl. Mater.* 240, p. 32-42.
- Wang, Q., Wang, L., Fei, H., Zhenhua, L., Zhentao, M., 2004. Study of deactivation and regeneration of Pd/Al<sub>2</sub>O<sub>3</sub> catalyst in hydrogen peroxide production by the anthraquinone process. *React. Kinet. Catal. Lett.* 81, pp. 297-304.
- Wareing, A., Trivedi, D., M Mignanelli, M. 2012. Assessment of potential radionuclide release from spent AGR fuel in a geological disposal facility, *NNL (10) 11377 Issue 3*.
- Weber W.J., Ewing R.C., Catlow C.R.A., Diaz de la Rubia T., Hobbs L.W., Kinoshita C., Matzke H., Motta A.T., Nastasi M., Salje E.K.H., Vance E.R., Zinkle S.J. 1998. Radiation effects in crystalline ceramics for the immobilisation of high-level waste and plutonium, *J. Mater. Res.* 13, pp.1434-1484.
- Werme, L.O., Johnson L.H., Oversby, V.M., King, F., Spahiu, K., Grambow, B., Shoesmith, D.W. 2004. Spent fuel performance under repository conditions: A model for use in SR-Can, SKB TR 04-19, Svensk Kärnbränslehantering AB.
- Wersin, P., Spahiu, K., Bruno, J. 1994. Time evolution of oxygen and redox conditions in HLW repository, SKB Technical Report TR 94-02, SKB, Stockholm.
- Wieselquist, W. A., Lefebvre, R.A., Jessee, M. A. Eds., 2020. SCALE Code System, Report ORNL/TM-2005/39, Version 6.2.4, Oak Ridge National Laboratory, Oak Ridge, TN, USA.
- Winsley, R.J., Baldwin, T.D., Hicks, T.W., Mason, R.M., Smith, P.N. 2015. Understanding the likelihood and consequences of post-closure criticality I a geological disposal facility, *Mineralogical Magazine*, 79 pp. 1551-1561.
- Wiss, T., J.-P. Hiernaut, D. Roudil, J.-Y. Colle, E. Maugeri, Z. Talip, A. Janssen, V.V. Rondinella, R.J.M. Konings, H. Matzke, W. Weber (2014). "Evolution of spent nuclear fuel in dry storage conditions for millennia and beyond". *Journal of Nuclear Materials* 451: 198-206.
- Wu, L., Beauregard, Y., Qin, Z., Rohani, S., Shoesmith, D.W. 2012. A model for the influence of steel corrosion products on nuclear fuel corrosion under permanent disposal conditions. *Corrosion Science*, 61, 83-91.
- Wu, L., Liu, N., Qin, Z., Shoesmith, D.W. 2014b. Modeling radiolytic corrosion of fractured nuclear fuel under permanent disposal conditions, *J. Electrochem. Soc.* 161(8) pp. E3259-E3266.
- Wu, L., Qin, Z., Shoesmith, D.W. 2014a. An improved model for the corrosion of used nuclear fuel inside a failed waste container under permanent disposal conditions. *Corrosion Science*, 84, pp. 85-95.
- Yang, M., Fidalgo, A.B., Sundin, S., Jonsson, M., 2013. Inhibition of radiation induced dissolution of UO<sub>2</sub> by sulphide-A comparison with the hydrogen effect, *J. Nucl. Mater.* 434 pp. 38-42.

### 3.1.1 Spent Nuclear Fuel; State-of-Knowledge

Zehavi, D., J. Rabani, J. 1972. Oxidation of aqueous bromide ion by hydroxyl radicals. Pulse radiolytic investigation, J. Phys. Chem. 76 pp. 312-319.

Zwicky H-U, Low J, Ekeröth E, 2011. Corrosion studies with high burnup light water reactor fuel. Release of nuclides into simulated groundwater during accumulated contact time of up to two years. TR-11-03 Svensk Kärnbränslehan